UNIVERSIDADE FEDERAL DO PARÁ
INSTITUTO DE GEOCIÊNCIAS
PROGRAMA DE PÓS-GRADUAÇÃO EM GEOLOGIA E GEOQUÍMICA

DISSERTAÇÃO DE MESTRADO Nº 564

CHARNOQUITOS DE OURILÂNDIA DO NORTE (PA): GEOLOGIA, NATUREZA E IMPLICAÇÕES TECTÔNICAS PARA A PROVÍNCIA CARAJÁS

Dissertação apresentada por:

WILLIAMY QUEIROZ FELIX
Orientador: Prof. Dr. Davis Carvalho de Oliveira (UFPA)

BELÉM
2019

Universidade Federal do Pará
Instituto de Geociências
Programa de Pós-Graduação em Geologia e Geoquímica

CHARNOQUITOS DE OURILÂNDIA DO NORTE (PA): GEOLOGIA, NATUREZA E IMPLICAÇÕES TECTÔNICAS PARA A PROVÍNCIA CARAJÁS
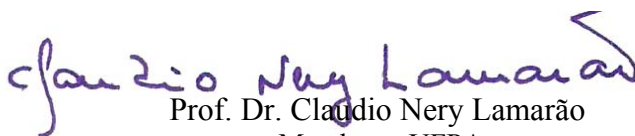
DISSERTAÇÃO APRESENTADA POR

WILLIAMY QUEIROZ FELIX

Como requisito parcial à obtenção do Grau de Mestre em Ciências na Área de **GEOLOGIA E GEOQUÍMICA**, linha de pesquisa **PETROLOGIA E EVOLUÇÃO CRUSTAL**

Data de Aprovação: 02 / 10 / 2019

Banca Examinadora:

Prof. Dr. Davis Carvalho de Oliveira
Orientador – UFPA

Prof. Dr. Claudio Nery Lamarão
Membro – UFPA

Prof. Dr. Júlio Cezar Mendes
Membro – UFRJ

À família, em especial minhas irmãs.

v

AGRADECIMENTOS

Meus sinceros agradecimentos às pessoas e entidades que direta ou indiretamente contribuíram para a realização deste trabalho, em especial:

- À Universidade Federal do Pará (UFPA), o Instituto de Geociências e ao Grupo de Pesquisa de Petrologia de Granitoides (GPPG), pelo fornecimento de infraestrutura necessária à realização deste trabalho.

- Ao Conselho Nacional de Desenvolvimento Científico e Tecnológico CNPQ pela concessão de bolsa de mestrado.

- Ao prof. Davis Carvalho de Oliveira por sua orientação, confiança e paciência ao longo destes anos.

- Ao laboratório de microanálises (MEV – Microssonda) do Instituto de geociências da Universidade Federal do Pará, em especial ao professor Cláudio Lamarão e as técnicas Gisele Tavares e Ana Paula, pelas ajudas na hora do sufoco, gostaria também de agradecer a oficina de laminação pela confecção das lâminas e pela competência, a todos esses fica o meu muito obrigado oportunidade de utilização das ferramentas que possibilitaram esse trabalho.

- Aos colegas do GPPG pela amizade e ajuda em discussões, etapas de campo e manuseio de equipamentos, em especial a Luana Camile e Diwhemerson Souza com quem tive a satisfação de realizar a etapa de campo. A Natânia Santos de quem herdei as amostras, ao Luciano Ribeiro pelas críticas construtivas e sugestões. Aos Pablo Leite, Bhrenno Marangoanha, Fernando Fernandes e Jully Milly, fica obrigado pela paciência ao longo desses anos.

- Aos amigos (ordem alfabética), Alexandre Cardoso, Brenda Marques, Crislene Silva, Daniella Vieira, Danilo Cruz e Evelyn Melo, por me aturarem todo esse tempo.

- A meus familiares por todo o carinho, incentivo e apoio e pela compreensão por todos os momentos que estive ausente. Em especial agradeço profundamente a meus pais Antônia Queiroz e João Felix, pelo amor, dedicação, educação, que apesar das dificuldades fizeram o possível para que eu alcançasse meus objetivos. A meu irmão Dayvidson, as minhas irmãs Alice, Leticia, Beatriz e Jéssica e aos meus sobrinhos, Ágatha, Maite e Salomão.

RESUMO

Estudos desenvolvidos nos granitoides com piroxênio e rochas máficas associadas que ocorrem na região de Ourilândia do Norte permitiram a individualização de 4 variedades petrográficas: (i) ortopiroxênio granodiorito, (ii) clinopiroxênio monzogranito e (iii) anfibólio monzogranito, e (iv) gabronorito. Este último ocorre espacialmente associado à variedade ortopiroxênio granodiorito. Tais rochas configuram cinco corpos alongados na direção NE-SW e E-W, onde o plúton principal atinge ~12 km de extensão. É formado pelas variedades clinopiroxênio monzogranito e ortopiroxênio granodiorito, enquanto a variedade anfibólio monzogranito forma três pequenos corpos lenticulares com cerca de 3 km de comprimento. Estes são alongados na direção E-W, mostram foliações na direção NE-SW e E-W e mergulhos subverticais (70-80º). Tais rochas exibem textura magmática bem preservada, são leucocráticas (M'=21,1 – 32,9), e de granulação média a grossa. Os minerais acessórios primários são allanita, epídoto, zircão, apatita, magnetita e ilmenita, sendo que a titanita ocorre somente nos monzogranitos e a olivina é restrita à variedade gabronorítica. São rochas metaluminosas de afinidade magnesiana, seguem o *trend* cálcio alcalino e cálcio alcalino de alto K. As razões Fe/(Fe+Mg) tanto nas biotitas quanto nos anfibólios, indicam condições intermediarias de fO_2, que é corroborado pela razão $Fe^{3+}/(Fe^{3+}+Fe^{2+})$ nos anfibólios que indica moderadas condições de fO_2 durante a cristalização (acima do tampão QFM). As temperaturas de cristalização para os piroxênios variam entre 855 a 1061 °C, 713 a 800 nos anfibólios, e a pressão de cristalização é de 1,9 a 3,1 kbar. A atividade de água no magma varia de 4,1 a 6,5. Textura em coroa formada por anfibólios bordejando piroxênios é comum em todas as variedades, o que pode ser explicado pela reação do *melt* anidro com água em estágio magmático, que resultaria na ausência de piroxênio na fácies anfibólio monzogranito. As microestruturas de recristalização em quartzo e feldspatos permitem inferir uma temperatura final de deformação cristal-plástica em torno de 400-450 ºC. Microfraturas submagmáticas preenchidas por quartzo e álcali feldspato também são encontradas, indicando que os charnoquitos de Ourilândia do Norte sofreram deformação na presença de *melt*. Isto está de acordo com a natureza sin-tectônica para colocação de seus magmas. O empobrecimento de HFSE em relação às rochas neoarqueanas de Carajás indica que a associação estudada possui uma fonte distinta e/ou sofreram diferentes processos de evolução. Modelamento geoquímico indica que tais granitoides evoluíram por cristalização fracionada a partir de um magma parental máfico, em contraponto à fusão parcial, admitida como principal processo responsável pela origem dos demais granitoides neoarqueanos de Carajás.

Palavras-chave: Geoquímica (PA). Petrologia. Mineralogia Química. Província Carajás. Cráton Amazônico.

ABSTRACT

ABSTRACT: The granite-charnockite association from Carajás Province is spatially associated with gabbronorites, which intrude Mesoarchean granitoids and form a NE-SW elongated pluton with subordinate lenses E-W oriented showing subvertical (70-80°) foliation. They consist of leucocratic rocks (M' = 21.1 - 32.9) with well-preserved magmatic textures and medium- to coarse-grained. The main mafic phases are pyroxene [enstatite/ferrosilite and augite/diopside ($Wo_1En_{66}Fs_{33}$ to $Wo_{49}En_{38}Fs_{14}$)], amphibole [hornblende ($0.88 \geq Mg/(Mg+Fe^{2+}) \leq 0.43$)], and biotite [$0.68 \geq Fe/(Fe + Mg) \geq 0.31$]. These rocks are considered syntectonic plutons emplaced in a postcollisional setting, which underwent dynamic recrystallization controlled by subgrain rotation (SGR; 400-450 °C) in a sinistral transpressive deformational regime driven by pure shear. The granite-charnockite association and gabbronorite present very similar geochemical behavior: magnesian affinity [whole-rock $0.8 \geq FeOt/(FeOt+MgO) \leq 0.5$], calc-alkaline and high-K calcic-alkaline trends and metaluminous character. Magma ascent and emplacement are reconstructed as a single-stage process with decreasing temperatures. Crystallization temperatures range from 1100 to ~700 °C for pyroxenes, and 809 to 713 °C for amphiboles. Calculated crystallization pressures were 190 to 310 MPa resulting in crystallization depths of 7.0 to 10.5 km. Observed mineral assemblages and compositions of the main mafic minerals imply crystallization under relatively oxidizing conditions (NNO -9.8 to -12.6). H_2O contents ranging from 4.1 to 6.5 wt% and indicates that water played an important role in the magmatic evolution of the studied rocks. Hydration was responsible for differences in the modal contents of monzogranite varieties. Gabbronorites were probably formed by partial melting of depleted mantle source (low HFSE), and orthopyroxene-bearing granitoids originated through fractional crystallization from magma similar in composition to gabbronorite.

Keywords: Charnockite. Carajás. Granitoids. Archean. Crystallization Parameters.

LISTA DE ILUSTRAÇÕES

amphibole with straight boundaries with Am1 and Bt1; e) well-preserved hypidiomorphic texture in the orthopyroxene granodiorite; f) mafic cluster of titanite and amphibole with straight boundaries; g) clinopyroxene partially transformed to Am2 and producing Qtz4; h) resorbed and ragged ilmenite inclusions in biotite; i) subhedral plagioclase displaying intragranular microfractures filled by quartz, indicating deformation in the presence of melt; j) core-mantle texture characterized by plagioclase porphyroclast bordered by quartz, plagioclase and alkali feldspar; k) recrystallized quartz showing core-mantle texture formed by a matrix of Qtz2. 22

LISTA DE TABELAS

SUMÁRIO

CAPÍTULO 1 INTRODUÇÃO

1.1 APRESENTAÇÃO

O termo charnoquito foi proposto por Holland (1900) para se referir a uma série de granitoides que possuíam ortopiroxênio como fase varietal. Ao longo dos anos este termo ganhou uma série de variações e também foi atribuído à rochas metamórficas (Howie 1955, Le Maitre 2002, Streckeisen 1976). As diversas nomenclaturas atribuídas a este grupo de rochas e as ambuiguidades quanto a sua origem, levaram Frost & Frost (2008) a sugerirem a eliminação dos vários termos específicos, além de propor o uso do termo charnoquito apenas para rochas ácidas onde o ortopiroxênio seja de origem ígnea. Charnoquitos não são específicos de um único ambiente tectônico ou período geológico, embora estejam presentes na maioria dos Crátons (Condie *et al.* 1982, Frost & Frost 2008, Rajesh 2012, Rajesh & Santosh 2004). A formação de granitoides ortopiroxênio requer condições especiais quando comparadas àquelas exigidas para formação de granitos com biotita e anfibólio (Carroll & Wyllie 1990, Frost *et al.* 2000, Naney 1983, Patiño Douce 1996). Neste caso, a estabilidade do piroxênio é controlada pela temperatura, pressão, composição e conteúdo de H_2O, e em a altas pressões (>8 kbar) o ortopiroxênio é restrito a condições anidras, e em a baixas pressões pode se formar tanto em condições anidras quanto hidratadas (Naney 1983). A crosta arqueana da Província Carajás é composta predominantemente por tonalito-trondhjemito e granodiorito (TTG) e leucogranitos (Almeida *et al.* 2011, Feio *et al.* 2013). Rochas ígneas com anfibólio e biotita são dominantes em relação àquelas com piroxênio, embora menos abundantes, essas rochas têm um papel importante durante os períodos de formação de crosta, além de serem imprescindíveis para entender a evolução do magmatismo neoarqueano de Carajás.

A área de Ourilândia do Norte (Figura 1), porção centro-oeste da Província Carajás, está situada na fronteira entre os domínios Rio Maria e Carajás. Trabalhos de mapeamento geológico em escala de semi-detalhe (1:50.000), desenvolvidos recentemente nesta região, aliados a estudos petrográficos e geoquímicos permitiram a individualização de diversos granitoides mesoarqueanos, além de granitoides com piroxênio intrusivos nas unidades mesoarqueanas (Santos & Oliveira 2016, Silva *et al.* 2018), os quais são o alvo desta dissertação de mestrado. Uma das principais diferenças entre o Domínio Rio Maria e Carajás

é a ausência de eventos magmáticos neoarqueanos registrados no DRM (Dall'Agnol *et al.* 2006, Vasquez *et al.* 2008). As rochas neoarqueanas da Província Carajás possuem uma intrínseca relação com rochas charnoquíticas (Cunha *et al.* 2016, Dall'Agnol *et al.* 2017, Feio *et al.* 2012), que devido à sua importância para a evolução geológica da província, os charnoquitos de Carajás ainda carecem de estudos mais detalhados que permitam uma discussão sobre sua origem e evolução.
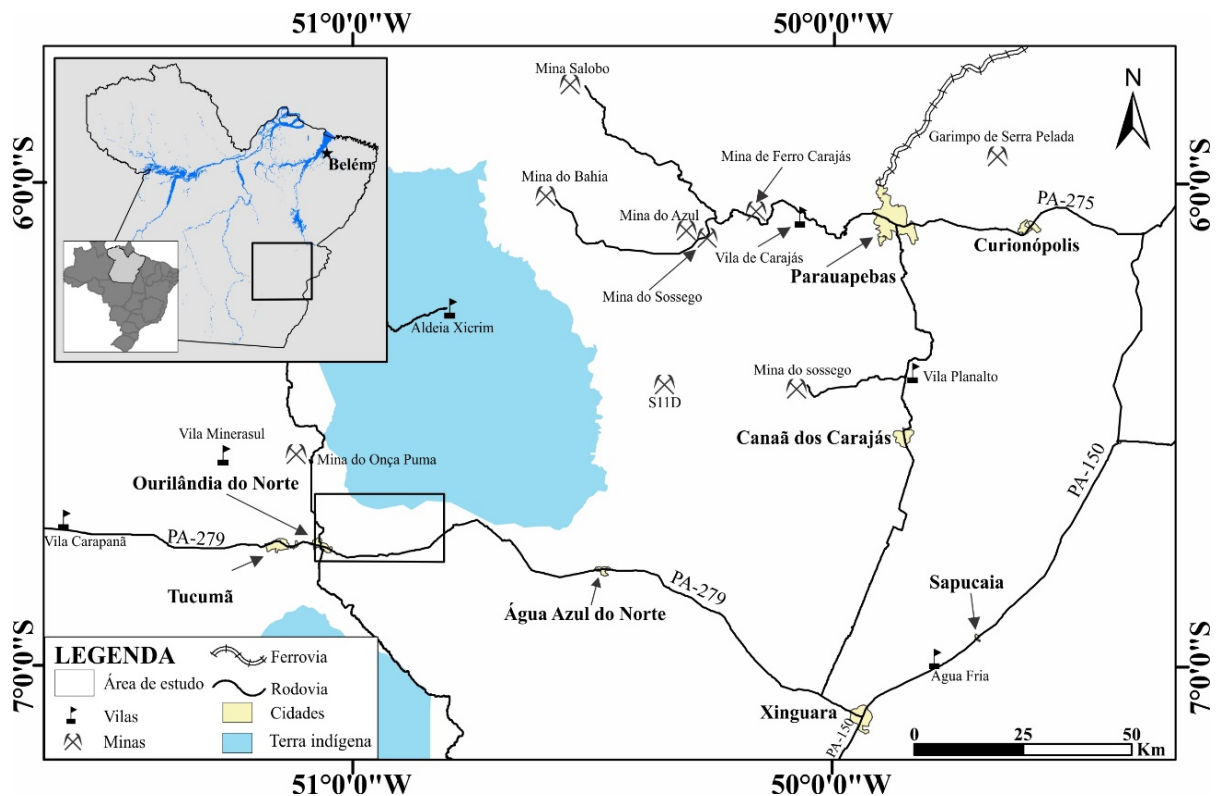
Figura 1- Mapa de localização da área de estudo, que é limitada a norte pela reserva indígena Xicrim Cateté e a oeste pela cidade de Ourilândia do Norte.

1.2   GEOLOGIA REGIONAL

A Província Carajás (PC - Figura 2), localizada na borda Sudeste do Cráton Amazônico (Almeida *et al.* 1981) faz parte do contexto geológico da Província Amazônia Central (Tassinari & Macambira 2004, 1999), embora Santos (2003) considere a PC como uma província geocronológica independente. Inicialmente, a Província Carajás foi dividida em dois segmentos crustais tectonicamente distintos: o primeiro ao sul é o Domínio Rio Maria de idade mesoarqueana, e o Domínio Carajás formado por rochas meso- e neoarqueanas, ao norte (Souza *et al.* 1996, Vasquez *et al.* 2008). O primeiro é composto por rochas mesoarqueanas incipientemente deformadas, enquanto o Domínio Carajás manteria o embasamento mesoarqueano, só que afetado por eventos tectonotermais neoarqueanos. A

divisão mais atual da Província Carajás foi proposta por (Dall'Agnol *et al*. 2013), onde os autores propuseram uma nova divisão tectono-estratigráfica para a Província Carajás, a qual seria segmentada em três domínios tectônicos principais, o Domínio Rio Maria e os domínios Canaã dos Carajás e Sapucaia, além da Bacia Carajás.

Dall'Agnol *et al*. (2006) definiram o **Domínio Rio Maria** (DRM) como um terreno essencialmente Mesoarqueano (3,0 a 2,87 Ga), caracterizado por associações *greenstone belts* do supergrupo Andorinhas (3,0 Ga a 2,9 Ga) e rochas granitoides diversas, como: **(a)** TTGs, que embora apresentem uma variação nas suas idades são essencialmente mesoarqueanos com idade de 2,96 Ga a 2,93 Ga, possuem características geoquímicas similares, sendo eles; Tonalito Arco Verde, Trondhjemito Mogno e Tonalito Mariazinha (Almeida *et al*. 2011, 2008). **(b)** Granitoides de alto-Mg (sanukitoides), que são formados pelo Granodiorito Rio Maria de 2,87 Ga e rochas associadas (Medeiros & Dall'Agnol 1988, Oliveira *et al*. 2009, Santos & Oliveira 2016); **(c)** rochas da Suíte Guarantã (2,87 Ga a 2,86 Ga), representadas por três plútons (Guarantã, Azulona e Trairão), localizados na porção sul do terro Rio Maria (Almeida *et al*. 2013, 2010, Althoff *et al*. 2000); Leucogranodioritos-granitos afins desta unidade foram caracterizados na região de Ourilândia do Norte (Santos *et al*. 2013); **(d)** Leucogranitos potássicos de afinidade cálcio-alcalina com idade 2,87 Ga, representados pelos granitos Mata Surrão e Xinguara (Almeida *et al*. 2013, Dall'Agnol *et al*. 2006, Lafon *et al*. 1994, Leite *et al*. 1999).

O **Domínio Sapucaia** (DS) está localizado entre os domínios Rio Maria e Canaã dos Carajás. É constituído de associações *greenstone belt*, rochas TTG, sanukitoides, granitoides alto Ba-Sr e potássicos, análogas àqueles encontrados no DRM, sendo afetados por eventos do Neoarqueano. As unidades mesoarqueanas incluem: **(i)** Greenstone belts do grupo Sapucaia, caracterizados por rochas metáficas, metaultramáficas e metassedimentares, com fácies metamórficas compatível com xisto verde a anfibolito (DOCEGEO 1988, Costa *et al*. 1994, Sousa *et al*. 2013); **(ii)** granitoides sódicos distintos dos TTG e sanukitoides arqueanos, representados pelo Tonalito São Carlos de 2,95 Ga, (Silva *et al*. 2014); **(iii)** associações TTG representados por uma estreita faixa NW-SE do Tonalito Caracol de 2,93 Ga (Almeida *et al*. 2011, Leite *et al*. 2004) e rochas afins do Tonalito Mariazinha, com estruturação N-S que ocorrem nas proximidades de Xinguara (Almeida *et al*. 2011). Nas proximidades da região de Vila Jussara, foi caracterizado o Trondhjemito Colorado de 2,87 Ga ±1, (Silva *et al*. 2010). (Leite-Santos & Oliveira 2014) mapearam rochas afins a esta unidade nas proximidades de Nova Canadá, que também ocorrem na região de Xinguara; **(iv)** foram reconhecidos

granitoides de alto-Mg nas proximidades da cidade de Água Azul do Norte, com afinidade sanukitoide com idade de cristalização U-Pb SHRIMP em zircão de 2,87 Ga (Gabriel & Oliveira 2014); **(v)** Leucogranodioritos-granitos de alto Ba-Sr ocorrem de forma expressiva no domínio Sapucaia e são representados pelo Leucogranodiorito Nova Canadá, caracterizados por leucogranodioritos a leucomozongranitos moderadamente deformados (Leite-Santos & Oliveira 2014, 2016, Santos 2014). Teixeira *et al.* (2013) descreveram leucogranodioritos porfiríticos com características de alto Ba-Sr na região de Vila Jussara; **(vi)** granitos de alto-K de afinidade cálcio-alcalina ocorrem de forma restrita no Domínio Sapucaia e são representados pelo Granito Xinguara (2,86 Ga - Almeida *et al.* 2011, Leite *et al.* 2004) e Leucogranito Velha Canadá de idade 2,74±2Ga (Leite-Santos & Oliveira 2016); **(vi)** granitoides subalcalinos sintectônicos semelhantes àqueles da Suíte Planalto (Feio *et al.* 2012) foram descritos por (Silva *et al.* 2014) na mesma região, e posteriormente agrupados e chamados de Suíte Vila Jussara (Dall'Agnol *et al.* 2017), são rochas com caráter mais oxidado e que apresentam uma variedade petrográfica maior quando comparados à Suíte Planalto.

O **Domínio Canaã dos Carajás** (DCC) de idade meso- a neoarqueana, sendo formado por rochas granitoides mesoarqueanas, é geologicamente distinto dos outros domínios por seu maior volume de rochas graníticas em relação aos TTG's. As unidades são compostas pelo Ortogranulito Chicrim-Cateté, Complexo Xingu, rochas ultramáficas da Suíte intrusiva Cateté, rochas máficas do Diopsídio Norito Pium, granitoides neoarqueanos, *greenstone belts*, além da presença de associações charnoquíticas (Dall'Agnol *et al.* 2013, Feio *et al.* 2013, Vasquez *et al.* 2008).

Os granitoides mesoarqueanos são: **(i)** granitoides sódicos distintos dos clássicos TTG arqueanos, representados pelo Tonalito Bacaba de 3,0 Ga (Moreto *et al.* 2011), Complexo Tonalítico Campina Verde de 2,87 a 2,85 Ga (Feio *et al.* 2013), e Trondhjemito Rio Verde com idade de 2,92 a 2,86 Ga (Feio *et al.* 2013) **(ii)** granitos potássicos de afinidade cálcio-alcalina, representados pelos plútons: Serra Dourada de 2,86 Ga (Moreto *et al.* 2011) e 2,83 Ga (Feio *et al.* 2013), Boa Sorte de 2,85-2,89 Ga (Rodrigues *et al.* 2010), Cruzadão de 2,84 Ga (Feio *et al.* 2013) e Bom Jesus de 2,83 Ga (Feio *et al.* 2013). O Granito Canaã dos Carajás de idade 2,95 Ga (Feio *et al.* 2013), tem caráter mais sódico e por isto é descrito separadamente. Na área de Ourilândia do Norte ocorrem granodioritos e monzogranitos mesoarqueanos, cálcico-alcalinos, alto-K, colocados em ambiente colisional, nas fases finais

de encurtamento regional do ciclo tectônico que moldaram o segmento norte do domínio Rio Maria (~2,87 Ga) (Santos & Oliveira 2016, Silva *et al.* 2018).

O Ortogranulito Chicrim-Cataté ocorre ao sul da Bacia Carajás e é descrito como um elipsoide de direção ENE-WSW, constituído por granulitos máficos e félsicos, cálcio alcalinos com textura granoblastica (Vasquez *et al.* 2008). Pidgeon *et al.* (2000) obteve idade de cristalização e metamorfismo (3,0 e 2,86 Ga, respectivamente) do protólito ígneo deste Complexo, essa idade é considerada a mesma para o Ortogranulito Chicrim-Cateté. O magmatismo ultramáfico da Suíte intrusiva Cateté é presentado por intrusões acamadadas, tais como: Complexo Serra da Onça, Complexo Luanga, Complexo acamadado Lago Grande, todos de idades neoarqueana ~2,76 Ga (Lafon *et al.* 2000, Macambira & Vale 1997, Machado *et al.* 1991, Teixeira *et al.* 2015). O magmatismo máfico neoarqueano do Domínio Canaã dos Carajás é representado pelo Diopídio-Norito Pium com idade de cristalização 2,74 Ga (Santos *et al.* 2013).

O magmatismo granitoide Neoarqueano inclui: **(i)** granitoides subalcalinos e sintectônicos, colocados em zonas de cisalhamento e que possuem assinatura tipo-A; representado pelo Complexo Estrela com 2,76 Ga (Barros *et al.* 2009, 2001), Granito Serra do Rabo de 2,74 Ga (Barros *et al.* 2009), Granito Igarapé Gelado datado de 2,73 Ga (Barros *et al.* 2009); e Suíte Planalto (2,75-2,71 Ga) (Feio *et al.* 2012); **(ii)** rochas charnoquíticas caracterizadas por ortopiroxênio tonalitos e granodioritos de idade 2,75 Ga (Feio *et al.* 2012, Santos *et al.* 2013, Gabriel *et al.* (2010); **(iii)** granitoides sódicos de assinatura toleítica da Suíte Pedra Branca (2,75 Ga - Feio *et al.* 2013), que ocorrem associados à Suíte Planalto; **(iv)** Suíte Plaquê é neoarqueana (2,73 Ga), composta por muscovita-biotita leucogranitos com assinatura metaluminosa a peraliminosa que ocorrem com corpos estratoides alongados na direção E-W (Araújo *et al.* 1988, Avelar *et al.* 1999). Estudos recentes vêm pondo em xeque a real existência da Suíte Plaquê, e mostrando que onde deveria ocorrer rochas da Suíte Plaquê na verdade ocorrem outras rochas neoarqueanas, principalmente rochas afins da Suíte Planalto e Vila Jussara (Dall'Agnol *et al.* 2017, Feio *et al.* 2012, Marangoanha *et al.* 2019, Oliveira *et al.* 2018) e até mesmo rochas mesoarqueanas (Santos & Oliveira 2016, Silva *et al.* 2018). Granitos tipo A paleoproterozóicos (1,88 Ga) e diques associados são encontrados intrudindo rochas em todos os domínios da Província Carajás (Dall'Agnol *et al.* 2005, Dall'Agnol & Oliveira 2007, Oliveira *et al.* 2008, Silva *et al.* 2016, Teixeira *et al.* 2017).
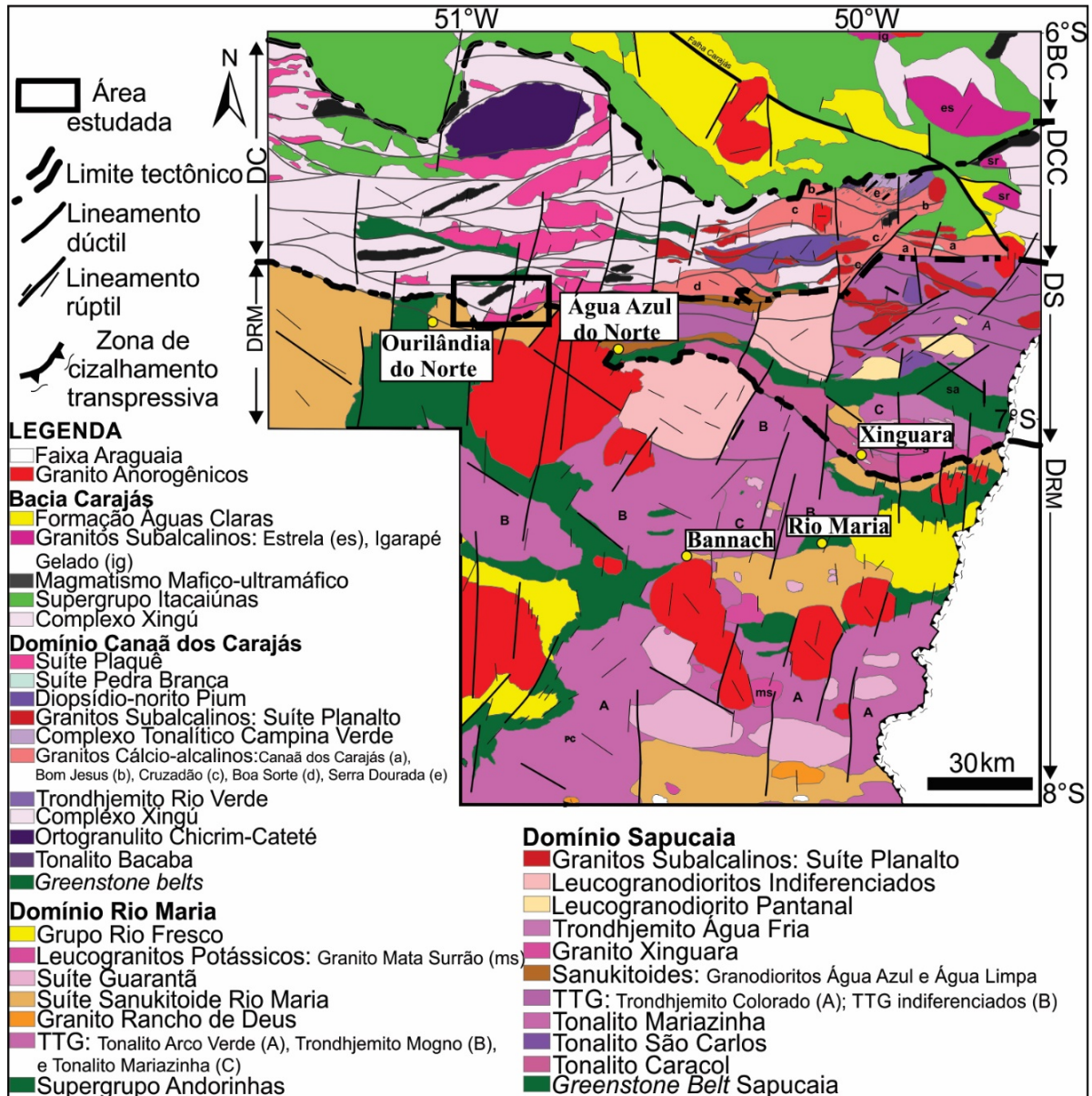
Figura 2- Mapa geológico da Província Carajás, modificado de Dall'Agnol *et al.* (2013), Feio *et al.* (2013), Oliveira *et al.* (2010), Santos *et al.* (2013), Vasquez *et al.* (2008).

1.3 JUSTIFICATIVA

A crosta arqueana da porção norte da Província de Carajás é composta predominantemente por granitos e granodioritos com subordinadas ocorrências de granitoides da série tonalito-trondhjemito-granodiorito (TTG; Feio & Dall'Agnol 2012, Gabriel & Oliveira 2014, Leite-Santos & Oliveira 2016, Silva *et al.* 2018). Embora a grande maioria desses granitoides contenha anfibólio e / ou biotita, os granitoides portadores de ortopiroxênio (série charnockítica-enderbítica) formam um componente menor, porém importante, que pode levar a uma melhor compreensão do crescimento episódico da crosta continental da Província de Carajás. No domínio Canaã dos Carajás, vários estudos identificaram ocorrências de

plutões neoarqueanos (2,73-2,76 Ga) com caráter ferroso a levemente magnesiano e afinidades com granitos do tipo A (Barros *et al.* 2009, Dall'Agnol *et al.* 2017, Feio *et al.* 2012, Marangoanha *et al.* 2019). Estes são comumente associados a rochas gabroicas (Norito Pium) e sua origem está diretamente ligada a magmas de natureza charnoquítica (Dall'Agnol *et al.* 2017, Feio *et al.* 2012). Embora importantes para explicar a evolução magmática no neoarqueano, trabalhos voltados para o estudo de rochas charnoquíticas são raros ou ausentes na província.

Trabalhos recentes desenvolvidos na região de Ourilândia do Norte descreveram uma série de granitoides indiferenciados portadores de ortopiroxênio que ocorrem como corpos intrusivos em granitoides mesoarqueanos e associados espacialmente às rochas máficas (Silva *et al.* 2018). Tais corpos ainda são desprovidos de estudos mais detalhados, necessário para entender as relações entre suas variedades petrográficas e capazes de explicar a origem e evolução de seus magmas, assim como elucidar a relação entre o magmatismo charnoquítico e as rochas neoarqueanas da Província Carajás. Desta forma, esta proposta de mestrado visa esclarecer os seguintes problemas:

(i)   Reavaliação e obtenção de novos dados de campo dos charnoquitos da área de Ourilândia do Norte;

(ii)   Ausência de classificação e individualização das variedades petrográficas das rochas sob estudo;

(iii)   Inexistência de estudos voltados para a classificação geoquímica, origem, evolução magmática e ambiente de formação;

(iv)   Ausência de estudos meso- e microestruturais e indefinição das condições de colocação do magma gerador destes plútons;

(v)   Inexistência de estudos sobre os parâmetros de cristalização e condições de formação dos magmas geradores dos charnoquitos estudados: pressão, temperatura, fugacidade de oxigênio e quantidade de água.

1.4   OBJETIVO

O objetivo geral desta dissertação visa definir a classificação, natureza e origem, assim como os processos responsáveis pela formação do magma que deu origem às rochas charnoquíticas de Ourilândia do Norte. Além destes aspectos, será apresentado uma discussão sobre os dados microestruturais destas rochas, com intuito de propor um modelo tectono-magmático para a formação e colocação deste magmatismo e colaborar para o avanço na

compreensão sobre a geologia do neoarqueano da Província Carajás. Para tanto foram atingidos os seguintes objetivos específicos:

a) Realização de análises modais e classificação e individualização dessas rochas em variedades petrográficas;

b) Reavaliação das relações de campo entre os charnoquitos e os diferentes granitoides mesoarqueanos;

c) Caracterização das microestruturas magmáticas e deformacionais observadas nessas rochas;

d) Definição de séries e tipologias magmáticas, visando compreender os possíveis ambientes de formação e os processos que controlaram a origem e evolução dos magmas geradores dessas rochas;

e) Estimar os parâmetros durante a cristalização dessas rochas (condições de fO_2, P, T e xH_2O);

f) Confecção de mapa geológico, em ambiente SIG (Sistema de Informação Geográfica), na escala de detalhe (1:50.000) dos plútons charnoquíticos;

g) Comparação das principais características dos charnoquitos de Ourilândia com ocorrências análogas tanto na Província Carajás como em outros terrenos arqueanos contribuindo para o avanço do conhecimento das afinidades petrológicas desses charnoquitos.

1.5   MATERIAL E MÉTODOS

1.5.1 Pesquisa Bibliográfica

Esta etapa constituiu no levantamento bibliográfico referente à geologia da região estudada, abrangendo uma síntese de grande parte dos dados publicados para a Província Carajás. O principal enfoque desta pesquisa está relacionado aos trabalhos mais recentes, referentes aos domínios Sapucaia, Canaã dos Carajás, além de forcar em artigos dedicados a charnoquitos. Para uma discussão mais profunda, serão utilizados artigos e livros sobre temas relacionados à geologia de terrenos arqueanos, com ênfase em rochas charnoquíticas.

1.5.2 Mapeamento Geológico

O mapeamento geológico destinado à coleta de dados deste estudo foi realizado em duas etapas, durante o desenvolvimento das dissertações de Santos (2015) e Silva (2017),

lideradas pelo Prof. Davis Carvalho de Oliveira: (i) entre 18 a 27 de outubro de 2013; e (ii) entre 23 a 25 de setembro de 2014; (iii) e de 08 a 11 de agosto de 2017.

Estes mapeamentos geraram um mapa geológico na escala 1:50.000, acompanhado de coleta sistemática de amostras (Fig. 3) para estudos petrográficos, geoquímicos e de química mineral. Para tanto, foram utilizadas imagens de satélite (Landsat7 e TM), mosaicos de radar (SRTM) e de cartas aero-radiométricas e aeromagnetométricas, e para a localização dos pontos foi utilizado aparelho GPS (*Global Position System*) com precisão de aproximadamente 3 m.

1.5.3 Petrografia

Para a realização desta etapa foi feito o exame macroscópico das amostras de rocha coletadas durante as etapas de campo, seguido do estudo em microscópio petrográfico para identificação e descrição sistemática dos minerais (Deer *et al.* 2013, Kerr 1959); estudo das texturas magmáticas, deformacionais e de alteração (Bard 1986, Hibbard 1995, MacKenzie *et al.* 1982, Passchier & Trouw 1996); obtenção de composições modais (Chayes 1956, Hutchison 1974) com contador automático de pontos da marca Swift (≤ 2.000 pontos por amostra) e classificação das rochas conforme estabelecido pela IUGS (Le Maitre 2002, Streckeisen 1976).

1.5.4 Química Mineral

O estudo de Química Mineral foi realizado através de microssonda eletrônica, no laboratório da própria UFPA (Lab. de Microanálises – IG) e a Microssonda eletrônica do Laboratório de Microssonda Eletrônica da Universidade de São Paulo, em seções pré-selecionadas de piroxênios, anfibólios, biotitas, minerais óxidos além de outros minerais acessórios. A presença de uma assembleia mineral contendo ortopiroxênio, clinopiroxênio, anfibólio, ilmenita e magnetita, faz dos charnoquitos um importante litotipo para a avalição das condições de formação do magma, tais como: pressão, temperatura e fugacidade de oxigênio (Anderson *et al.* 2008, Anderson & Smith 1995, Frost & Frost 2008, Wells 1977).

1.5.5 geoquímica

Os dados geoquímicos em rocha total das amostras NDP foram obtidos durante o desenvolvimento da dissertação de Santos (2015), e serão utilizados nessa dissertação. As análises químicas em rocha total foram realizadas no Laboratório ***Acme Analytical Laboratories Ltd***, onde obteve-se os conteúdos de elementos maiores e menores, traço e terras

raras, em amostras representativas das diferentes variedades faciológicas dos plútons. A caracterização geoquímica foi realizada com base nos procedimentos indicados em Ragland (1989) e Rollinson (1993), e a avaliação do comportamento dos elementos maiores, menores e traço foi feita por meio de diagramas de variação clássicos (Baker & Rutherford 1996, Debon & Le Fort 1983, Frost *et al.* 2001, Harker 1965, Irvine & Baragar 1971, O'Connor 1965) com o objetivo de caracterizar as rochas estudadas, identificando as suas séries magmáticas, ambiente de formação e os processos que controlaram a evolução magmática.
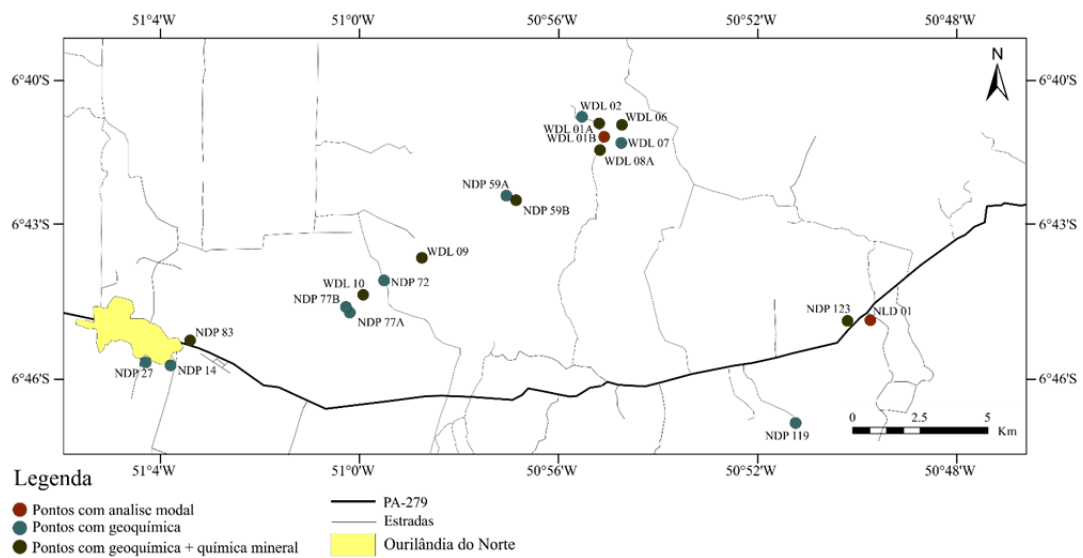
Figura 3- Mapa de amostragem referente às etapas de campo realizadas na área de Ourilâdia do Norte.

CAPÍTULO 2 Igneous charnockites from Carajás Province, southeastern Amazonian Craton (northern Brazil): petrogenetic constraints and intensive crystallization parameters

Williamy Queiroz Felix[1,2] (williamy@ufpa.br), Davis Carvalho de Oliveira[1,2] (davis@ufpa.br), Luciano Ribeiro da Silva[1,2] (lucianor@ufpa.br)

[1]Programa de Pós-Graduação em Geologia e Geoquímica (PPGG), Instituto de Geociências (IG), Universidade Federal do Pará (UFPA), Endereço, CEP-66075-110, Belém, Pará, Brasil.

[2] Grupo de Pesquisa Petrologia de Granitoides (GPPG), IG, UFPA, Brasil.

ABSTRACT: The granite-charnockite association from Carajás Province is spatially associated with gabbronorites, which intrude Mesoarchean granitoids and form a NE-SW elongated pluton with subordinate lenses E-W oriented showing subvertical (70-80°) foliation. They consist of leucocratic rocks (M' = 21.1 - 32.9) with well-preserved magmatic textures and medium- to coarse-grained. The main mafic phases are pyroxene [enstatite/ferrosilite and augite/diopside ($Wo_1En_{66}Fs_{33}$ to $Wo_{49}En_{38}Fs_{14}$)], amphibole [hornblende ($0.88 \geq Mg/(Mg+Fe^{2+}) \leq 0.43$)], and biotite [$0.68 \geq Fe/(Fe + Mg) \geq 0.31$]. These rocks are considered syntectonic plutons emplaced in a postcollisional setting, which underwent dynamic recrystallization controlled by subgrain rotation (SGR; 400-450 °C) in a sinistral transpressive deformational regime driven by pure shear. The granite-charnockite association and gabbronorite present very similar geochemical behavior: magnesian affinity [whole-rock $0.8 \geq FeOt/(FeOt+MgO) \leq 0.5$], calc-alkaline and high-K calcic-alkaline trends and metaluminous character. Magma ascent and emplacement are reconstructed as a single-stage process with decreasing temperatures. Crystallization temperatures range from 1100 to ~700 °C for pyroxenes, and 809 to 713 °C for amphiboles. Calculated crystallization pressures were 190 to 310 MPa resulting in crystallization depths of 7.0 to 10.5 km. Observed mineral assemblages and compositions of the main mafic minerals imply crystallization under relatively oxidizing conditions (NNO -9.8 to -12.6). H_2O contents ranging from 4.1 to 6.5 wt% and indicates that water played an important role in the magmatic evolution of the studied rocks. Hydration was responsible for differences in the modal contents of monzogranite varieties. Gabbronorites were probably formed by partial melting of depleted mantle source (low HFSE), and orthopyroxene-bearing granitoids originated through fractional crystallization from magma similar in composition to gabbronorite.

Keywords: Charnockite. Orthopyroxene. Crystallization Parameters. Carajás. Archean.

2.1   INTRODUCTION

The term charnockite was originally proposed for quartz-, feldspar- and orthopyroxene (usually hypersthene)-bearing igneous rocks (Holland, 1900), although it has also been applied to metamorphic rocks, making the origin of these rocks controversial (Bohlender *et al.* 1992, Frost & Frost, 2008, Howie 1955, Rajesh & Santosh 2012). The generation of anhydrous rocks can be related either to dry metamorphism (granulite facies) or to magmatic crystallization whenever $p(CO_2)$ predominates over $p(H_2O)$. To make the term charnockite less ambiguous and petrologically relevant, Frost & Frost (2008) proposed using this term only for pyroxene-bearing granitoids that have clear igneous origin.

A close relationship between hydrous and anhydrous ($aH_2O < 1$) magmatic lithotypes with different degrees of preservation of their primary igneous characteristics has been noted in different periods of Earth evolution, and the origin of this association has been attributed to distinct tectonic settings: rift-related, deeply eroded cordilleran-type plutons, Caledonian-type plutons and deep crustal melting related to granulite metamorphism (Frost & Frost 2008, Rajesh 2012). Significant contrasts in composition from ferroan to magnesian types have been identified in these rocks (Frost & Frost 2008). Orthopyroxene rocks are dominant or widely scattered in many igneous plutons and are commonly associated with pyroxene-free amphibole- and biotite-rich granitoids (e.g., Bohlender *et al.* 1992, Frost *et al.* 2000, Frost & Frost 2009), which are generally interpreted as derived from water-rich magmas compared to water-poor or anhydrous charnockitic magmas (Frost & Frost 2009, Laurent *et al.* 2014, Rapopo 2010). Although extensively distributed, orthopyroxene-bearing granitoids are rare or absent in many complexes, and the dominant rocks have amphibole and biotite as the main mafic phases (Mikhalsky *et al.* 2006). Frost & Frost (2008) considered that the hydrated varieties correspond to rocks emplaced at upper crustal levels and pyroxene granitoids to deeper levels of charnockitic plutons.

The Archean crust of northern Carajás Province is predominantly composed of granites and granodiorites with subordinate tonalite-trondhjemite-granodiorite (TTG) series (Feio & Dall'Agnol 2012, Gabriel & Oliveira 2014, Leite-Santos & Oliveira 2016, Silva *et al.* 2018). Although the vast majority of these granitoids contain amphibole and/or biotite, orthopyroxene-bearing granitoids (charnockite-enderbite series) form a minor but important component that may lead to a better understanding of the episodic continental growth of Carajás Province crust. In the Canaã dos Carajás domain, several studies have identified occurrences of Neoarchean (2.73–2.76 Ga) plutons having ferroan to slightly magnesian

characters and A-type granites affinity (Barros *et al.* 2009, Dall'Agnol *et al.* 2017, Feio *et al.* 2012). They are commonly associated with gabbroic rocks and emplaced along anastomosing high-strain shear zones, concordant with the dominant E–W regional trend (Marangoanha *et al.* 2019). Their origin has been associated with partial melting of mafic to intermediate lower crustal rocks (Feio *et al.* 2012). All these Neoarchean granite units have amphibole and biotite as the main mafic phases, contain rare relicts of clinopyroxene and are devoid of orthopyroxene (e.g., Feio *et al.* 2012, Marangoanha *et al.* 2019). Although comparatively rarer in Carajás Province, Neoarchean granitoids of sodic affinity have also been described. This group of granitoids is exposed in the Canaã dos Carajás domain as small stocks intrusive in the Mesoarchean basement and spatially associated with noritic, quartz-noritic (Pium norite) and biotite-hornblende granite (Planalto and Vila União suites) rocks. The tonalitic-trondhjemitic association (Pedra Branca trondhjemite) and orthopyroxene-bearing trondhjemite (enderbite from the Ouro Verde area) differ from the TTG units by their higher Zr and lower Rb contents (Feio *et al.* 2012, Marangoanha 2018). The Planalto and Vila Jussara suites are closely associated with charnockites rocks and have been interpreted as corresponding to hydrated charnockitic/granitic intrusions emplaced at high crustal levels (Cunha *et al.* 2016, Dall'Agnol *et al.* 2017, Feio *et al.* 2012).

The Ourilândia do Norte area, located in the central-west portion of Carajás Province (straddling the border between the Rio Maria and Carajás domains), is predominantly formed by 2.87 Ga Mesoarchean plutons of sanukitoid affinity, leucogranites, and younger intrusions of clinopyroxene-bearing granitoids (Santos & Oliveira 2016). As a result of the present study, geological mapping performed in this area allows us to identify different lithologic types among the pyroxene-bearing plutons, which are akin to the charnockite-enderbite series and differ from typical hornblende-biotite granites. Although not yet dated, these rocks may be correlated to postorogenic Neoarchean plutonic structures. Although several recent papers have proposed origin for the Neoarchean magmatism in Carajás Province, petrogenetic information concerning the charnockites sensu lato and the associated mafic rocks is lacking. Accordingly, the present paper introduces a set of new data with information about the mineralogical, deformational and geochemical characteristics of these peculiar Neoarchean pyroxene-bearing granitoids and compares them with similar occurrences. In addition, we estimate the formation conditions of the charnockitic rocks and their petrogenetic link with the plutons containing primary hydrous assemblage. New mineral chemical data are presented and discussed in order to determine the intensive parameters of crystallization (P, T, and fO_2), which control orthopyroxene stability in acidic magmas, making charnockite granitoids a very

powerful tool to study crystallization parameters (Carroll & Wyllie 1990, Frost *et al.* 2000, Frost & Frost 2008, Naney 1983; Patiño Douce 1996).

2.2   GEOLOGICAL SETTING

The Amazonian Craton occupies the northern part of the South American platform (Fig. 1a) and has been separated into several provinces based on their distinct ages, structural patterns and geodynamic evolution (Fig. 1b; Tassinari & Macambira 2004). The Archean nucleus preserved in the southeastern sector of the craton is denominated Carajás Province (Fig. 1b, c), in which two distinct tectonic domains are distinguished (Dall'Agnol *et al.* 2006, Santos 2003, Souza *et al.* 1996). The older domain lies in the southern part and is known as the Mesoarchean (3.0-2.87 Ga) Rio Maria domain (Dall'Agnol *et al.* 2013, 2006, Feio *et al.* 2013, Vasquez *et al.* 2008), while the northern part of the province is represented by the Carajás domain, which consists of extensive Mesoarchean crust affected by Neoarchean events (3.0-2.73 Ga; Barros *et al.* 2009, Feio *et al.* 2013, Marangoanha *et al.* 2019, Dall'Agnol *et al.* 2006). According to the most recent geologic framework established by Dall'Agnol *et al.* (2013), the Carajás domain can be divided into two subdomains separated by ductile transcurrent shear zones: Sapucaia and Canaã dos Carajás (Fig. 1c). These authors consider the latter to be the basement of the Carajás basin (Fig. 1d), which is composed of 2.76–2.55 Ga metavolcanic rocks and banded iron formations belonging to the Itacaiúnas supergroup and subalkaline granitoids represented by the Igarapé Gelado, Estrela and Serra do Rabo granites (~2.76–2.73 Ga, (Barros *et al.* 2009, Sardinha *et al.* 2006).

The Rio Maria domain has been considered by different authors as a classic Archean juvenile terrane composed of greenstone belts (2.97 Ga, Souza *et al.* 2001) and a variety of Archean granitoids: (1) older TTG series (2.98–2.93 Ga, Almeida *et al.* 2011, Althoff *et al.* 2000), (2) younger TTG series (2.87–2.86 Ga, Almeida *et al.* 2011, Leite *et al.* 2004); (3) Rio Maria sanukitoid suite (2.87 Ga; Oliveira *et al.* 2009); and (4) high Ba- and Sr-bearing leucogranodiorite-granite suite and high-K calc-alkaline leucogranites (2.87–2.86 Ga; Almeida *et al.* 2013, 2010). The Sapucaia domain (~3.0–2.73 Ga) shows strong lithological similarity to the Rio Maria domain (Gabriel and Oliveira 2014, Leite-Santos & Oliveira 2016, Santos *et al.* 2013, Silva *et al.* 2018). However, the rocks of the Sapucaia domain were intensely affected by Neoarchean events, represented by deformed A-type granitoids (Dall'Agnol *et al.* 2017). The Canaã dos Carajás domain (3.0–2.72 Ga) is marked by widespread Mesoarchean granitic magmatism associated with Neoarchean granites, quartz norites and charnockitic rocks, as well as sodic granitoids (Pedra Branca trondhjemite) and A-

type granites of the Planalto, Vila União and Vila Jussara suites (Feio *et al.* 2013, 2012, Marangoanha *et al.* 2019, Oliveira *et al.* 2018, Santos *et al.* 2013). The ultramafic rocks include large layered intrusions hosting lateritic Ni deposits, e.g., the Serra da Onça complex (2.76 Ga; Lafon *et al.* 2000), Luanga complex (2.763 Ga; Machado *et al.* 1991), and Lago Grande layered complex (2.72 Ga; Teixeira *et al.* 2015).

Figure 1- **a)** South American platform with the Amazonian Craton highlighted (Almeida *et al.* 1981); **b)** Amazonian Craton geochronological provinces (Tassinari & Macambira 2004); **c)** Carajás Province subdivision proposed by Dall'Agnol *et al.* (2013); **d)** detailed geological map of Canaã dos Carajás and Sapucaia domains (modified from Dall'Agnol *et al.* (2013), Feio *et al.* (2013), Oliveira *et al.* (2010), Santos *et al.* (2013), Vasquez *et al.* (2008); **e)** map showing the Ourilândia do Norte area and the studied rocks.

2.3   GENERAL ASPECTS OF THE CHARNOCKITE ASSOCIATION

In this section, we present a map on a semi-detailed scale (~1:50.000), and new geological, meso-microscopic petrographic, and quantitative modal composition data. Microscopic observations were concentrated on 19 thin sections whose mineralogical and microstructural aspects were analyzed. The quantitative analysis was made using a Stageledge automatic point counter (2000 points counted with the Endeeper Hardledge software), and the results were plotted in suitable diagrams, according to the International Union of Geological Sciences – IUGS (Le maitre 2002; Fig. 2).

2.3.1   Geology

The geological map shows that the pyroxene-bearing granitoids comprise four NE-SW to E-W elongated lenticular stocks (Fig. 1e). The main granitoid pluton in the central portion of the map has length and width of ~12.5 km and ~2.5 km, respectively. This pluton intrudes Mesoarchean leucogranites, shows granodioritic and monzogranitic compositions and is spatially associated with mafic intrusions. The three smaller bodies are formed by monzogranites with E-W elongated/lenticular shapes having lengths of ~3-4 km and widths < 2 km. In general, all studied bodies show a planar fabric defined by a NE-SW to E-W trend and steep dip (70-85°), which is consistent with trends imprinted during the development of regional shear zones.

2.3.2   Classification and textural aspects

Based on their modal composition (see Table 1; Fig. 2), the studied rocks can be classified as gabbronorites (mafic member) and granitoids, among the studied granitoids, three distinct petrographical facies are identified: (i) orthopyroxene granodiorite, (ii) clinopyroxene monzogranite, and (iii) amphibole monzogranite; the granitoids make up the granite-charnockite association. The existence of several representative outcrops in a NE-SW direction allows the delimitation of gabbronorite as an intrusion that occupies the northern portion of the main pluton (Fig. 3a and Fig. 1e). These rocks are dark gray, usually leuco- to mesocratic (M' ~ 30.3%) and fine to medium grained (1-5 mm). In the sample identified as quartz gabbro (WDL-07), the presence of equant aggregates (up to 1 cm) of anhedral and late-stage quartz immersed in a fine-grained matrix is remarkable (Fig. 3b). Olivine occurs as an accessory mineral in most samples, but it is eventually a varietal phase (>5%) in the olivine gabbronorites (sample WDL-06; Table 1; Fig. 3c). Granophyric intergrowths involving quartz and alkali feldspar occur near the rim of a zoned plagioclase crystal (Fig. 3d). Clinopyroxene

commonly occurs as reaction rims around olivine and orthopyroxene (Fig. 3e-g). All studied rocks contain coexisting clino- and orthopyroxenes with exsolution textures; host orthopyroxene crystals contain large clinopyroxene lamellae, which in turn exsolve into thin lamellae of orthopyroxene due to subsolidus re-equilibration. Such lamellae occur as intergrowths that display parallel and herringbone textures (Fig. 3f).

The granite-charnockite association comprises leucocratic rocks (22≥M'≤ 30%; Table 1 and Fig. 2), medium dark greenish- to pinkish-gray (Fig. 4a and b), in which the feldspars are 2.5 mm in size. They are medium to coarse grained (1-5 mm), with hypidiomorphic, equigranular and occasionally porphyritic texture. The granodiorites are slightly more impoverished in ferromagnesian minerals than the mafic rocks; orthopyroxene remains a common phase, and olivine is absent (Fig. 4c-e). Although the monzogranites show ferromagnesian minerals contents similar to those of the other varieties, orthopyroxene is rare or absent and the amphibole/clinopyroxene ratio is highly variable among these rocks (Table 1); clinopyroxene is recognized as a trace mineral (<1%) in the amphibole-enriched monzogranite, although it is present in the clinopyroxene-bearing monzogranite as the main ferromagnesian phase (up to 20%; Fig. 4e). The widespread replacement of anhydrous by hydrous minerals is commonly observed in monzogranites, where pyroxene is preserved as a relict core within amphibole (corona texture) in the more evolved varieties (Fig. 4f and g). The amphibole monzogranite facies shows some differences in felsic and accessory minerals contents and in the deformational history from the other facies.

Plagioclase shows moderate to intense saussuritization, and deformational structures are more intense and better represented by microfractures filled up by quartz and alkali feldspar (Fig. 4i). The primary quartz (Qtz_1) occurs with hypidiomorphic faces and generally shows core-mantle microstructures (Fig. 4j and k); the mantle is represented by aggregates of recrystallized quartz crystals (Qtz_2; Fig. 4k); Qtz_3 occurs as xenomorphic crystals in association with alkali feldspar forming granophyric texture (Fig. 3b and d); and Qtz_4 consists of fine-grained inclusions associated with amphibole destabilization (Fig. 4g). K-feldspar shows a bimodal grain size distribution pattern: Kfs_1 is hypidiomorphic with a perthitic texture; Kfs_2 is xenomorphic and, together with Qtz_3, forms a granophyric texture (Fig. 3d); and Kfs_3 is the product of the deformation that affected monzogranites and is associated with Qtz_2 (Fig. 4j and k).

Magmatic epidote is present as idiomorphic crystals with zoned allanite cores and partially enclosed by biotite and hornblende. Apatite and zircon have been observed as inclusions in feldspar and mafic minerals. Fe-Ti oxide minerals are magnetite and ilmenite

and generally occur associated with mafic mineral aggregates, where titanite forms continuous rims around ilmenite (Fig. 4h).

Table 1- Modal composition of the studied rocks from Ourilândia do Norte.

Rock type	Gabbronorite				Granite-charnockite association															
					Opx-Granodiorite				Cpx-Monzogranite						Amp-Monzogranite				
Sample	WDL	WDL	WDL	WDL	WDL	WDL	WDL	WDL	WDL	NDP	NDP	WDL	NDP	NDP	NDP	NLD	NDP	NDP	NDP
Minerals	06	07	08B	08A	01B	01A	09	02	10	77B	77A	59A	59B	72	119	01	123	27	83
Quartz	2.1	4.7	9.1	11.2	15.8	17.2	19.7	20.9	20.9	23.9	25.7	28.9	29.2	30.1	28.2	28.5	30.0	30.6	33.8
Alkali-feldspar	-	2.3	6.4	1.5	10.5	6.1	5.8	12.3	22.5	19.5	19.9	16.7	17.5	10.8	14.9	27.3	14.6	20.3	18.1
Plagioclase	66.6	65.1	56.0	54.5	51.7	48.0	48.8	46.4	31.4	28.8	29.0	32.6	28.2	30.9	25.1	22.4	25.6	20.8	21.0
Amphibole	7.6	4.1	2.3	6.9	9.5	6.5	10.2	9.5	3.3	7.6	2.6	4.7	3.2	3.3	26.9	19.0	26.5	21.0	22.2
Orthopyroxene	4.0	10.9	5.8	7.4	3.9	9.2	3.4	3.4	0.7	-	-	-	-	-	-	-	-	-	-
Clinopyroxene	12.9	11.0	17.2	16.6	5.4	10.4	9.2	4.8	16.7	16.1	19.0	14.7	18.3	20.7	Tr	Tr	0.5	0.9	1.1
Olivine	5.8	0.5	1.4	Tr	-	-	-	-	-	-	-	-	-	-	-	-	-	-	-
Biotite	1.0	1.0	1.2	1.3	1.9	1.3	1.6	1.5	3.3	2.6	2.9	1.2	2.6	4.0	3.4	1.1	1.0	6.4	2.4
Titanite	-	-	-	-	-	-	-	-	-	-	-	-	-	-	0.8	1.2	1.1	Tr	0.5
Opaques	0.2	0.7	0.8	0.8	1.4	1.5	1.5	1.2	1.0	1.8	0.9	1.5	1.0	0.2	-	0.3	-	-	0.3
Epidote	-	-	-	-	-	-	-	-	0.3	-	-	-	Tr	-	0.6	0.4	0.7	-	0.6
Mafic	31.4	28.0	28.6	32.9	22.0	28.7	25.8	20.3	25.1	28.0	25.4	22.0	25.1	28.2	30.3	20.3	28.0	28.3	25.0
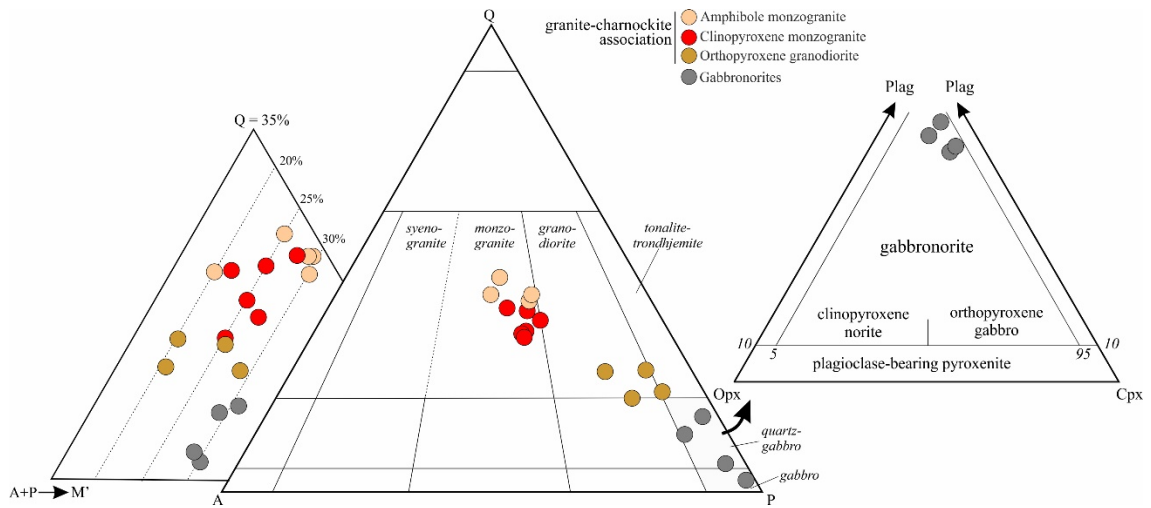
Figure 2- Q-A-P, Q-(A+P)-M and Opx-Cpx-Plg plots for the studied rocks from Ourilândia do Norte, after (Le Maitre 2002).
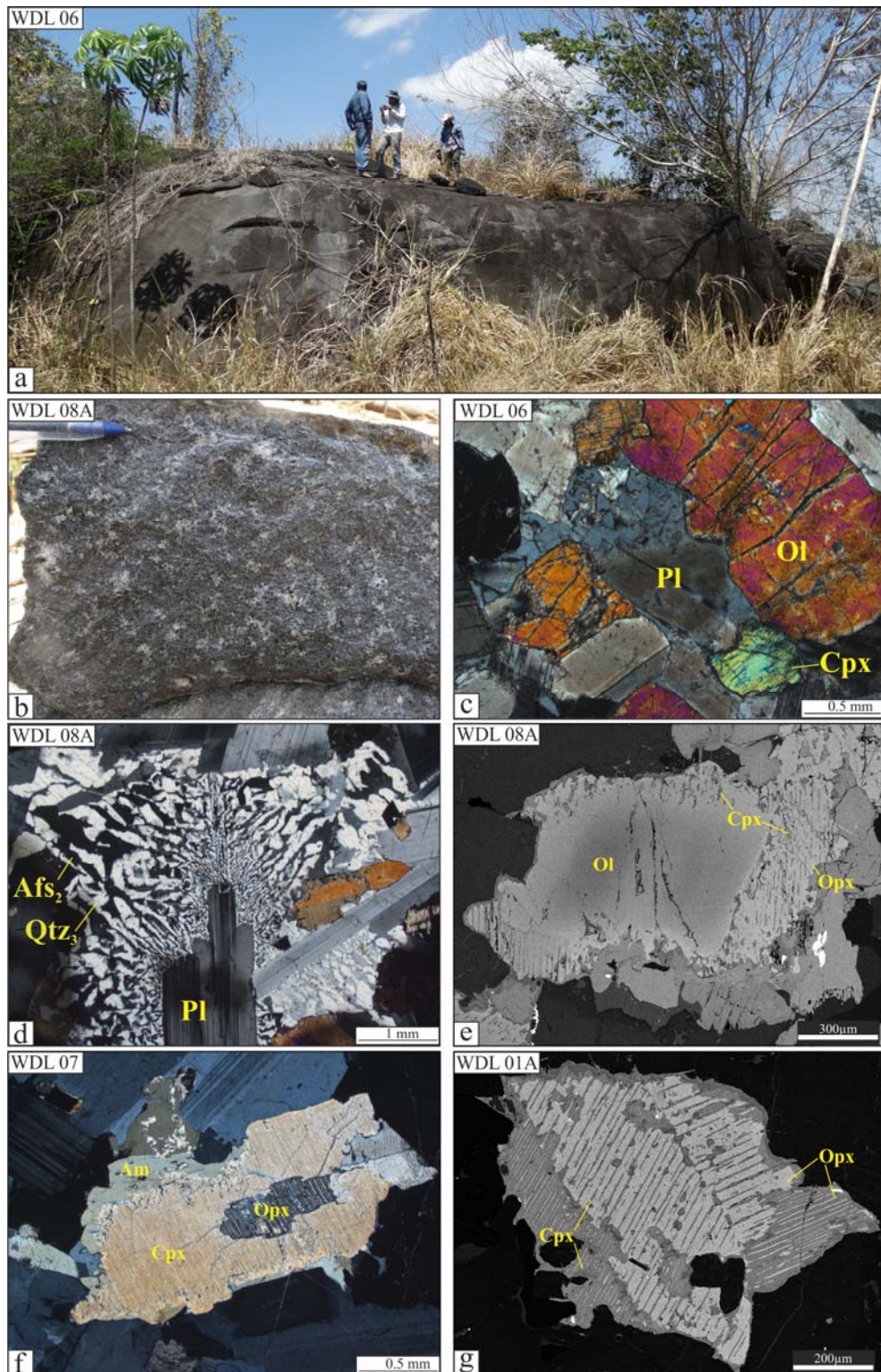
Figure 3- Textural aspects of gabbronorites associated with the granite-charnockite association from Ourilândia do Norte; **a)** field aspect of the gabbronorite; **b)** gabbronorite rich in quartz; **c)** olivine, clinopyroxene and plagioclase forming intergranular texture in the gabbronorite; **d)** granophyric texture formed by **Pl₁** surrounded by **Qtz₃** and **Afs₂**; **e)** olivine crystal with reaction rim (exsolution lamellae) surrounded successively by clinopyroxene and orthopyroxene; **f and g)** orthopyroxene showing exsolution of clinopyroxene (herringbone textures) cored by clinopyroxene with orthopyroxene exsolution.
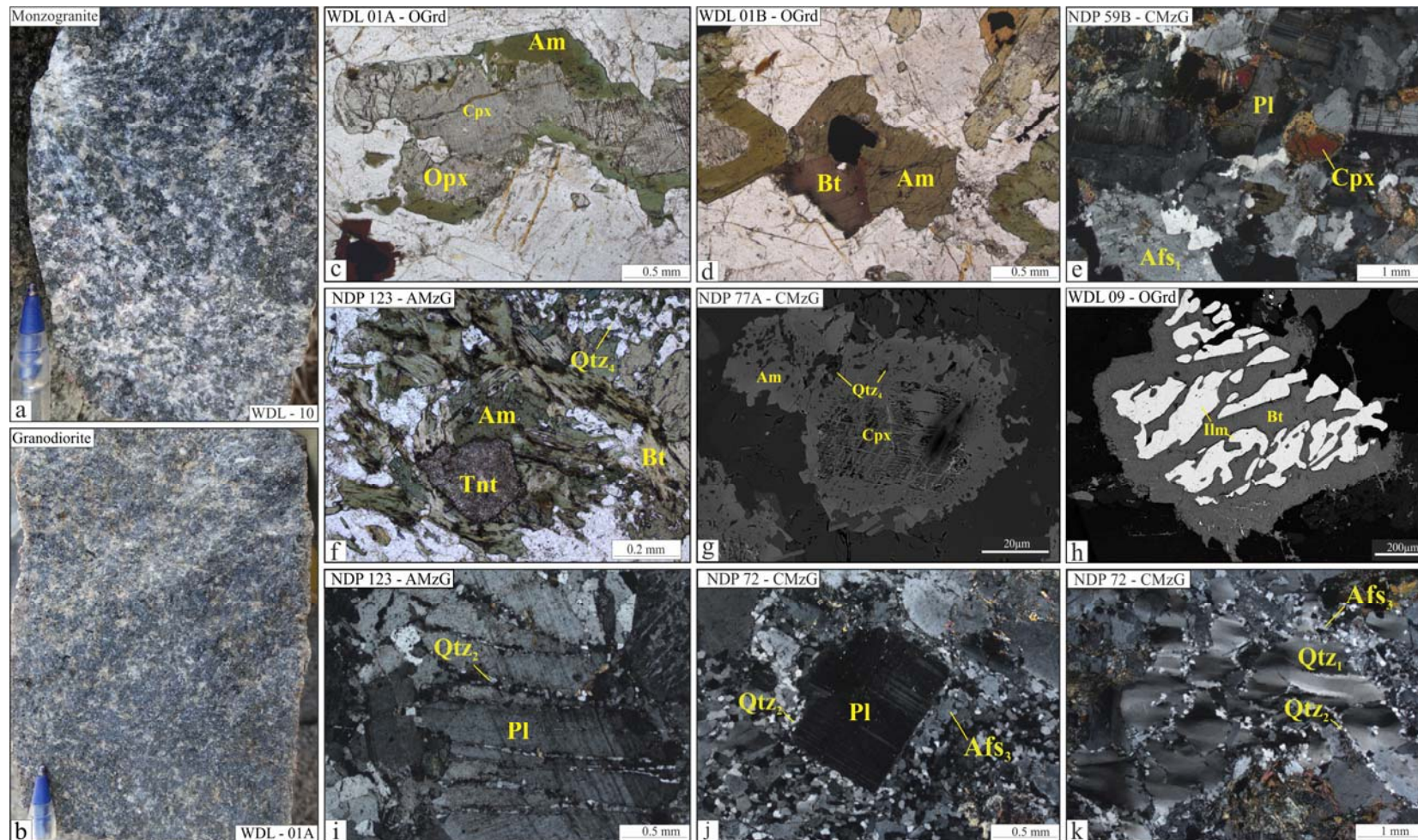
Figure 4- Textural aspects of the granite-charnockite association from Ourilândia do Norte: **a)** clinopyroxene monzogranite; **b)** orthopyroxene granodiorite; **c)** clinopyroxene partially transformed into **Am; d)** clinopyroxene partially transformed into amphibole with straight boundaries between **Am** and **Bt; e)** well-preserved hypidiomorphic texture in the clipyroxene monzogranite; **f)** mafic cluster of titanite and amphibole with straight boundaries; **g)** clinopyroxene partially transformed into **Am** and producing Qtz_4; **h)** resorbed and ragged ilmenite inclusions in biotite; **i)** subhedral plagioclase displaying intragranular microfractures filled by quartz, indicating deformation in the presence of melt; **j)** core-mantle texture characterized by plagioclase porphyroclast bordered by quartz, plagioclase and alkali feldspar; **k)** recrystallized quartz showing core-mantle texture formed by Qtz_1 int the core mantled by Qtz_2.

2.4   GEOCHEMISTRY

Based on field and petrographic criteria, the granite-charnockite association and gabbronorite are assigned to four facies (Table 1). The geochemical data of the granite-charnockite association and mafic rocks from Ourilândia do Norte, summarized in Table 2, comprise 16 whole-rock chemical analyses for the most representative samples of each group identified as follow: 3 samples of gabbronorites; 3 specimens of orthopyroxene-bearing granodiorite; and 10 samples of granite – 5 of clinopyroxene-bearing monzogranite and 5 of amphibole-bearing monzogranite. The SiO_2 content in the analyzed samples ranges from 55.6 - 64.7 wt%; the granite-charnockite association shows a range between 59.9 and 64.6 wt%, and the mafic rocks vary from 55.6 to 56.7 wt%. Harker variation diagrams of selected major and trace elements for the different varieties show that granitoids are more enriched in large ion lithophile elements (LILEs; Rb, K and Ba, except Sr) and high field strength elements (HFSEs; Zr, Y and Ti) and more impoverished in mantle rock-forming elements (Mg, Fe, Ca and Al) than gabbronorites (Fig. 5 and Table 2). The monzogranite samples are clearly more evolved than the granodiorites and, consequently, than the gabbronorites, for which overall negative correlations are observed for compatible elements [Al_2O_3 (16.9 – 13.4 wt%), CaO (9.8 – 3.9 wt%), Fe_2O_3t (9.8 – 7.2 wt%), MgO (6.7 - 1.9 wt%), Mg# (60 - 30) and Sr (355 - 205 ppm)] with increasing SiO_2 through colinear trends (Fig. 5 and Table 2). Positive correlations can be observed between SiO_2 and TiO_2 (0.3 – 0.7 wt%), K_2O (0.7 – 3.6 wt%), Rb (26 - 107.4 ppm), Ba (255 -798 ppm), Zr (42.0 – 155.3 ppm) and Y (7.0 – 21.5 ppm) (Fig. 5 and Table 2). The high Rb/Zr ratios (> 0.5) recorded in these rocks do not show a clear correlation with SiO_2 (Fig. 5h). Collinearity showed in these rocks could indicate cogeneticity between their magmas.

Analytical data of rare earth elements (REEs) are normalized using the values of (Evensen *et al.* 1978). Despite the petrographical differences, REE and multielement behavior of the studied rocks are quite similar (Fig. 6a and b). In general, the granite-charnockite association shows light REEs contents slightly higher than those of heavy REE, with variations in the La/Yb ratio between 8.2 and 13.5. Gabbronorites exhibit the same pattern, although they are more fractionated in REE. The granite-charnockite association has discrete negative Eu anomalies (Eu/Eu* 0.6 – 0.9), while in gabbronorites, these anomalies are absent or positive (Eu/Eu* 0.8 – 1.2). In the mantle-normalized multielemental diagram, the studied rocks display LILE-enriched patterns (Rb, Ba, Sr and K). The granitoids show discrete negative Nb, P and Ti anomalies compared to the accentuated anomalies in the gabbronorites,

which are also relatively more depleted in HFSEs and show dissimilar patterns in both REE and multielemental diagrams compared with other Neoarchean suites (Fig. 6c, d) that are enriched in HFSE.

Table 2- Geochemical analyses of pyroxene-bearing rocks from Ourilândia do Norte. Major (wt%) and trace elements (ppm).

	Pyroxene Bearing Rocks From Ourilândia do Norte															
Facies	Gabbronorites			Opx Granodiorite			Cpx Monzogranite					Amp Monzogranite				
Sample	WDL 6	WDL 7	WDL 08A	WDL 01A	WDL 9	WDL 2	NDP 59A	NDP 59B	NDP 77A	NDP 77B	NDP 72	NDP 123	NDP 27	NDP 14	NDP 83	NDP 119
SiO_2	55.6	56.7	57.2	59.8	61.5	64.3	63.6	63.6	64.0	64.2	64.7	62.4	63.9	64.2	64.3	64.6
TiO_2	0.3	0.4	0.4	0.7	0.6	0.6	0.6	0.6	0.6	0.6	0.6	0.7	0.6	0.6	0.6	0.6
Al_2O_3	17.0	15.6	15.4	14.2	15.0	14.1	13.9	13.7	13.8	14.0	13.9	13.7	13.4	13.6	13.9	13.6
FeOt	7.1	7.9	7.2	8.8	7.3	6.8	7.0	6.9	6.8	6.5	6.4	8.1	6.9	6.8	6.5	6.5
MnO	0.2	0.2	0.1	0.1	0.1	0.1	0.1	0.1	0.1	0.1	0.1	0.1	0.1	0.1	0.1	0.1
MgO	6.7	4.8	4.8	3.3	2.9	2.4	2.5	2.5	2.3	2.3	2.3	2.2	2.1	1.9	2.3	2.0
CaO	9.7	8.5	8.4	6.8	6.1	5.0	4.5	4.8	4.6	4.7	4.5	4.8	3.9	4.3	4.6	4.3
Na_2O	2.8	3.1	3.1	3.2	3.3	3.5	3.7	3.4	3.4	3.5	3.7	3.2	3.1	3.6	3.6	3.2
K_2O	0.7	1.1	1.2	1.8	2.1	2.2	2.2	2.3	2.5	2.5	2.6	2.5	3.6	2.8	2.4	2.9
P_2O_5	0.0	0.1	0.1	0.1	0.1	0.2	0.1	0.1	0.1	0.1	0.1	0.1	0.2	0.1	0.1	0.1
Total	100.8	99.2	98.6	99.8	99.7	99.9	98.9	98.9	98.9	99.3	99.7	98.7	98.5	98.6	99.0	98.8
Ba	255.0	421.0	465.0	578.0	623.0	789.0	621.0	760.0	698.0	805.0	706.0	869.0	1207.0	854.0	737.0	798.0
Rb	26.0	47.3	53.9	79.2	98.9	91.8	68.6	92.2	103.6	97.4	96.0	68.8	102.8	107.4	93.4	105.5
Sr	355.0	370.0	333.0	311.0	316.0	319.0	281.2	298.4	263.4	267.1	269.2	205.1	206.1	267.6	300.8	239.5
Th	2.3	3.9	4.6	7.2	8.0	8.3	10.9	8.0	9.4	9.5	9.6	8.3	7.9	9.4	9.8	11.5
Hf	1.2	1.8	2.2	3.5	3.2	3.6	3.3	2.5	3.1	3.8	2.9	3.7	2.8	4.3	4.1	4.4
Zr	42.0	64.0	86.0	130.0	116.0	133.0	118.5	108.0	121.0	136.1	105.0	131.6	103.9	152.9	155.3	152.3
Nb	1.7	2.9	3.2	5.2	5.7	6.3	5.9	5.9	6.4	6.3	6.3	6.8	6.5	6.2	6.2	6.5
Ta	0.2	0.3	0.4	0.5	0.6	0.7	0.7	0.6	0.8	0.8	1.0	1.2	0.8	1.0	0.9	0.7
Y	7.0	12.0	12.2	16.7	13.9	21.1	14.4	13.6	15.2	14.9	12.6	18.7	15.0	21.5	15.0	15.8
Ni	121.0	80.0	83.0	36.0	33.0	46.0	51.0	32.0	31.0	30.0	25.0	31.0	37.0	22.0	28.0	31.0
La	8.4	15.1	17.7	23.4	23.7	31.7	25.1	26.2	26.9	24.0	25.7	31.2	26.6	31.6	28.9	31.6
Ce	15.3	28.1	32.6	44.1	44.4	53.1	49.1	49.1	48.4	49.2	50.1	52.9	50.1	50.1	56.1	54.4
Pr	1.7	3.2	3.6	5.0	4.8	6.5	5.1	5.5	5.4	5.2	5.4	6.3	5.2	6.4	6.0	6.3
Nd	6.4	11.9	12.9	17.6	17.3	23.9	17.8	19.6	18.9	17.7	18.5	21.6	20.1	24.6	22.2	22.0
Sm	1.2	2.4	2.7	3.3	3.1	4.6	3.3	3.1	3.1	3.4	3.4	3.9	3.6	4.3	3.7	4.1
Eu	0.5	0.7	0.6	0.8	0.8	1.1	0.9	0.9	0.8	0.8	0.7	1.0	1.0	1.1	0.7	0.8
Gd	1.2	2.0	2.1	2.8	2.6	3.9	3.0	3.0	3.3	3.1	3.1	3.8	3.3	3.8	3.3	3.6
Tb	0.2	0.3	0.3	0.5	0.4	0.6	0.5	0.5	0.5	0.5	0.5	0.6	0.5	0.6	0.5	0.5
Dy	1.2	2.1	2.0	2.7	2.4	3.4	2.5	2.8	2.6	2.7	2.5	3.4	3.1	3.3	2.7	3.1
Ho	0.2	0.4	0.4	0.6	0.5	0.7	0.5	0.6	0.6	0.5	0.5	0.7	0.6	0.8	0.5	0.6
Er	0.7	1.2	1.2	1.7	1.5	2.1	1.5	1.4	1.6	1.4	1.5	2.0	1.6	1.9	1.5	1.6
Tm	0.1	0.2	0.2	0.3	0.2	0.3	0.2	0.2	0.3	0.3	0.2	0.3	0.2	0.3	0.2	0.3
Yb	0.7	1.2	1.2	1.6	1.3	1.9	1.5	1.4	1.5	1.4	1.4	1.8	1.6	2.0	1.4	1.7
Lu	0.1	0.2	0.2	0.3	0.2	0.3	0.2	0.2	0.2	0.3	0.2	0.3	0.2	0.3	0.2	0.2
FeO*	0.5	0.6	0.6	0.7	0.7	0.7	0.7	0.7	0.8	0.7	0.7	0.8	0.8	0.8	0.7	0.8
FeOt/MgO	1.0	1.6	1.5	2.7	2.5	2.9	2.8	2.7	2.9	2.9	2.9	3.7	3.3	3.6	2.8	3.3
$TiO_2+P_2O_5$	0.3	0.5	0.5	0.8	0.7	0.8	0.7	0.7	0.7	0.7	0.7	0.8	0.7	0.7	0.7	0.7
Zr+Nb+Ce+Y	66.0	107.0	134.0	196.0	180.0	213.5	187.9	176.6	191.0	206.5	174.0	210.0	175.5	230.7	232.6	229.0
Zr+Y	49.0	76.0	98.2	146.7	129.9	154.1	132.9	121.6	136.2	151.0	117.6	150.3	118.9	174.4	170.3	168.1
Sr/Y	50.7	30.8	27.3	18.6	22.7	15.1	19.5	21.9	17.3	17.9	21.3	10.9	13.7	12.4	20.0	15.1
#Mg	0.6	0.5	0.5	0.4	0.4	0.4	0.4	0.4	0.4	0.4	0.4	0.3	0.4	0.3	0.4	0.4
A/NK	3.2	2.5	2.4	2.0	1.9	1.7	1.6	1.7	1.7	1.6	1.6	1.7	1.5	1.5	1.6	1.6
A/CNK	0.7	0.7	0.7	0.7	0.8	0.8	1.6	1.7	1.7	1.7	1.6	1.7	1.5	1.5	1.6	1.6
MALI	-6.2	-4.3	-4.7	-1.8	-0.7	0.8	1.4	0.9	1.3	1.3	1.7	0.9	2.9	2.1	1.4	1.8
La/YbN	8.2	8.6	10.1	9.6	12.2	11.3	11.5	12.6	12.0	11.2	12.1	11.7	11.3	10.9	13.5	12.8
Eu/Eu#	1.2	0.9	0.8	0.8	0.8	0.8	0.9	0.9	0.7	0.7	0.7	0.8	0.9	0.8	0.6	0.6

Abbreviations: Mg# = $Mg^{2+}/(Mg^{2+}Fe)$ molecular ratio; (Eu/Eu)# = $Eu_N/((Sm_N+Gd_N)/2)$; A/CNK = $Al_2O_3/(CaO+Na_2O+K_2O)$ molar ratios; A/NK = $Al_2O_3/(Na_2O+K_2O)$ molar ration; FeO*= FeOt/(FeOt+MgO); MALI = Na_2O+K_2O-CaO. Major and minor element analyses were performed using inductively coupled plasma atomic emission spectrometry (ICP-AES), and trace elements were analyzed by ICP mass spectrometry (ICP-MS). Detailed analytical procedures are available on the laboratory websites (www.acmelab.com and www.alsglobal.com).
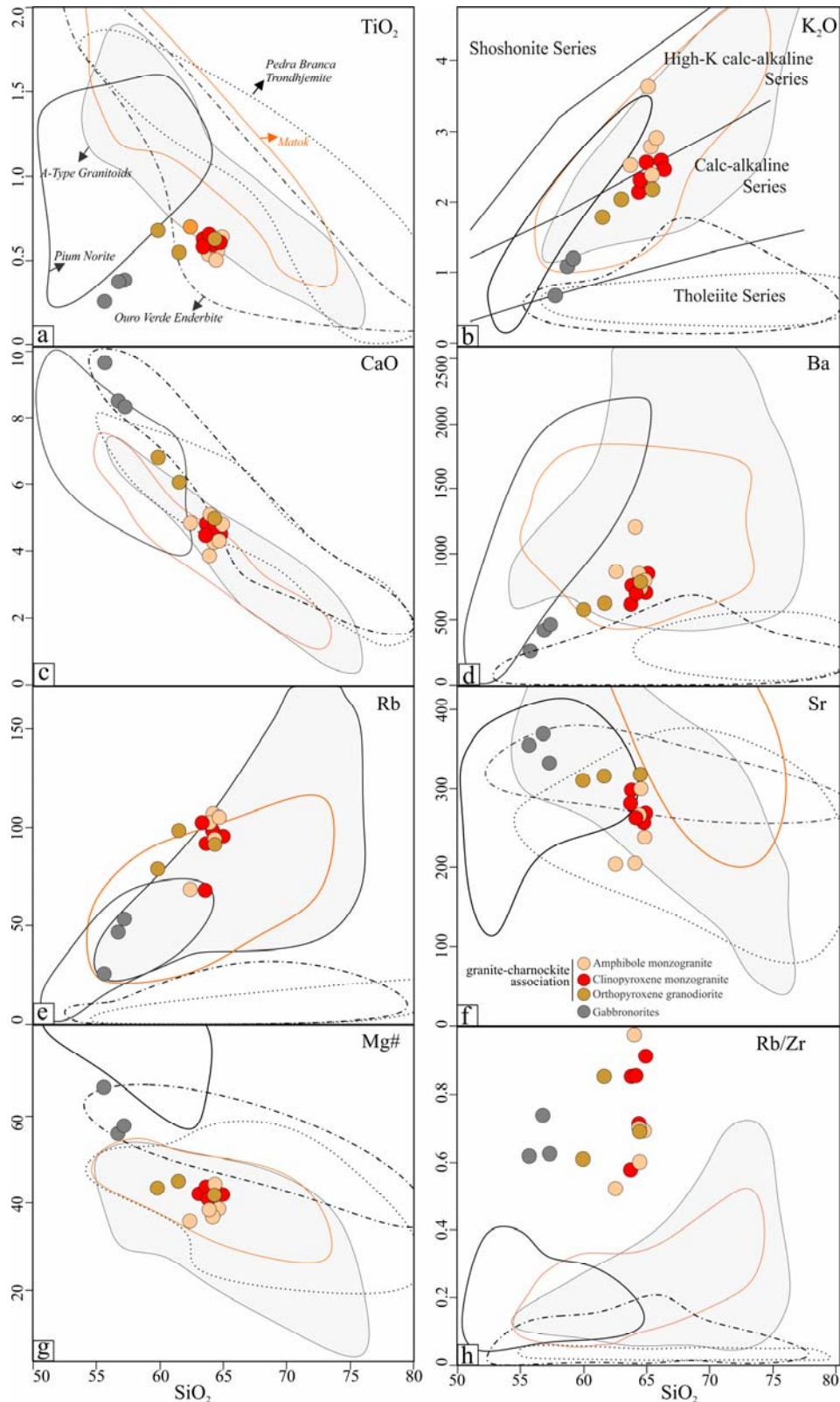
Figure 5- Major and minor element Harker diagrams (in wt%) of the studied rocks compared with Neoarchean A-type granitoids (Dall'Agnol *et al.* 2017, Feio *et al.* 2012, Marangoanha *et al.* 2019, Oliveira *et al.* 2018), charnockite from the Ouro Verde area (Maragoanha 2018), Pium diopside norite (Santos *et al.* 2013), Pedra Branca trondhjemite (Feio *et al.* 2013, Gomes & Dall'Agnol 2007), and charnockites from Matok pluton (Bohlender 1992).
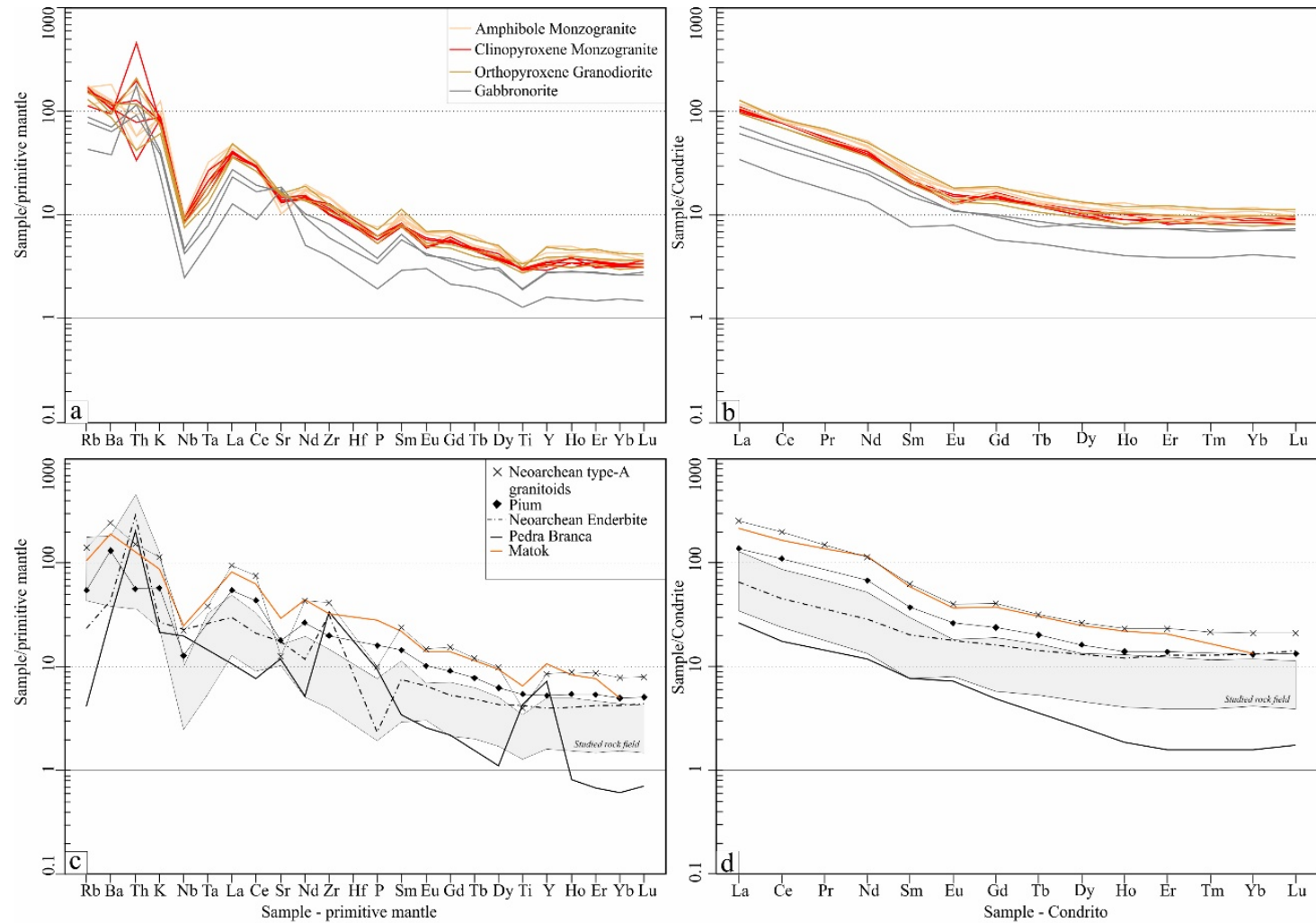
Figure 6- Rare earth element and multielement patterns of the studied rocks: **(a)** diagrams showing REE and **(b)** multielements of the pyroxene-bearing rocks from Ourilândia do Norte; **c)** and **d)** diagrams showing the field (in gray) for pyroxene-bearing rocks from Ourilândia do Norte and average from Neoarchean suites. Chondrite normalization values are from Evensen et al. (1978), and primitive mantle normalization values are from McDonough and Sun (1995).

2.4.1 Classification and Magmatic Series

Another way to identify and separate intrusive rocks in this investigation is to use established chemical classification and discrimination diagrams for the characterization of different rock groups. Most of the granitoids included in the granite-charnockite association are classified as granodiorites using the P-Q classification diagram (Fig. 7a; Debon & Lefort 1988). In this scheme, the mafic rocks plot in the quartz diorite field. All these varieties are metaluminous with the aluminum saturation index (ASI) ≤ 0.9, as defined by Shand (1950) (Fig. 7b). According to the SiO_2 vs. Fe* diagram of Frost *et al.* (2001), the studied rocks are mostly magnesian, where the granitoid types plot near the boundary with the ferroan field. Two samples (clinopyroxene-free monzogranites) plot outside the field of magnesian rocks and are slightly ferroan (Fig. 7c). According to the criteria of Miyashiro (1974) on the same diagram, these rocks belong to the tholeiitic series. In the modified alkali-lime index (MALI; Frost *et al.* 2001) diagram, gabbronorite and granodiorite are calcic, while the most siliceous varieties plot in the calc-alkaline field (Fig. 7d). Similar behavior is observed in the K_2O vs. SiO_2 diagram of Peccerillo & Taylor (1976); these rocks show affinity with calc-alkaline (gabbronorite and granodiorite) to high-K calc-alkaline (monzogranites) series (Fig. 5b).
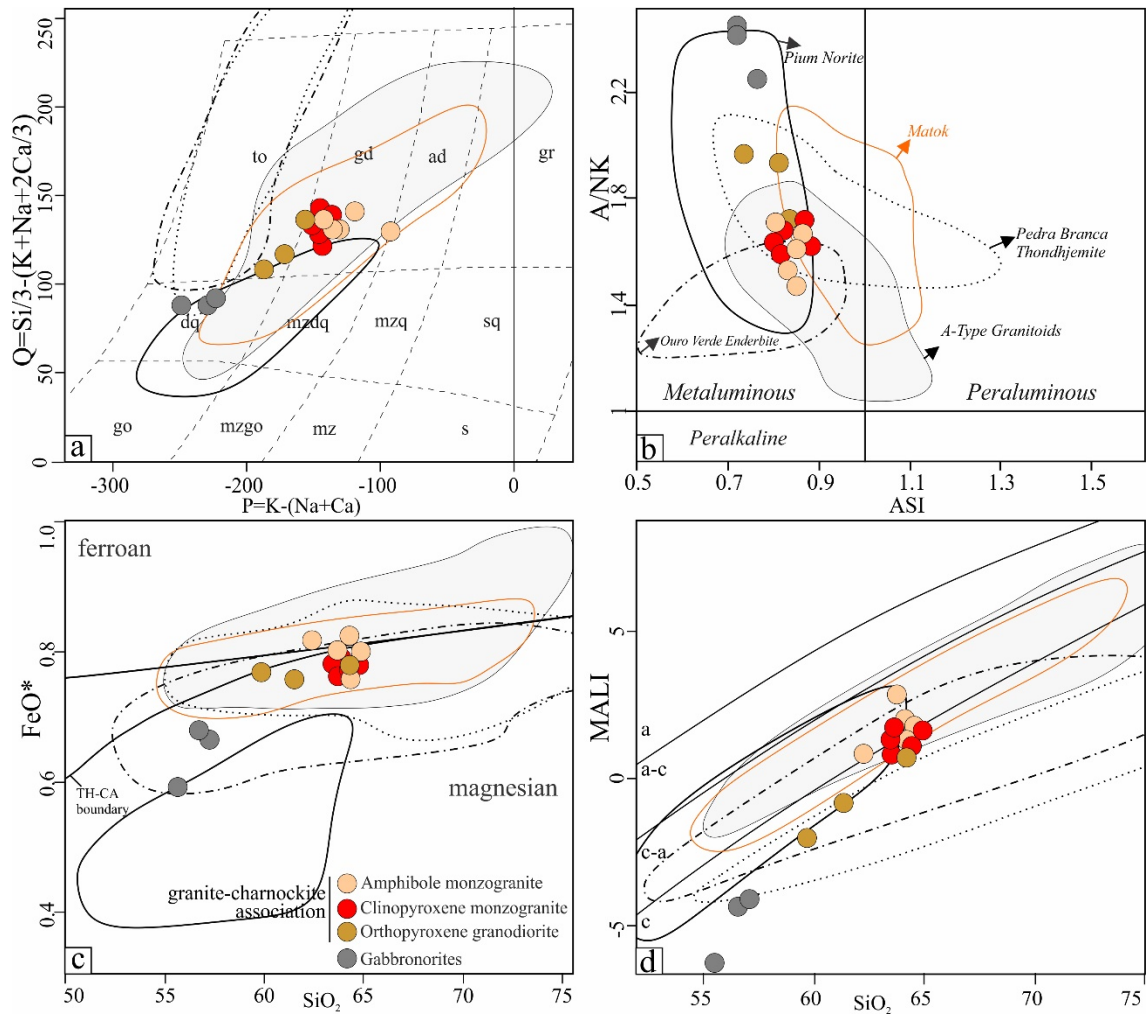
Figure 7- Geochemical classification and magmatic series plots for the pyroxene-bearing rocks from Ourilândia do Norte: **a)** P-Q diagram (Debon & Lefort 1988) showing that the studied charnockites plot mostly in the granodiorite field; **b)** A/CNK [$Al_2O_3/(CaO+Na_2O+K_2O)$] vs. A/NK [$Al_2O_3/(Na_2O+K_2O)$] diagram (Shand 1950); **c)** SiO_2 vs. FeOt/(FeOt+MgO) diagram (Frost *et al.* 2001), TH-CA boundary of Miyashiro (1974), TH, tholeiitic; CA, calc-alkalic; **d)** Na_2O+K_2O-CaO (MALI) vs. SiO_2 diagram (Frost *et al.* 2001) fields: a, alkalic; a-c, alkali-calcic; c-a, calc-alkalic; c, calcic.

2.5   MINERAL CHEMISTRY

2.5.1   Analytical procedures

Mineral chemistry analyses were performed with a JEOL JXA-8230 microprobe at the Microanalyses Laboratory of the Geosciences Institute of the Federal University of Pará. Wavelength dispersive spectroscopy (WDS) microanalyses and scanning electron microscopy (SEM) images of selected crystals of pyroxene, amphibole, biotite, and plagioclase were obtained in 30 μm-thick polished sections. WDS analyses were performed under the following operating conditions: a column accelerating voltage of 15 kV; a current of 20 nA; couting time of 20 s for major elements and 40 s for minor and trace elements; and beam diameters of 10 microns for feldspars and 1 micron for all other minerals. Matrix effects were corrected by the atomic number, X-ray absorption, and fluorescence (ZAF) method, and the analytical precisions were ±1% and ±10% for major and minor elements, respectively. The crystals used for the analyses were PETH for Cl and V; LIF for Mn, Fe, Ni, Ti, and Ba; PETJ for K, Ca, Cr, and Sr; TAP for Na, Si, Al, and Mg; and LDE1 for F. The standards used for instrument calibration were andradite (Si and Ca), microcline (Al and K), hematite (Fe), olivine (Mg), albite (Na), pyrophanite (Ti and Mn), vanadinite (V and Cl), and topaz (F).

2.5.2   Amphibole

Amphiboles were analyzed using H_2O-free content, and the structural formula was calculated based on 23 oxygen atoms, according to the method of Leake *et al.* (1997) and Hawthorne *et al.* (2012). The Fe^{+3}/Fe^{+2} ratios were estimated based on charge balancing (Schumacher 1997). For structural formula calculation, cations were collected into a set of 13 cations minus Ca, Na, and K (13-CNK). Amphiboles were classified using the nomenclature scheme of Leake *et al.* (1997). In the investigated rocks, the amphiboles are calcic and classified mainly as magnesiohornblende and ferrohornblende (Fig. 8). These amphiboles are characterized by variable total Al and Si contents (0.8 - 1.5 and 6.9 - 7.9 apfu, respectively), with Ca contents of 1.6 - 1.9 apfu (Table 3). Regarding Mg/(Fe+Mg) ratios, all analyses vary between 0.4 and 0.7 (Fig. 8), except for sample WDL-06 (gabbronorite), which shows ratios from 0.8 to 0.9.

Table 3- Representative electron microprobe analyses of amphiboles from the studied rocks.

	PYROXENE BEARING ROCKS FROM OURILÂNDIA DO NORTE											
Facies	Gabbronorite			Orthopyroxene Granodiorite			Clinopyroxene Monzogranite			Amphibole Monzogranite		
Sample	WDL-06	WDL-08A	WDL-08A	WDL-09	WDL-01A	WDL-01A	WDL-10	WDL-10	NDP-59B	NDP-123	NDP-83	NDP-83
Analysis	c1-amp1-1	c1-amp1-3	c6-amp1-2	c5-amp1-3	c4-amp1-1	c3-amp2-3	c7-amp1-1	c3-amp2-4	c5-amp3-1	c1-amp2-1	c3-amp1-1	c2-amp1-3
SiO_2	51.04	46.15	46.70	46.65	44.38	45.18	46.33	48.20	47.88	46.65	46.53	45.43
TiO_2	0.31	1.45	1.64	1.26	1.94	1.58	1.46	0.55	0.81	0.49	1.65	0.13
Al_2O_3	6.06	7.44	7.87	6.76	7.62	7.62	6.74	5.77	5.86	7.87	6.65	8.48
FeO*	11.62	18.62	16.46	21.21	21.91	21.11	22.34	21.53	19.92	19.40	18.47	21.58
MnO	0.18	0.23	0.27	0.31	0.32	0.30	0.53	0.53	0.39	0.29	0.26	0.37
MgO	16.64	10.78	11.89	9.12	8.72	9.13	7.86	9.20	9.84	9.72	10.93	8.39
CaO	11.64	11.17	11.43	10.67	10.65	10.55	10.63	10.97	11.25	11.87	10.68	11.77
Na_2O	0.63	1.08	1.25	1.10	1.27	1.33	1.34	1.00	1.08	0.89	1.57	1.01
K_2O	0.62	0.91	0.93	0.76	1.03	0.99	0.95	0.63	0.64	1.02	0.89	0.75
Soma	98.74	97.82	98.43	97.84	97.82	97.78	98.18	98.37	97.67	98.20	97.64	97.91
Structural formulae based on 23 oxygen atoms												
Si	7.13	6.83	6.83	6.96	6.68	6.76	6.99	7.15	7.15	6.95	6.91	6.84
Al^{iv}	0.87	1.17	1.17	1.04	1.32	1.24	1.01	0.85	0.85	1.05	1.09	1.16
Al^{vi}	0.13	0.13	0.18	0.15	0.03	0.11	0.18	0.16	0.18	0.33	0.07	0.34
Ti	0.03	0.16	0.18	0.14	0.22	0.18	0.17	0.06	0.09	0.05	0.18	0.01
Cr	0.00	0.00	0.00	0.00	0.00	0.00	0.00	0.00	0.00	0.00	0.00	0.00
Fe^{3+}	0.91	0.67	0.51	0.74	0.83	0.79	0.48	0.66	0.44	0.35	0.61	0.54
Fe^{2+}	0.45	1.63	1.51	1.91	1.92	1.85	2.34	2.02	2.05	2.07	1.69	2.18
Mn	0.02	0.03	0.03	0.04	0.04	0.04	0.07	0.07	0.05	0.04	0.03	0.05
Mg	3.46	2.38	2.59	2.03	1.96	2.04	1.77	2.04	2.19	2.16	2.42	1.88
Ca	1.74	1.77	1.79	1.71	1.72	1.69	1.72	1.74	1.80	1.89	1.70	1.90
Na	0.17	0.31	0.35	0.32	0.37	0.39	0.39	0.29	0.31	0.26	0.45	0.30
K	0.11	0.17	0.17	0.14	0.20	0.19	0.18	0.12	0.12	0.19	0.17	0.14
Ba	0.00	0.01	0.00	0.00	0.00	0.00	0.01	0.00	0.00	0.00	0.01	0.00
Sr	0.01	0.01	0.00	0.00	0.01	0.01	0.00	0.00	0.01	0.01	0.01	0.01
F	0.00	0.05	0.11	0.01	0.08	0.06	0.00	0.00	0.00	0.00	0.04	0.01
Cl	0.01	0.03	0.03	0.02	0.03	0.03	0.03	0.03	0.02	0.16	0.02	0.02
OH*	1.99	1.91	1.86	1.96	1.89	1.92	1.97	1.97	1.98	1.84	1.94	1.97
Total	17.03	17.27	17.33	17.17	17.30	17.28	17.30	17.15	17.24	17.35	17.33	17.35
$Mg/(Mg+Fe^{2+})$	0.88	0.59	0.63	0.52	0.50	0.52	0.43	0.50	0.52	0.51	0.59	0.46
$Fe^{3+}/(Fe^{3+}+Al^{vi})$	0.88	0.84	0.74	0.83	0.97	0.88	0.72	0.80	0.71	0.52	0.89	0.61
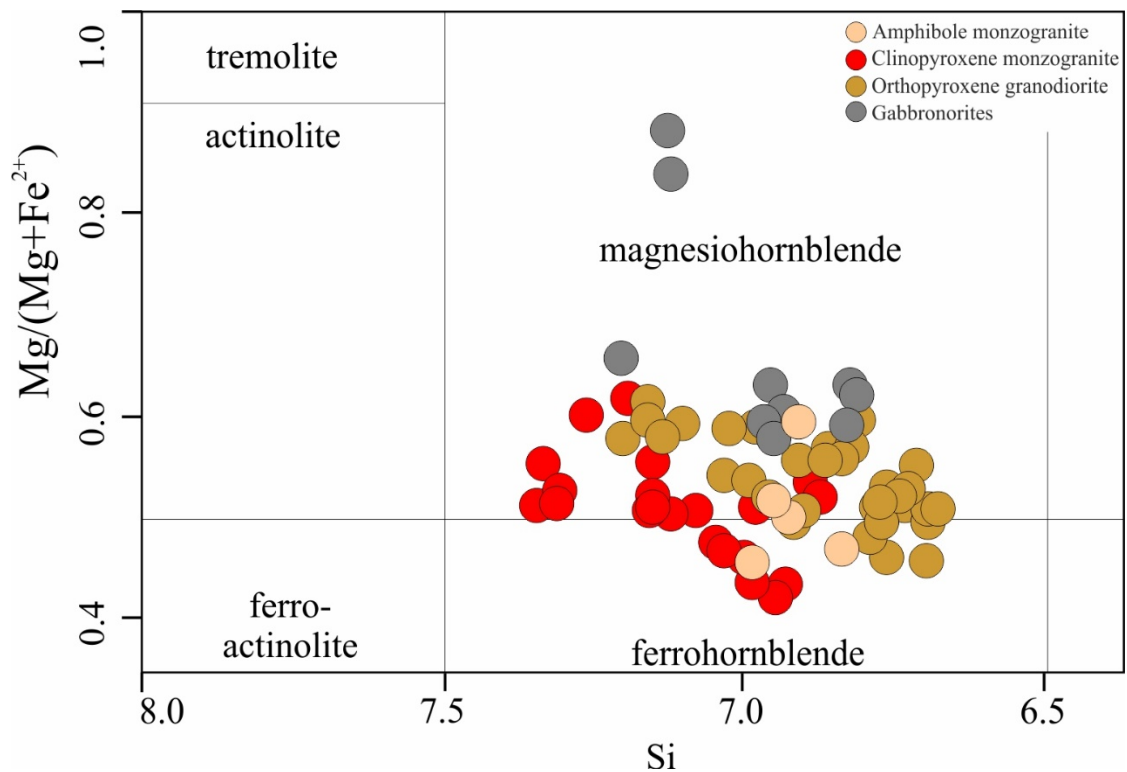
Figure 8- Classification diagram (Leake *et al.* 1997) for representative amphiboles from the Ourilândia do Norte pyroxene-bearing rocks.

2.5.3 Pyroxene

Orthopyroxene crystals are restricted to the gabbronorite and granodiorite, and they have CaO ranging from 0.66 to 2.5 wt% (Table 4). Those from gabbronorite are richer in MgO, as indicated by the FeO/(FeO+MgO) ratios (Fig. 9). In the gabbronorite, the orthopyroxene plots in the field of enstatite, while in granodiorite in the field of ferrosilite (accorfing Marimoto 1988). The compositional range of orthopyroxene is $Wo_1En_{66}Fs_{33}$ to $Wo_3En_{55}Fs_{42}$. In contrast, clinopyroxene has CaO ranging from 8.6 to 23.4 wt%. Clinopyroxenes are diopside and augite, and pigeonite occurs by exsolution in granodiorite; the range of compositions is $Wo_{29}En_{42}Fs_{30}$ to $Wo_{49}En_{38}Fs_{14}$ (Fig. 9).

Table 4- Representative electron microprobe analyses of pyroxenes from the studied rocks.

	PYROXENE BEARING ROCKS FROM OURILÂNDIA DO NORTE										
Facies	Gabbronorite			Orthopyroxene Granodiorite			Clinopyroxene Monzogranite				
Sample	WDL-06$_{Opx}$	WDL-08A$_{Opx}$	WDL-06$_{Cpx}$	WDL-01$_{Opx}$	WDL-01$_{Cpx}$	WDL-09$_{Cpx}$	WDL-10$_{Cpx}$	WDL-10$_{Cpx}$	NDP-59B$_{Cpx}$	NDP-123$_{Cpx}$	NDP-123$_{Cpx}$
Analysis	c3-px-1-2	c3-px-1-3	c1-px-2-1	c4-px-1-1	c4-px-2-1	c4-px-1-1	c2-px-1-3	c8-px1-3	c1-px-1-1	c2-px-1-1	c3-px-1-2
SiO$_2$	54.243	52.44	53.19	50.69	51.88	52.18	53.30	52.89	51.14	52.86	51.97
TiO$_2$	0.122	0.29	0.29	0.14	0.34	0.22	0.30	0.18	0.40	0.23	0.46
Al$_2$O$_3$	0.618	0.81	1.97	0.49	1.51	1.68	1.30	0.70	1.47	0.63	1.55
FeO*	21.102	24.95	8.10	32.19	13.71	12.62	8.56	14.25	14.70	13.11	14.38
MnO	0.493	0.55	0.23	0.73	0.33	0.32	0.32	0.51	0.39	0.44	0.49
MgO	22.978	19.17	14.49	14.44	10.88	14.31	13.02	9.78	12.58	10.92	12.26
CaO	0.902	1.62	22.01	0.77	21.02	17.80	23.41	21.99	17.43	20.81	17.94
Na$_2$O	0.028	0.03	0.38	0.03	0.32	0.24	0.31	0.47	0.27	0.28	0.35
K$_2$O	0.020	0.01	0.02	0.01	0.03	0.01	0.03	0.03	0.00	0.02	0.02
Soma	100.506	99.85	100.69	99.48	100.01	99.37	100.54	100.81	98.38	99.29	99.42
Structural formulae based on 6 oxygen atoms											
					T-site						
Si	1.98	1.98	1.96	1.99	1.97	1.96	1.97	2.00	1.94	1.99	1.97
Al^{IV}	0.02	0.02	0.04	0.01	0.03	0.04	0.03	0.00	0.06	0.01	0.03
Total	**2.00**	**2.00**	**2.00**	**2.00**	**2.00**	**2.00**	**2.00**	**2.00**	**2.00**	**2.00**	**2.00**
					M1-site						
Al^{VI}	0.01	0.01	0.04	0.01	0.04	0.04	0.03	0.03	0.01	0.02	0.03
Ti	0.00	0.01	0.01	0.00	0.01	0.01	0.01	0.01	0.01	0.01	0.01
Cr	0.00	0.00	0.00	0.00	0.00	0.00	0.00	0.00	0.05	0.00	0.00
Mg	0.98	0.98	0.79	0.84	0.62	0.80	0.72	0.55	0.71	0.61	0.69
Fe^{2+}	0.00	0.00	0.14	0.14	0.34	0.15	0.24	0.41	0.22	0.36	0.26
Total	**1.00**	**1.00**	**1.00**	**1.00**	**1.00**	**1.00**	**1.00**	**1.00**	**1.00**	**1.00**	**1.00**
					M2-site						
Mg	0.27	0.10	0.00	0.00	0.00	0.00	0.00	0.00	0.00	0.00	0.00
Fe^{2+}	0.68	0.82	0.10	0.94	0.11	0.25	0.04	0.06	0.26	0.13	0.23
Mn	0.02	0.02	0.01	0.02	0.01	0.01	0.01	0.02	0.01	0.01	0.02
Ca	0.04	0.07	0.87	0.03	0.85	0.72	0.93	0.89	0.71	0.84	0.73
Na	0.00	0.00	0.03	0.00	0.02	0.02	0.02	0.03	0.02	0.02	0.03
Total	**1.00**	**1.00**	**1.00**	**1.00**	**1.00**	**1.00**	**1.00**	**1.00**	**1.00**	**1.00**	**1.00**
Wo	2	3	46	1	45	37	48	47	37	43	38
En	64	55	42	43	32	42	37	29	37	32	36
Fs	34	42	13	55	23	21	14	25	25	25	26
FeO*/(FeO*+MgO)	0.48	0.57	0.36	0.69	0.56	0.47	0.40	0.59	0.54	0.55	0.54
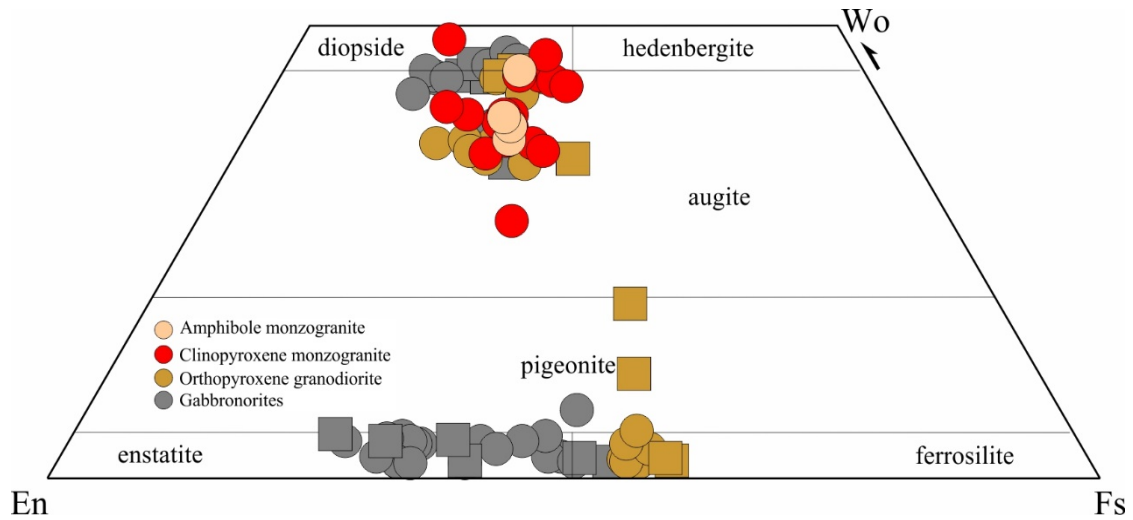
Figure 9- Wollastonite–enstatite–ferrosilite classification diagram (Morimoto 1988) for pyroxenes from the Ourilândia do Norte charnockites. The squares represent exsolution lamellae in the pyroxenes.

2.5.4 Plagioclase

Plagioclase does not show significant differences in the end-member orthoclase ($Or_{0.6}$ to $Or_{2.1}$). The major differences are in the end-members albite (Ab_{37} to Ab_{86}) and andesine (An_{13} to An_{61}), where An decreases from the gabbronorite to the amphibole monzogranite facies. Plagioclases from gabbronorites are predominantly labradorite, while those from granodiorite and clinopyroxene-bearing monzogranite are labradorite and andesine. Plagioclase from amphibole monzogranites plots in the andesine and oligoclase fields (see Fig. 10a; Table 5).

Table 5- Representative electron microprobe analyses of plagioclases from the studied rocks.

	PYROXENE BEARING ROCKS FROM OURILÂNDIA DO NORTE											
Facies	Gabbronorite			Orthopyroxene Granodiorite			Clinopyroxene Monzogranite					
Sample	WDL-06	WDL-08A	WDL-08A	WDL-09	WDL-01A	WDL-01A	WDL-10	WDL-11	NDP-59B	NDP-123	NDP-82	NDP-83
Analysis	c4-plg-1-1	c1-plg-1-2	c5-plg-1-5	c4-plg-1-3	c5-plg-2-1	c6-plg-1-1	c7-plg-1-2	c8-plg-1-1	c1-plg-1-1	c2-plg-1-1	c6-plg-1-2	c6-plg-2-1
SiO2	53.55	55.04	55.05	54.36	57.26	55.00	54.17	56.86	55.50	63.81	55.25	56.15
TiO2	0.01	0.03	0.05	0.00	0.04	0.05	0.01	0.07	0.03	0.00	0.04	0.03
Al2O3	29.51	27.77	27.31	27.69	26.50	27.21	28.75	26.96	26.79	22.01	27.54	27.26
FeO	0.60	0.17	0.37	0.21	0.19	0.28	0.23	0.09	0.08	0.04	0.19	0.09
MgO	0.01	0.00	0.00	0.00	0.00	0.01	0.00	0.00	0.00	0.00	0.00	0.00
CaO	12.31	10.95	10.80	10.87	8.87	10.19	11.71	9.59	9.82	3.67	10.33	9.75
Na2O	4.61	5.48	5.73	5.52	6.65	5.77	5.15	6.41	6.10	9.68	5.87	6.27
K2O	0.26	0.25	0.37	0.16	0.15	0.24	0.12	0.14	0.15	0.16	0.16	0.16
Total	100.84	99.69	99.68	98.82	99.65	98.76	100.13	100.12	98.48	99.37	99.37	99.71
Structural formulae based on 8 oxygen atoms												
Si	2.41	2.49	2.50	2.49	2.58	2.51	2.45	2.55	2.54	2.84	2.51	2.53
Ti	0.00	0.00	0.00	0.00	0.00	0.00	0.00	0.00	0.00	0.00	0.00	0.00
Al	1.57	1.48	1.46	1.49	1.41	1.47	1.53	1.43	1.44	1.15	1.47	1.45
Fe	0.02	0.01	0.01	0.01	0.01	0.01	0.01	0.00	0.00	0.00	0.01	0.00
Mg	0.00	0.00	0.00	0.00	0.00	0.00	0.00	0.00	0.00	0.00	0.00	0.00
Ca	0.59	0.53	0.53	0.53	0.43	0.50	0.57	0.46	0.48	0.17	0.50	0.47
Na	0.40	0.48	0.50	0.49	0.58	0.51	0.45	0.56	0.54	0.83	0.52	0.55
K	0.01	0.01	0.02	0.01	0.01	0.01	0.01	0.01	0.01	0.01	0.01	0.01
Total	5.01	5.01	5.03	5.02	5.01	5.02	5.01	5.01	5.01	5.01	5.02	5.02
Si+Al	3.98	3.98	3.96	3.98	3.99	3.98	3.98	3.98	3.98	3.99	3.98	3.98
Ca+Na+K	1.01	1.03	1.05	1.03	1.02	1.02	1.02	1.03	1.03	1.02	1.03	1.03
An	58.71	51.74	49.99	51.63	42.06	48.71	55.32	44.88	46.68	17.16	48.87	45.79
Ab	39.83	46.84	47.96	47.47	57.08	49.94	43.99	54.33	52.48	81.93	50.21	53.31
Or	1.45	1.42	2.05	0.90	0.86	1.34	0.69	0.80	0.84	0.91	0.92	0.90

2.5.5 Biotite

Biotite has TiO_2 contents between 1.79 and 5.4 wt% and Fe contents between 1.61 and 3.96 apfu (Table 6). Granite-charnockite association rocks exhibit low Mg# (Mg/(Mg+Fe) = 0.32 – 0.69) and Ti (0.21 - 0.58) contents. Mg# of the gabbronorites are slightly higher (0.46-0.69) and they are richer in TiO_2 than the other lithotypes. High TiO_2 contents in biotite suggest that this mineral formed at magmatic temperatures (Nachit *et al.* 2005); most biotites plot in the magmatic fields (Fig. 10b). In the total Al vs. Mg diagram (Fig. 10c; Nachit *et al.* 1985), biotite shows compositions near annite end-member and plots in the subalkaline field (Fig. 10c). These aspects are also observed in Neoarchean suites of the Carajás Province (e.g., Cunha *et al.* 2016, Dall'Agnol *et al.* 2017, Oliveira *et al.* 2018).

Table 6- Representative electron microprobe analyses of biotites from the studied rocks.

	PYROXENE BEARING ROCKS FROM OURILÂNDIA DO NORTE										
Facies	Gabbronorite			Orthopyroxene Granodiorite			Clinopyroxene Monzogranite				
Sample	WDL-06	WDL-06	WDL-08A	WDL-09	WDL-01A	WDL-01A	WDL-10	NDP-59B	NDP-59B	NDP-83	NDP-83
Analysis	c2-bt-1-1	c3-bt-1-2	c4-bt-1-1	c5-bt-1-1	c2-bt-1-2	c4-bt-1-1	c1-bt-1-1	c4-bt-1-2	c4-bt-1-3	c3-bt-1-1	c3-bt1-2
SiO_2	39.50	39.35	37.10	35.55	35.63	35.99	36.01	35.68	35.53	36.24	35.54
TiO_2	3.33	2.73	5.03	3.93	4.98	4.18	2.62	2.58	1.79	2.08	2.09
Al_2O_3	13.95	14.68	13.85	14.41	13.27	13.72	14.57	14.49	14.44	15.66	15.75
FeO	13.78	13.55	20.44	25.80	25.69	25.51	26.39	25.74	26.21	23.26	24.28
MnO	0.07	0.07	0.08	0.10	0.14	0.11	0.23	0.22	0.25	0.24	0.24
MgO	16.73	17.05	10.63	6.75	6.85	7.50	7.41	7.75	7.99	8.32	8.32
CaO	0.02	0.01	0.03	0.02	0.02	0.00	0.02	0.00	0.01	0.01	0.00
Na_2O	0.06	0.08	0.07	0.13	0.07	0.05	0.13	0.07	0.07	0.11	0.11
K_2O	9.60	9.39	9.40	9.26	9.21	9.26	9.22	9.41	9.30	9.44	9.30
SrO	0.13	0.00	0.03	0.00	0.11	0.07	0.06	0.00	0.04	0.00	0.06
BaO	0.16	0.17	0.21	0.00	0.00	0.11	0.12	0.09	0.18	0.00	0.07
F	0.27	0.12	0.21	0.02	0.22	0.16	0.13	0.20	0.11	0.26	0.20
Cl	0.46	0.23	0.16	0.15	0.12	0.12	0.27	0.62	0.73	0.13	0.12
NiO	0.05	0.09	0.06	0.00	0.01	0.00	0.02	0.02	0.06	0.04	0.05
Li_2O^*	1.78	1.74	1.10	0.65	0.67	0.78	0.78	0.69	0.65	0.85	0.65
H_2O^*	3.98	4.12	3.88	3.81	3.72	3.78	3.76	3.61	3.60	3.75	3.76
Subtotal	103.89	103.39	102.29	100.58	100.71	101.35	101.73	101.18	100.96	100.38	100.52
O=F,Cl	0.22	0.10	0.13	0.04	0.12	0.09	0.11	0.22	0.21	0.14	0.11
Total	103.68	103.29	102.16	100.54	100.59	101.25	101.61	100.96	100.75	100.24	100.41
Si	5.60	5.57	5.53	5.52	5.54	5.55	5.55	5.54	5.55	5.57	5.49
Al iv	2.33	2.43	2.43	2.48	2.43	2.45	2.45	2.46	2.45	2.43	2.51
Al vi	0.00	0.03	0.00	0.16	0.00	0.04	0.20	0.20	0.21	0.40	0.36
Al total	2.33	2.45	2.43	2.64	2.43	2.49	2.65	2.65	2.66	2.84	2.87
Ti	0.36	0.29	0.56	0.46	0.58	0.48	0.30	0.30	0.21	0.24	0.24
Fe	1.63	1.61	2.55	3.35	3.34	3.29	3.40	3.34	3.43	2.99	3.14
Mn	0.01	0.01	0.01	0.01	0.02	0.01	0.03	0.03	0.03	0.03	0.03
Mg	3.54	3.60	2.36	1.56	1.59	1.72	1.70	1.79	1.86	1.90	1.92
Ni	0.01	0.01	0.01	0.00	0.00	0.00	0.00	0.00	0.01	0.00	0.01
Li*	1.02	0.99	0.66	0.41	0.42	0.48	0.48	0.43	0.41	0.52	0.40
Ca	0.00	0.00	0.00	0.00	0.00	0.00	0.00	0.00	0.00	0.00	0.00
Na	0.02	0.02	0.02	0.04	0.02	0.02	0.04	0.02	0.02	0.03	0.03
K	1.74	1.70	1.79	1.84	1.83	1.82	1.81	1.86	1.85	1.85	1.83
Sr	0.01	0.00	0.00	0.00	0.01	0.01	0.01	0.00	0.00	0.00	0.01
Ba	0.01	0.01	0.01	0.00	0.00	0.01	0.01	0.01	0.01	0.00	0.00
OH*	3.77	3.89	3.86	3.95	3.86	3.89	3.87	3.74	3.75	3.84	3.87
F	0.12	0.06	0.10	0.01	0.11	0.08	0.06	0.10	0.06	0.13	0.10
Cl	0.11	0.05	0.04	0.04	0.03	0.03	0.07	0.16	0.19	0.03	0.03
Mg/Mg+Fe	0.68	0.69	0.48	0.32	0.32	0.34	0.33	0.35	0.35	0.39	0.38
Fe/Fe+Mg	0.32	0.31	0.52	0.68	0.68	0.66	0.67	0.65	0.65	0.61	0.62
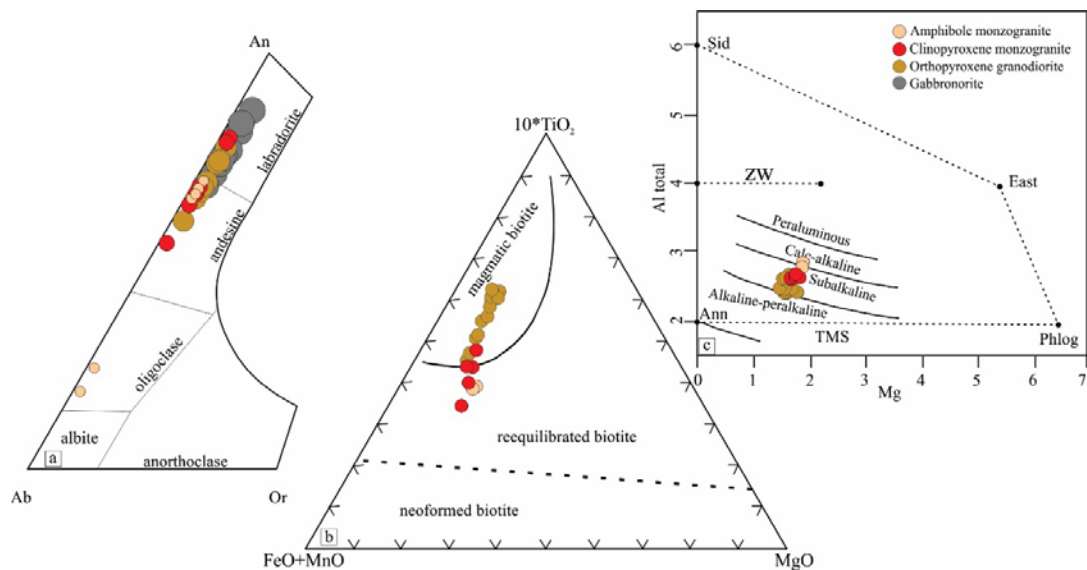
Figure 10- Classification diagrams for plagioclase and biotites from the Ourilândia do Norte charnockites: **a)** nomenclature of feldspar; **b)** biotite compositions in the 10*TiO_2-FeO+MnO-MgO ternary diagram (wt%), with limits for magmatic, re-equilibrated and neoformed biotite from Nachit *et al.* (2005); **c)** Al^{IV} vs. Mg diagram (fields Nachit *et al.* 1985). Abbreviations: Sid - siderophyllite; East - eastonite; Phlog - phlogopite; Ann - annite; TSM - tetrasilicic mica; Zw - zinnwaldite.

2.6   DISCUSSION

2.6.1   Microtextural considerations

Textural features identified in the studied rocks can be divided into magmatic and syn- to postdeformational. The magmatic textures are hypidiomorphic, intergranular, granophyric and exsolution involving olivine and pyroxene crystals. Deformational features are undulatory extinction, core-mantle structures in quartz and filled microcracks. Regarding igneous texture, granophyric intergrowth is normally formed by the simultaneous crystallization of quartz and feldspar from a melt along the eutectic boundary (Smith 1974). Exsolution textures between olivine and pyroxene are common in the gabbronorite and represent evidence of a cotectic relationship between the augite series and olivine (Fig. 3e). These texture form when the magma becomes richer in calcium relative to iron and magnesium (Poldervaart & Hess 1951). In contrast, exsolution features involving clino- and orthopyroxenes (herringbone textures) are frequent in all varieties. In plutonic rocks, slowly cooled orthopyroxenes exsolve diopside-augite as fine lamellae parallel to (100) from saturated basaltic magmas (Poldervaart & Hess 1951). Clinopyroxene destabilization into amphibole generates quartz (**Qtz$_4$**; Fig. 4c, d) in the magmatic stage through peritectic reactions (Ellis & Thompson 1986). In addition, amphibolite-biotite straight boundaries indicate that both minerals crystallized in equilibrium during the magmatic stage (Fig. 4d). Other reactions predict hydration crystallization such as those observed in partially reacted and resorbed oxide minerals (ilmenite) mantled by biotite (which in this rock is rich in Ti) (Fig. 4h). In particular, hydration crystallization reactions are likely to have strong influence on the evolution and composition of late hydrous plutons (Beard *et al.* 2004). This process seems to have played an important role in the evolution of the granite-charnockite association, which can be observed in their monzogranite varieties. Concerning the origin of the A-type Neoarchean granite suites from the Carajás Province, this process seems to have reached the highest levels of hydration, resulting in plutons formed by pyroxene-free monzogranite (Cunha *et al.* 2016, Dall'Agnol *et al.* 2017, Feio *et al.* 2012).

Deformational aspects identified in the granite-charnockite association, such as undulatory extinction and core-and-mantle microstructure, occur mostly in quartz (Fig. 4f-h) and formed by dynamic recrystallization controlled by subgrain rotation (SGR), indicating moderate-temperature solid-state deformation (400 - 450 °C; Passchier & Trouw 2005, Vernon 2004). These features suggest pretectonic crystallization; however, microcracks in plagioclase filled with residual minerals indicate that deformation also occurred in the presence of melt (e.g., Blenkinsop 2000, Bouchez *et al.* 1992, Passchier & Trouw 2005)

through submagmatic flow, suggesting a syntectonic relationship between the origin and deformation of the studied rocks (Fig. 4i). This configuration is also observed in other Neoarchean granitoids from the Carajás Province (Barros *et al.* 2009, Oliveira *et al.* 2018, Marangoanha *et al.* 2019).

2.6.2   Crystallization parameters

Crystallization parameters were estimated using biotites, amphiboles, plagioclases and pyroxenes. These minerals were chosen based on their textural aspects and chemical compositions. We selected the early magmatic minerals that do not show evidence of further transformations. All calculations for pyroxene and amphiboles were performed using the WinPyrox (Yavuz 2013) and WinAmptb programs (Yavuz & Döner 2017), and their parameters are given in Table 7.

2.6.2.1 Temperature and pressure

Considering that the Ca-in-orthopyroxene thermometer of (Köhler & Brey 1990) can be used to calculate temperatures for single orthopyroxenes, this thermometer shows temperatures higher than 1194 and up to 1573 °C, establishing orthopyroxenes as the mafic phase with the highest temperatures (Table 7). A graphical thermometer is also used to estimate the values for two-pyroxene crystallization (Lindsley & Andersen 1983 - Fig. 11a), which vary from 1100 to ~700 °C. A two-pyroxene thermometer on the join $Mg_2Si_2O_6$-$CaMgSi_2O_6$ proposed by Carlson & Lindsley (1988) has similar values (708-1060 °C), and a single-clinopyroxene thermometer shows temperatures of 833 to 904 °C (Molin & Zanazzi 1991). Overall, orthopyroxene shows a decrease in temperature from gabbronorite to granodiorite (Table 7), while the clinopyroxene temperatures are similar in all rocks (833 – 906 °C). The amphibole-plagioclase thermometer by Blundy and Holland (1990) suggests a pressure-dependent thermometer considering the albite content of silica-saturated rocks. This thermometer, allied to the calibration of Hammarstrom & Zen (1986), provides temperatures of crystallization for the studied rocks between 725 and 819 °C (Table 7). In turn, the Holland & Blundy (1994) quasi-solidus hornblende-plagioclase equilibrium thermometer using the calibration of Schmidt (1992) yields values of 676 to 816 °C. The amphibole-only thermometer by Ridolfi *et al.* (2010) provides temperatures with minor difference among the thermometers used, varying from 713 to 809 °C (Fig. 11b). The estimated temperature of ~900 °C is petrologically consistent with the near-liquidus temperatures expected for charnockitic rocks, result also obtained by several charnockite worldwide (Table 8).

Although the cores and rims of hornblende crystals in the studied rocks have mostly similar compositions, the pressure is estimated using only the composition of hornblende rims. Employing the Al-in-hornblende geobarometer proposed by Hammarstrom & Zen (1986), Hollister *et al.* (1987) and Anderson & Smith (1995), the pressures estimated for the emplacement (and crystallization) of the granite-charnockite association and gabbronorite are similar and range from 110 to 350 MPa (Fig. 11c). Using the geobarometer of Johnson & Rutherford (1989), the pressure tends to be lower and varies from 100 to 270 MPa (Table 7). The equations of Schmidt (1992) and Ague (1997) indicate higher pressures but not very different in the interval from 190 to 390 MPa. The P-T diagram based on the equations of Mutch *et al.* (2016) and Ridolfi *et al.* (2010) shows pressures varying from 190 to 310 MPa, where the monzogranite rocks have low values P and T of 190 to 250 Mpa and 713 to 774 °C, respectively (Fig. 11b). According to the conversion factor (100 MPa = 3.7 km) proposed by Brown *et al.* (1992), the studied rocks crystalized at depths of 7.0 to 11.5 km. We estimate pressure values of 190 to 310 Mpa to the emplacement of the granite-charnockite association and associated mafic rocks. Analogous conditions have been determined for other Neoarchean plutons of the Carajás Province, for example the Estrela and Serra do Rabo granites that were emplaced in low- to intermediate-grade metavolcanic rocks and banded iron formations at lower pressures of ~200 to 300 MPa (Barros *et al.* 2001, Sardinha *et al.* 2006).

Table 7- Estimated crystallization parameters for the Ourilândia do Norte pyroxene-bearing rocks.

Authors/Facies	Gabbronorite	Opx Grano	Cpx Monzo	Amp Monzo
Crystallization Temperature (°C)				
Ridolfi et al. (2010) Amp	765-809	768-800	713-772	760-774
Blundy and Holland (1990) Amp	726-773	745-819	725-798	766-784
Holland and Blundy (1994) Amp	684-767	699-816	676-776	710-788
Putirka (2016)	731-781	717-777	666-738	706-758
Molin and Zanazzi (1991) Cpx	836-904	833-906	864-905	885-896
Carlson and Lidsley (1988) Cpx-Opx	708-1021	717-1060	-	-
Brey and Köhler (1990) Cpx-Opx	723-943	726-918	-	-
Taylor (1998) Cpx-Opx	855-1061	887-1043	-	-
Brey and Köhler (1990) Opx	1194-1573	1244-1485	-	-
Amphibole crystallization pressure (kbar)				
Hammarstrom and Zen (1986)	1.8-3.0	2.4-3.4	1.2-2.5	2.0.2.3
Hollister et al. (1987)	1.7-3.0	2.3-3.5	1.1-2.6	2.4-2.9
Johnson and Rutherford (1989)	1.4-2.3	1.9-2.7	1.0-1.9	1.5-1.8
Schmidt (1992)	2.4-3.5	3.0-3.9	1.9-3.0	2.6-2.9
Anderson and Smith (1995)	2.0-2.8	1.1-3.1	1.5-2.1	1.8-2.1
Ague (1997)	2.6-3.4	3.0-3.7	2.2-3.1	2.7-2.9
Mutch et al. (2016)	2.1-2.8	2.5-3.1	1.9-2.5	2.3-2.4
Water activity (wt%)				
Ridolfi et al. (2010)	4.2-6.3	5.0-6.1	4.1-6.5	4.7-5.9
Oxigen fugacity QFM (negative values)				
Fegley (2013)	12.1-10.1	11.9-10	12.6-11.3	12.3-11.2
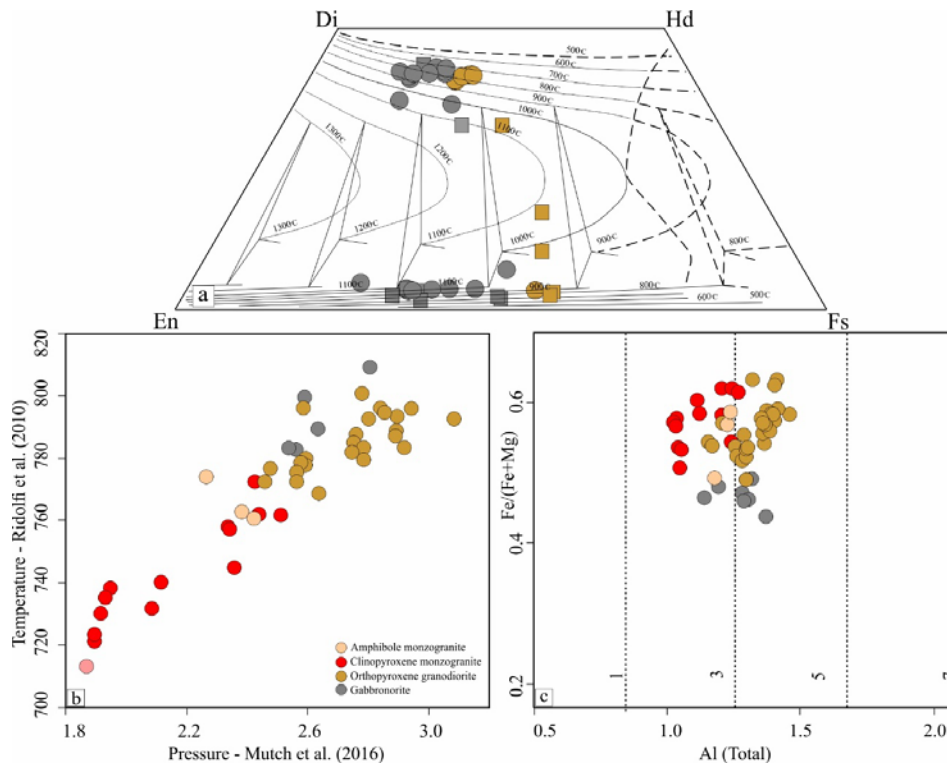
Figure 11- Graphical representation of temperatures and pressures for pyroxene and amphibole of the pyroxene-bearing rocks from Ourilândia do Norte: **a)** recalculated two-pyroxene compositions plotted in the Di–Hd–En–Fs diagram for thermometry at 1 atm (Lindsley and Andersen 1983); **b)** diagram showing temperature (Ridolfi *et al.* 2010) vs. pressure (Mutch *et al.* 2016) for crystallization of amphiboles from Ourilândia do Norte pyroxene-bearing rocks; **c)** Fe/(Fe +Mg) vs. $Al^{IV}+Al^{VI}$ diagram for amphiboles in the studied rocks (isobars from Anderson & Smith 1995) showing the possible crystallization pressure range.

2.6.2.2 Oxygen fugacity

Oxygen fugacity (fO_2) is the main parameter that controls the formation of iron-titanium oxide minerals; experimental studies show that fO_2 is strongly dependent on temperature, but it can also be modified through variations in pressure (Anderson and Smith 1995, Carmichael 1991, Frost & Lindsley 1991, Frost 1991). The Fe/(Fe+Mg) ratio in amphiboles and biotites is indicative of fO_2, which become progressively richer in magnesium with increasing fO_2 (e.g., Anderson *et al.* 2008, Anderson & Smith 1995, Wones 1981). In the Fe/(Fe+Mg) vs. Al^{IV} diagram (Anderson & Smith 1995), amphiboles from all studied rocks plot in the field of intermediate fO_2 (Fig. 12a). In the Fe/(Fe+Mg) vs. total Al diagram (Fig. 12b) the analyzed biotite plots in the magnetite-series granite field of (Anderson *et al.* 2008). These two diagrams show that the studied rocks crystallized under relatively oxidizing conditions as they plot in the intermediate fO_2 field. They are akin magnetite-series granites (NNO $\pm$ 0.5 and NNO +1; Fig. 13b). The molar ratio $Fe^{3+}/(Fe^{3+}+Fe^{2+})$ in the calcic amphiboles from the Ourilândia granite-charnockite association and gabbronorites ranges from 0.12 to 0.25, indicating fO_2 above the QFM buffer and suggesting crystallization under moderate to oxidizing conditions (e.g., Campos *et al.* 2016, Clowe *et al.* 1988). The estimation of fO_2 (NNO buffer) from amphibole compositions using the equation of (Fegley 2013) provides values varying from -12.1 to -9.8 and shows a positive correlation with temperature (Fig. 12c; Table 7). Both groups of rocks crystallized under similar fO_2 conditions, but monzogranite varieties crystallized under more oxidizing conditions (NNO +1); such behavior has also been recognized in the Matok pluton (e.g., Rapopo 2010). In relation to fO_2 conditions, the granite-charnockite association rocks of Ourilândia are similar to oxidized members of the Neoarchean A-type granite suites of the Carajás Province (Vila Jussara and Vila União), and the granite-charnockite from Carajás province contrast with many charnockites crystallized under more reduced conditions (Table 8). Thus, considering the contrasting fO_2 conditions attributed to the crystallization of charnockite magmas, we can conclude that they can crystallize under oxidized and reduced conditions.

2.6.2.3 Water activity

Worldwide, charnockite series in general show pyroxene-free facies where biotite and hornblende are the dominant ferromagnesian phases (Bohlender *et al.* 1992, Frost *et al.* 2000, Hubbard 1988, Rajesh *et al.* 2014b). Neoarchean granite plutons related to charnockite magmas with A-type geochemical signatures have been described in the Carajás Province (Dall'Agnol *et al.* 2017, Feio *et al.* 2012). They have amphibole and biotite as the main mafic

phases, with rare relicts of clinopyroxene, and are devoid of orthopyroxene. The occurrence of amphibole as an important phase in these plutons indicates that the water content had a direct influence on the mineral stability during magma evolution and that the magma contained between 4 and 7 wt% H_2O (Cunha *et al.* 2016, Dall'Agnol *et al.* 2017). Pyroxene is stable only in magmas with low water contents, although at low pressure (~200 MPa), while orthopyroxene is stable under both hydrated (~6 wt%) and anhydrous conditions (Naney 1983). For the studied rocks, H_2O contents in the melt are calculated according to Ridolfi *et al.* (2010) and range between 4.1 and 6.5 wt% (Table 3; Fig. 12d), similar to those estimated for worldwide charnockites and associated rocks ($\geq$ 4 wt% - Table 8). According to Frost & Frost (2008), hornblende-bearing granites can be produced from hydrated residual melt derived from charnockite magma. Textural and mineral chemistry evidence indicates that granite-charnockite association melts reacted with magmatic water during crystallization, resulting in peritectic reactions during magma evolution. Regarding the contrast in modal contents of pyroxene and amphibole among granite-charnockite association rocks, which have restricted geochemical variation, the hydration process is also admitted to have played an important role in their evolution. The highest H_2O saturation levels in the monzogranite varieties were favored by their lower fO_2 and temperature.
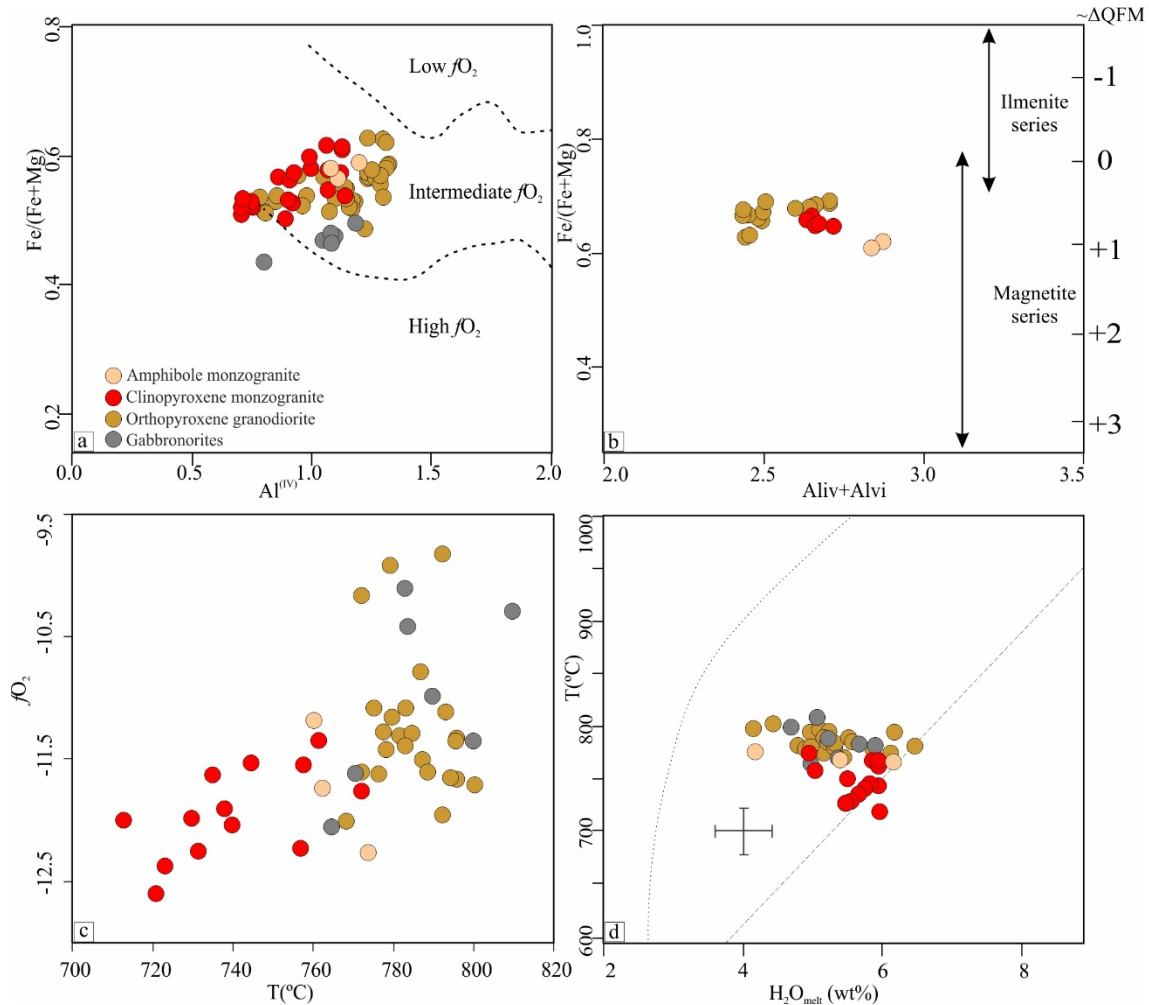
Figure 12- Binary diagrams showing crystallization parameters for the Ourilândia do Norte rocks: **a)** binary Al^{IV} vs. Fe/(Fe+Mg) plot for amphibole (Anderson & Smith 1995); **b)** Fe/(Fe+Mg) vs. $Al^{IV}+Al^{VI}$ diagram showing the compositional variations in biotite from the Ourilândia do Norte pyroxene-bearing rocks (Anderson *et al.* 2008); **c)** fO_2 vs. temperature, both calculated according to Ridolfi *et al.* (2010); **d)** temperature vs. H_2O content, both calculated according to Ridolfi *et al.* (2010), where black bars indicate the maximum relative error σest (0.4 wt%), the upper line is the maximum stability curve and the lower line is the limit of consistent amphibole crystallization.

Table 8- Comparison between the main crystallization parameters of selected worldwide charnockites and associated rocks.

	Temperature (°C)	Emplacement Pressure (Mpa)	Oxygen fugacity	H_2O content wt%	References
Studied Rocks	833-1061[CO]	190-310[M]	Oxidized < FMQ	4-6	This Study
Estrela Complex	782-893*	180-340[4]	Reduced < FMQ	-	Barros et al. (2001)
Serra do Rabo Granite	750-1020*	180-380[+]	Reduced < FMQ	-	Sardinha et a. (2004)
Planalto Suite	831-910***	300-500[+]	Reduced FMQ ± 0.5	>4	Cunha et al. (2016)
Vila Jussara Suite	833-917***	230-770[#]	FMQ ± 0.5 to NNO + 1	>4	Dall'Agnol et al. (2017)
Vila União Granites	831-926***	532-814[4]	FMQ ± 0.5 to NNO ± 0.5	>4	Oliveira et al. (2010)
Matok pluton	800-900*	330-860[#]	Oxidized > NNO	>5	Rapopo (2010)
Venda Nova Pluton	908-958**	550-600[1]	Reduced < FMQ	-	Mendes and Campos (2012)
Louis Lake Batholith	~800[IV]	500-700 and ~300[3]	FMQ 1.5 to 1.8	~2-4	Frost et al. (2010 a,b)

Notes: *Zircon-saturation temperature (Watson & Harrison 1983); **Opx-Cpx temperatures (Wood & Banno 1973); ***Ridolfi *et al.* (2010) geothermometer; [#]Al-in-amphibole geobarometer (Ridolfi *et al.* 2010, Johnson & Rutherford 1989, Anderson & Smith 1995); [+]estimated; [CO]Molin & Zanazzi (1991) geothermometer; [IV]Andersen *et al.* (1993) geothermometers; [1]Schmidt (1992) geobarometer; [3]Estimated.

2.6.3   Geochemical affinities and petrological model

The Ourilândia granite-charnockite association shows major elements concentrations similar to worldwide A-type granites (Fig. 13a). A-type plutons are widespread in the Carajás Province and represent two important periods of formation. Rapakivi granites are Paleoproterozoic in age and have anorogenic and ferroan character (Dall'Agnol & Oliveira 2007, Oliveira *et al.* 2008), while Neoarchean plutons are magnesian to ferroan granitoids, emplaced and crystallized in a regional stress field in the northern Carajás Province (Dall'Agnol & Oliveira 2007, Dall'Agnol *et al.* 2017, Oliveira *et al.* 2018, Marangoanha *et al.* 2019). Deformational features identified in the studied granitoids and afore described eliminate any possibility of linking these rocks with the Proterozoic magmatism. Even in the absence of geochronological data, we suggest from the deformational framework overprinted on these plutons, forming an E-W and NE-SW-trending elongated massif crosscutting the 2.87 Ga Mesoarchean rocks, that they were emplaced and recrystallized along of shear zones reactivated in the Neoarchean.

Neoarchean granitoids are relatively abundant in the northern Carajás Province, especially deformed ones, which differ from classic Proterozoic anorogenic magmatism (Fig. 1). To establish a more complete scenario of the magmatic event that originated the granite-charnockite association rocks of Ourilândia, here it is present a geochemical and petrological comparison with Neoarchean granitoids from Carajás Province. The database comprises 200 samples of Neoarchean granitoids from Carajás Province: A-type granitoid suites (Feio *et al.* 2012, Dall'Agnol *et al.* 2017, Marangoanha *et al.* 2019), enderbites from the Ouro Verde area (Marangoanha 2018), Pedra Branca trondhjemite (Feio *et al.* 2013, Gomes & Dall'Agnol 2007), and Pium norite (Santos *et al.* 2013). Igneous charnockite of the Matok Complex (Limpopo Belt) is used to compare with worldwide known examples (Bohlender *et al.* 1992).

Although the granite-charnockite association and gabbronorite from Ourilândia do Norte share similarities in the mode of occurrence and tectonic regime of emplacement with the other Neoarchean rocks of the Carajás Province, they differ in terms of their compositional ranges. Overall, the studied granitoids are highlighted by a narrower range of SiO_2 (59.9 to 64.6 wt%), which form a cluster of samples in distinct geochemical diagrams, contrasting with the wide compositional field defined by other Neoarchean plutons (Fig. 5). Harker diagrams consistently show that, regarding the SiO_2 range of the granite-charnockite association, these rocks are more impoverished in HFSEs (e.g., Zr, Y, Nb, and Ti) compared to other granitoid groups, contrasting sharply with the higher contents in the Neoarchean A-

type granitoids and Matok pluton (low Rb/HFSE; Fig. 13b). In addition, the granite-charnockite association is distinguished from the sodic rocks (enderbite) of the Ouro Verde area and the Pedra Branca trondhjemite by its enrichment in LILEs (K, Rb and Ba) and Fe_2O_3, combined with slight impoverishment in Al_2O_3, CaO and Sr and lower Mg#. Similarly, the gabbronorite is more enriched in Fe_2O_3 (lower Mg#) with lower HFSE contents than the Pium norite.

Chemical and modal compositions of granitoids are related factors such as magmatic sources and differentiation processes. However, the chemical composition of granitoids can be used to establish genetic links between spatially associated granitoid rocks. In the Carajás Province, Neoarchean rocks show a wide compositional spectrum, ranging from gabbro and diorite to syenogranite and monzogranite, which implies distinct nature. Altogether, the mafic rocks have been derived from enriched mantle sources, and granitoid rocks could have been generated by extensive partial melting of a radiogenic crust (Feio *et al.* 2012, Marangoanha *et al.* 2019). However, diverse processes have been suggested to explain the variations in magma compositions observed within Neoarchean granitoids from Carajás. Among the processes are (i) distinct sources, as shown in the discriminant diagram of Laurent *et al.* (2014), where sodic and high HFSE plutons closely match the composition of experimental melts derived from low- and high-K mafic rocks, respectively (Fig. 13c), and (ii) mixing of two contrasting felsic and mafic magmas (Marangoanha *et al.* 2019). In this sense, the charnockites from the Matok pluton are similar to Neoarchean A-type granitoid suites, whose wide range of bulk compositions is related to dehydration melting of metamorphic rocks (Rajesh *et al.* 2014a, 2014b) or a more complex process involving interactions between granitic and mantle-derived melts (Laurent *et al.* 2014). In contrast, the granite-charnockite association of Ourilândia exhibits a restricted compositional range that can be interpreted as indicating evolution from a single batch of magma or derived from source rocks of a specific composition.

Petrographic and mineralogical data show close similarities between the gabbronorites and granite-charnockite association rocks of Ourilândia. They present similar REE and multielement patterns and a nearly collinear arrangement between their samples in Harker diagrams (Fig. 5). These similarities suggest that they are comagmatic in origin. In addition, the granite-charnockite association and gabbronorite rocks define a single calc-alkaline trend, which is commonly interpreted as the result of magmatic differentiation (Barker & Arth 1976, Bohlender *et al.* 1992, Petersen 1980). Gradational decreases in residual elements such as Fe, Mg, Ca and Ti and linear increases in Si and alkalis are interpreted as the products of

fractional crystallization of a common parental magma, as admitted for charnockite-granite rocks of the Kleivan Complex in southern Norway (Petersen 1980) and the Matok Complex (Bohlender *et al.* 1992). Decreasing modal plagioclase and An content from the gabbronorite to the granitoids is also characteristic of magma differentiation. Considering the geochemical signature of the studied rocks, the most primitive magma was likely extracted from a normal or depleted mantle (low HFSE contents).
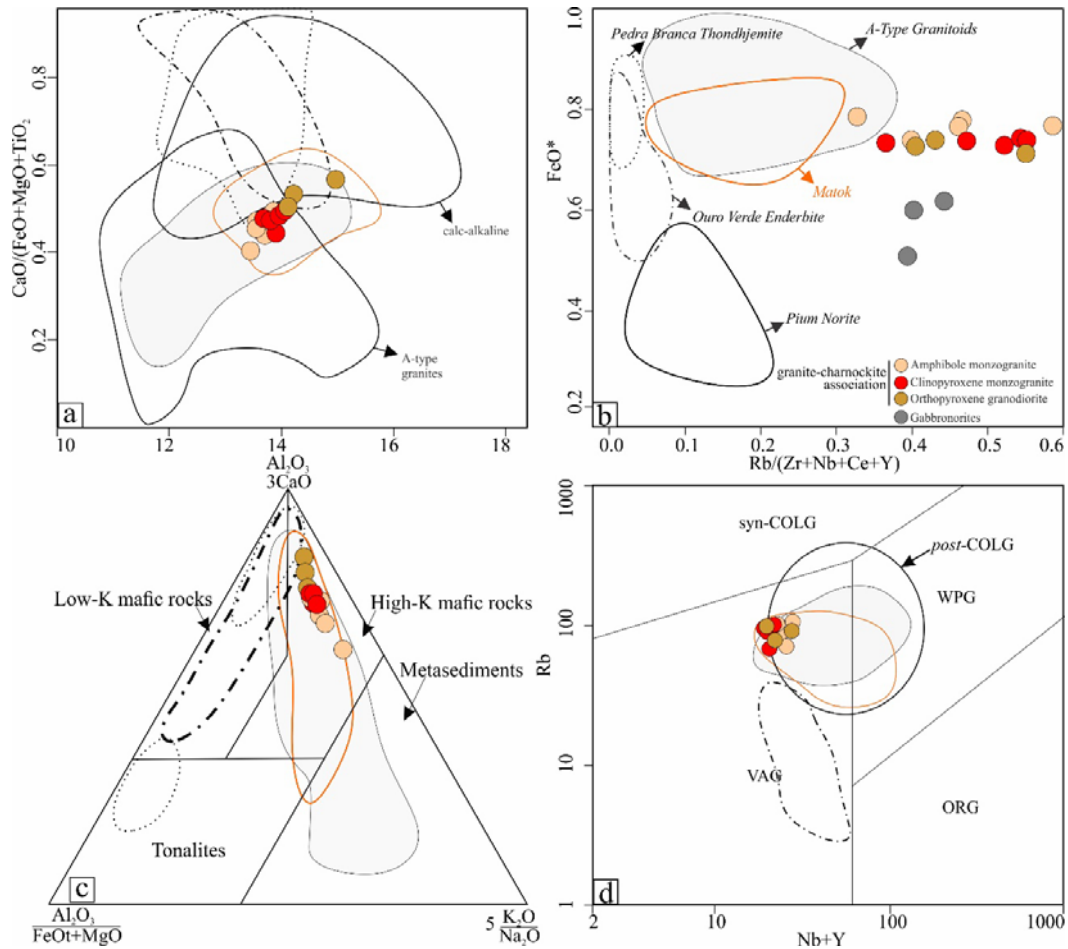
Figure 13- Discriminant geochemical diagrams for the pyroxene-bearing rocks from Ourilândia do Norte: **a)** CaO/(FeO*+MgO+TiO₂) vs. Al₂O₃ diagram (Dall'Agnol & Oliveira 2007); **b)** FeOt/(FeOt+MgO) vs. Rb/(Zr+Nb+Ce+Y) showing the pyroxene-bearing rocks from Ourilândia do Norte; **c)** petrogenetic classification ternary diagram Al₂O₃/(FeOt + MgO)–3∗CaO–5∗(K₂O/Na₂O) (fields from Laurent *et al.* 2014); **d)** Rb vs. Nb+Y granitoid discrimination diagram (Pearce 1996) suggesting the postcollisional character of the granite-charnockite association.

Based on these aspects, a geochemical modeling using REE is presented considering fractional crystallization as the primary process responsible for differentiation and that mantle-derived melts were the parental magma of all granite-charnockite association rocks. The less evolved granitoid (orthopyroxene granodiorite) can be obtained from the fractional crystallization of a silica-rich gabbronorite (sample WDL-07) magma involving extractions of plagioclase, pyroxene, olivine, amphibole and biotite. The calculated proportions are approximately 66% plagioclase, 12% clinopyroxene, 9% olivine, 8% amphibole, 4% orthopyroxene and 1% biotite with 45% crystallization of the source melt (Fig. 14). This process would explain the slightly depleted REE patterns of the charnockite magma. This model agrees with those obtained for other plutons with similar geochemical signatures and in close association with gabbroic rocks (e.g., Venda Nova pluton from the Neoproterozoic Aracuai Belt, Brazil; Mendes & Campos 2012). As shown in the geochemical section, the studied granite-charnockite rocks display very similar behavior, and fractional crystallization can be admitted not to have been the only process responsible for their textural and mineralogical differences, which are also attributed to different crystallization conditions of the magma (i.e., determined by the effects of parameters such as fO_2 and melt H_2O contents). Elemental relationships are consistent with the charnockitic and granitic rocks being comagmatic while the residual magma was progressively enriched in H_2O.
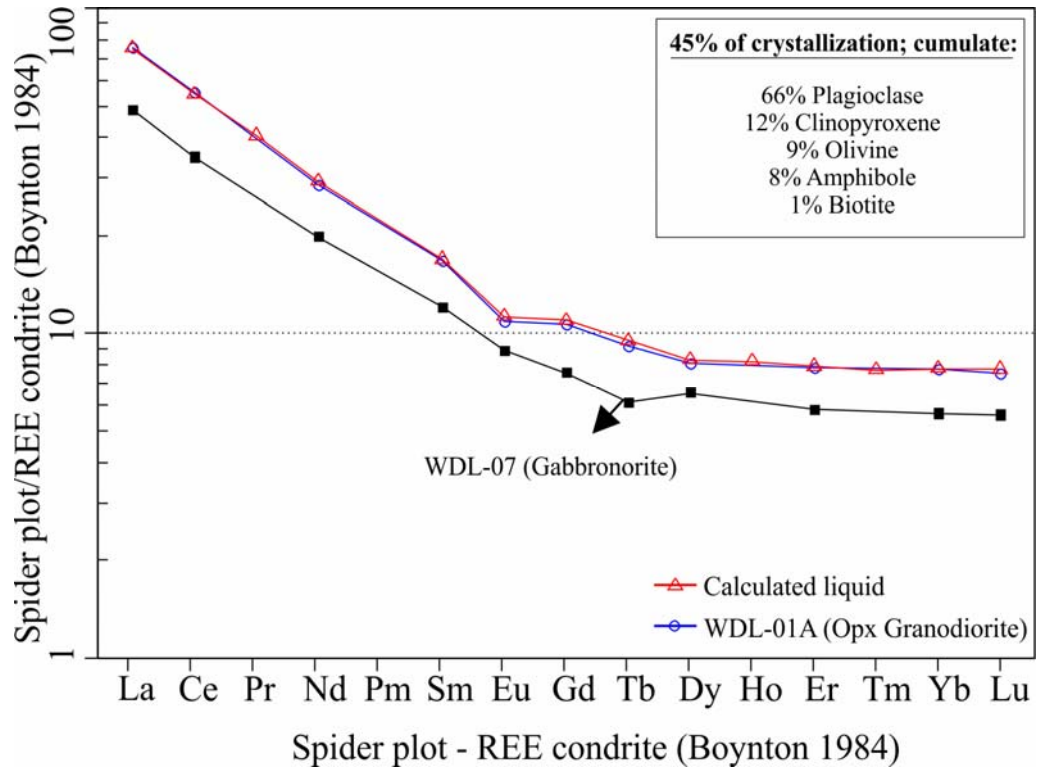
Figure 14- REE modeling for the generation of orthopyroxene granodiorite rocks by fractional crystallization of a gabbronorite; chondrite normalization values are from Boynton (1984); the mineral partition coefficients and formulas used are from Rollinson (1993) and https://earthref.org/KDD/.

2.6.4 Tectonic setting and emplacement

The Neoarchean granites of the Carajás Province are usually classified as syntectonic A-type granitoids deformed during the closure of the Carajás basin, approximately 2.75 to 2.73 Ga (Barros *et al.* 2001, 2009). However, Tavares *et al.* (2018) admitted a (rift-related) pretectonic emplacement for these plutons, which were only deformed and metamorphosed during the later closure event (in a collisional setting) of the Carajás basin (~2.09 Ga). Therefore, as the granite-charnockite association rocks of Ourilândia crosscut 2.87 Ga Mesoarchean granitoids formed in a collisional scenario (Silva *et al.* 2018), postulating that the formation of these rocks took place in a postcollisional orogenic setting after the metamorphic peak at 2.89-2.84 Ga is reasonable (Feio *et al.* 2013, Machado *et al.* 1991, Pidgeon *et al.* 2000). In this context, the postcollisional period would involve different types of magmatism that started in an intracontinental environment but still experienced large horizontal terrane movements along megashear zones (Liégeois 1998). The geochemical affinity of these rocks with the postcollisional Matok pluton and other Neoarchean A-type granites indicates that these rocks could share a similar tectonic setting (Fig. 13d). A postcollisional setting could explain the formation of the Carajás Basin and a syntectonic emplacement of Neoarchean rocks could be considered the most appropriate tectonic setting for the studied rocks. In this context, signs of mixing between contrasting magmas are used to unravel the delamination and mantle-crust interaction process in the Carajás Province (Marangoanha 2018).

The internal structure and geometry of plutons combined with their microstructural information and relationship with surrounding country rocks can provide patterns of magma ascent, emplacement and deformation mechanisms (Neves 2012, Blenkinsop 2000, Paterson *et al.* 1989). Field and microstructural observations in the granite-charnockite association rocks of Ourilândia do Norte indicate that the different magmas of these areas were generated and emplaced under an overall deformational setting. The foliation of the granitoids is subparallel to the borders of the plutons and preserves a strike parallel to that of the regional foliation printed in the Mesoarchean host rocks, pointing to solid-state foliation resulting from regional stress. The consistent NE-SW trending foliation arrangement of the main pluton, concordant with that of the country rocks, allows the postulation that the ascent and emplacement of the granite-charnockite association and gabbronorite magmas involved syntectonic migration using NE-SW to E-W regional-scale shear zones. Pre-existing conduits were active during the sinistral transpressive regime controlled by pure shear and penetrative

flow, with continuity between submagmatic and solid-state flows until relatively low temperatures (~ 450 °C; see section 7.2). Ascent through shear zones allowed magmatic mineral crystallization at different depths, confirming the variations in pressure (190 to 310 Mpa) and temperature (~670 to > 1200 °C) estimated for the studied rocks. Magma emplacement in an epizonal environment (7.0 to 11.5 km), near the boundary with the mesozone, indicates that the mantle-derived magmas from which the studied rocks originated were transported by translithospheric shear zones through the lower and middle crust into the upper crust.

2.7   CONCLUSIONS

The Carajás Province granite-charnockite association rocks exhibit well-preserved magmatic textures and can be divided in three granitoid varieties: orthopyroxene granodiorite, clinopyroxene (augite and diopside) monzogranite and amphibole (hornblende) monzogranite; gabbronorite occurs spatially associated to these rocks. They occur as a NE-SW elongated pluton with minor lenses of E-W orientation formed in a sinistral transpressive regime. Dynamic recrystallization controlled by subgrain rotation (SGR) under moderate-temperature solid-state deformation (400-450ºC). Filled up microcracks in plagioclase indicate a syntectonic crystallization, whose emplacement was controlled by trans-lithospheric scale shear zone acting as preexisting conduit for migration of mantellic magmas to epizonal levels (7.0 to 10.5 Km), in a post-collisional setting.

The studied rocks were formed at high temperatures (1100 to ~700ºC for pyroxenes, and 809 to 713 ºC for amphiboles) and crystallized under relatively oxidizing conditions (NNO -9.8 to -12.6). They differ from the Neoarchean A-type granites and sodic rocks (enderbite and trondhjemite) by their low contents in HSFE (high Rb/HFSE ratio) and enrichment in LILE, respectively. The geochemical affinity between the granite-charnockite association and gabbronorite rocks suggests in an origin from a single batch of magma (comagmatic). Geochemical modeling that the granite-charnockite association rocks were originated by fractional crystallization from a magma akin to gabbronorite. Water content (4.1 to 6.5 wt%) plays an important role in the magmatic evolution of the granite-charnockite association, which is also responsible by mineralogical differences of the monzogranitic varieties.

References

Ague J.J. 1997. Thermodynamic calculation of emplacement pressures for batholithic rocks, California: implications for the aluminum-in-hornblende barometer. *Geology,* **25** (6):563-566. doi:10.1130/0091-7613(1997)025<0563:TCOEPF>2.3.CO;2

Almeida J.A.C. de., Dall'Agnol R., Oliveira M.A.de., Macambira M.J.B., Pimentel M.M., Rämö O.T., Guimarães F.V., Leite A.A. da S., Almeida J. de A.C., Dall'Agnol R., Oliveira M.A.de., Macambira M.J.B., Pimentel M.M., Rämö O.T., Guimarães F.V., Leite A.A.S.da. 2011. Zircon geochronology, geochemistry and origin of the TTG suites of the Rio Maria granite-greenstone terrane: Implications for the growth of the Archean crust of the Carajás province, Brazil. *Precambrian Research,* **187** (1-2): 201–221. doi:10.1016/j.precamres.2011.03.004.

Almeida J. de A.C. de., Dall'Agnol R., Leite A.A.S.da. 2013. Geochemistry and zircon geochronology of the Archean granite suites of the Rio Maria granite-greenstone terrane, Carajás Province, Brazil. *Journal of South American Earth Sciences,* **42**, 103–126.

Almeida F.F.M., Hasui Y., Brito Neves B.B.de., Fuck R.A. 1981. Brazilian structural provinces: an introduction. *Earth-Science Reviews,* **17**, 1–29. doi:10.1016/0012-8252(81)90003-9.

Almeida J. A.C.de., Dall'Agnol R., Dias S.B., Althoff F.J. 2010. Origin of the Archean leucogranodiorite-granite suites: evidence from the Rio Maria terrane and implications for granite magmatism in the Archean. *Lithos,* **120**, 235–257. doi:10.1016/j.lithos.2010.07.026.

Almeida J. Oliveira M., Dall'Agnol R., Althoff F. 2008. *Relatório de mapeamento geológico na escala 1: 100.000 da Folha Marajoara (SB-22-zc v).* Belém, CPRM–Serviço Geológico do Bras. 147p. (Programa GeoBrasil).

Althoff F., Barbey P., Boullier A.M. 2000. 2.8–3.0 Ga plutonism and deformation in the SE Amazonian craton: the Archaean granitoids of Marajoara (Carajás Mineral Province, Brazil). *Precambrian Research,* **104**, 187–206. doi:10.1016/S0301-9268(00)00103-0.

Andersen D.J., Lindsley D.H., Davidson P.M. 1993. QUILF: A pascal program to assess equilibria among FeMgMnTi oxides, pyroxenes, olivine, and quartz. *Computers and Geosciences,* **19**, 1333–1350. doi:10.1016/0098-3004(93)90033-2.

Anderson J.L., Barth A.P., Wooden J.L., Mazdab F. 2008. Thermometers and Thermobarometers in Granitic Systems. *Reviews in Mineralogy and Geochemistry,* **69**, 121–142. doi:10.2138/rmg.2008.69.4.

Anderson J.L., Smith D.R. 1995. The effects of temperature and fO2 on the Al-in-hornblende barometer. *American Mineralogist,* **80**, 549–559. doi:10.1016/0031-9201(95)03018-R.

Baker L.L., Rutherford M.J. 1996. The effect of dissolved water on the oxidation state of silicic melts. *Geochimica et Cosmochimica Acta.* Pergamon **60**, 2179–2187. doi:10.1016/0016-7037(96)00090-7.

Barros C.E.M., Barbey P., Boullier A.M. 2001. Role of magma pressure, tectonic stress and crystallization progress in the emplacement of syntectonic granites. The A-type Estrela granite complex (Carajás Mineral Province, Brazil). *Tectonophysics,* **343**, 93–109. doi:10.1016/S0040-1951(01)00260-8.

Barros C.E.M., Sardinha A.S., Barbosa J.D.P.O.De., Macambira M.J.B., Barbey P., Boullier A.M. 2009. Structure, petrology, geochemistry and zircon u/pb and pb/pb geochronology of the synkinematic archean (2.7 ga) a-type granites fromthe carajás metallogenic province, northern Brazil. *Canadian Mineralogist,* **47**, 1423–1440. doi:10.3749/canmin.47.6.1423.

Beard J.S., Ragland P.C., Rushmer T. 2004. Hydration Crystallization Reactions between Anhydrous Minerals and Hydrous Melt to Yield Amphibole and Biotite in Igneous Rocks: description and implications. *J. Geol*, **112**, 617–621. doi:10.1086/422670.

Blenkinsop T. 2000. *Deformation microstructures and mechanisms in minerals and rocks.* Dordrecht, Kluwer Academic Publishers, p.150. doi:10.1007/0-306-47543-X

Blundy J.D., Holland T.J.B. 1990. Calcic amphibole equilibria and a new amphibole-plagioclase geothermometer. *Contributions to Mineralogy and Petrology,* **2**, 208-224 doi:10.1007/BF00306444.

Bohlender F., Van Reenen D.D., Barton J.M. 1992. Evidence for metamorphic and igneous charnockites in the Southern Marginal Zone of the Limpopo Belt. *Precambrian Research,* **55**, 429–449. doi:10.1016/0301-9268(92)90038-P.

Bohlender F. Unpublished Ph.D. thesis 1992. Igneous and metamorphiccharnockitic ocks in the Southern Marginal Zone of the Limpopo Belt with spe-cial emphasis on the Matok enderbitic-granitic suite. Rand Afrikaans University, pp. 261

Bouchez J.L., Delas C., Gleizes G., Nedelec A., Cuney M. 1992. Submagmatic microfractures in granites. *Geology,* **20**, 35–38. doi:10.1130/0091-7613(1992)020<0035:SMIG>2.3.CO.

Brown G.C., Hawkesworth C.J., Wilson R.C.L. 1992. *Understanding the Earth.* Milton Keynes, UK, Departament of Earth Sciences the open university, p. 229.

Bucher K. & Frost B.R. 2006. Fluid Transfer in High-grade Metamorphic Terrains Intruded by Anorogenic Granites: the Thor Range, Antarctica. *Journal of Petrology,* **47**, 567–593. doi:10.1093/petrology/egi086.

Campos B.C.S., Vilalva F.C.J., Nascimento M.A.L. do., Galindo A.C. 2016. Crystallization conditions of porphyritic high-K calc-alkaline granitoids in the extreme northeastern Borborema Province, NE Brazil, And geodynamic implications. *Journal of South American Earth Sciences,* **70**, 224–236. doi:10.1016/j.jsames.2016.05.010.

Carlson W.D. & Lindsley D.H. 1988. Thermochemistry of pyroxenes on the join Mg2Si2O6-CaMgSi2O6. *American Mineralogist,* **73** (3-4), 242-252.

Carmichael I.S.E. 1991. The redox states of basic and silicic magmas: a reflection of their source regions? *Contributions to Mineralogy and Petrology*. Springer-Verlag, **106**, 129–141.

doi:10.1007/BF00306429.

Carroll M.R., Wyllie P.J., 1990. The system tonalite-H2O at 15 kbar and the genesis of calc-alkaline magmas. *American Mineralogist,* **75**, 345–357. doi:10.1177/1525740109354775.

Clowe C.A., Popp R.K., Fritz S.J. 1988. Experimental investigation of the effect of oxygen fugacity on ferric-ferrous ratios and unit-cell parameters of four natural clinoamphiboles. *American Mineralogis,t* **73**, 487.

Cunha I.R.V.da., Dall'Agnol R., Feio G.R.L. 2016. Mineral chemistry and magnetic petrology of the Archean Planalto Suite, Carajás Province – Amazonian Craton: Implications for the evolution of ferroan Archean granites. *Journal of South American Earth Sciences,* **67**, 100–121. doi:10.1016/j.jsames.2016.01.007.

Dall'Agnol R., Cunha I.R.V.da., Guimarães F.V., Oliveira D.C.de., Teixeira M.F.B., Feio G.R.L., Lamarão C.N. 2017. Mineralogy, geochemistry, and petrology of Neoarchean ferroan to magnesian granites of Carajás Province, Amazonian Craton: The origin of hydrated granites associated with charnockites. *Lithos,* **277**, 3–32. doi:10.1016/j.lithos.2016.09.032.

Dall'Agnol R. & Oliveira D.C.de. 2007. Oxidized, magnetite-series, rapakivi-type granites of Carajás, Brazil: implications for classification and petrogenesis of A-type granites. *Lithos,* **93**, 215–233. doi:10.1016/j.lithos.2006.03.065.

Dall'Agnol R., Oliveira D.C.de, Guimarães F. V., O., Gabriel E.O., Feio G.R.L., Lamarão C.N., Althoff F.J., Patrick A. S., Teixeira M.F.B., Alice C. Silva, Daniel S. Rodrigues, Max J. P. Santos, Chrystophe R. P. Silva, Roseli D. Santos, P.J.L.S. 2013. Geologia do subdomínio de transição do domínio carajás – implicações para a evolução arqueana da província carajás – pará. *In:* 13 Simpósio Geol. da Amazônia. *Anais.* 1 CDrom.

Dall'Agnol R., Oliveira M.A., Almeida J.A.C., Althoff F.J., Leite A.A.S., Oliveira D.C., Barros C.E.M. 2006. Archean and Paleoproterozoic granitoids of the Carajás metallogenetic province, eastern Amazonian craton. *In:* Symp. Magmat. Crustal Evol. Metallog. Amaz. Craton. *Abstr.* Vol. F. Trips Guid.

Debon F. & Lefort P. 1988. A cationic classification of common plutonic rocks and their magmatic associations: principles, method, applications. *Bulletin de Minéralogie.* **5,** 493-510 p.

Ellis D.J. & Thompson A.B. 1986. Subsolidus and partial melting reactions in the quartz-excess CaO + MgO + Al2O3 + SiO2 + H2O system under water excess and water-deficient conditions to 10 kbar: some implications for the origin of peraluminous melts from mafic rocks. *J. Petrol,* **27**, 91–121.

Evensen N.M.M., Hamilton P.J.J., O'Nions R.K.K. 1978. Rare-earth abundances in chondritic meteorites. *Geochim. Cosmochim. Acta,* **42**, 1199–1212. doi:10.1016/0016-7037(78)90114-X.

Fegley B. 2013. Practical Chemical Thermodynamics for Geoscientists, Practical Chemical Thermodynamics for Geoscientists. doi:10.1016/C2009-0-22615-8.

Feio G.R.L., Dall'Agnol R. 2012. Geochemistry and petrogenesis of the Mesoarchean granites from the Canaã dos Carajás area, Carajás Province, Brazil: Implications for the origin of Archean granites. *Lithos,* **154**, 33–52. doi:10.1016/j.lithos.2012.06.022.

Feio G.R.L., Dall'Agnol R., Dantas E.L., Macambira M.J.B., Gomes A.C.B., Sardinha A.S., Oliveira D.C., Santos R.D., Santos P.A. 2012. Geochemistry, geochronology, and origin of the Neoarchean Planalto Granite suite, Carajás, Amazonian craton: A-type or hydrated charnockitic granites? *Lithos,* **151**, 57–73. doi:10.1016/j.lithos.2012.02.020.

Feio G.R.L., Dall'Agnol R., Dantas E.L., Macambira M.J.B., Santos J.O.S., Althoff F.J., Soares J.E.B., 2013. Archean granitoid magmatism in the Canaã dos Carajás area: Implications for crustal evolution of the Carajás province, Amazonian craton, Brazil. *Precambrian Res,* **227**, 157–185. doi:10.1016/j.precamres.2012.04.007.

Frost B.R., Barnes C.G., Collins W.J., Arculus R.J., Ellis D.J., Frost C.D. 2001. A geochemical classification for granitic rocks. *J. Petrol,* **42,** doi:10.1093/petrology/42.11.2033.

Frost B.R. & Frost C.D. 2009. On charnockites: Reply to the discussion by C. Bhattacharyya and B. Goswami. *Gondwana Res,* **15**, 218–219. doi:10.1016/J.GR.2008.09.003.

Frost B.R. & Frost C.D. 2008. On charnockites. *Gondwana Res,* **13**, 30–44. doi:10.1016/j.gr.2007.07.006.

Frost B.R., Frost C.D., Hulsebosch T.P., Swapp S.M. 2000. Origin of the Charnockites of the Louis Lake Batholith, Wind River Range, Wyoming. *J. Petrol,* **41**, 1759–1776.

Frost B.R. & Lindsley D.H. 1991. Occurrence of Iron-Titanium Oxides in Igneous Rocks. *Rev. Mineral.* doi:10.2138/rmg.1991.25.12.

Frost R. 1991. Oxide minerals: Petrologic and magnetic significance. *Rev. Mineral.* **25**, 481–509. doi:10.1016/0037-0738(93)90062-A.

Gabriel E.O., Oliveira D.C., Macambira M.J.B. 2010. Caracterização geológica, petrográfica e geocronológica de ortopiroxênio-trondhjemitos (leucoenderbitos) da região de Vila Cedere III, Canaã dos Carajás-PA, Província Mineral de Carajás. *In:* SBG, Congresso Brasileiro de Geologia, 45. CDrom (in Portuguese).

Gabriel E.O. & Oliveira D.C. 2014. Geologia, petrografia e geoquímica dos granitoides arqueanos de alto magnésio da região de Água Azul do Norte, porção sul do Domínio Carajás, Pará. *Bol. do Mus. Para. Emílio Goeldi* - Série Ciências Nat. **9**, 533–564.

Gomes A.C.B. & Dall'Agnol R. 2007. Nova associação tonalítica-trondhjemítica neoarqueana na região de Canaã dos Carajás: TTGS com altos conteúdos de Ti, Zr e Y. *Rev. Bras. Geociências,* **37**, 182–193. doi:10.25249/0375-7536.2007371182193.

Hammarstrom J.M. & Zen E. 1986. Aluminum in hornblende: an empirical igneous geobarometer. *Am. Mineral.* doi:10.1016/S0022-2836(03)00574-6.

Hawthorne F.C., Oberti R., Harlow G.E., Maresch W. V., Martin R.F., Schumacher, J.C.,

Welch, M.D. 2012. Nomenclature of the amphibole supergroup. *Am. Mineral.* **97**, 2031–2048. doi:10.2138/am.2012.4276.

Holland T. & Blundy J. 1994. Non-ideal interactions in calcic amphiboles and their bearing on amphibole-plagioclase thermometry. *Contrib. to Mineral. Petrol.* **116**, 433–447. doi:10.1007/BF00310910.

Holland T.H. 1900. The charnockite series, a group of Archaean hypersthenic rocks in peninsular India. *Geol. Surv. India Mem.*

Hollister L.S., Grissom G.C., Peters E.K., Stowell H.H., Sisson V.B., 1987. Confirmation of the empirical correlation of Al in hornblende with pressure of solidification of calc-alkaline plutons. *Am. Mineral.*

Howie R.A. 1955. The Geochemistry of the Charnockite Series of Madras, India. *Trans. R. Soc. Edinburgh,* **62**, 725–768. doi:10.1017/S0080456800009431

Hubbard F.H. 1988. Basic intrusion, charnockite-rapakivi granite plutonism and crustal depletion, S.W. Sweden. *Soc. Ital. di Mineral. e Petrol.* **43**, 543–554.

Johnson M.C. & Rutherford M.J. 1989. Experimental calibration of the aluminum-in-hornblende geobarometer with application of Long Valley caldera (California) volcanic rocks. *Geology,* **17**, 837–841. doi:10.1130/0091-7613(1989)017<0837:ECOTAI>2.3.CO;2.

Köhler T. & Brey G.. 1990. Calcium exchange between olivine and clinopyroxene calibrated as a geothermobarometer for natural peridotites from 2 to 60 kb with applications. *Geochim. Cosmochim. Acta,* **54**, 2375–2388. doi:10.1016/0016-7037(90)90226-B.

Lafon J.M. Macambira M.J.B.; Pidgeon R.T. Zircon U-Pb SHRIMP dating of Neoarchean magmatism in the southwestern part of the Carajás Province (eastern Amazonian Craton, Brazil). *In:* International Geological Congress, 31., 2000, Rio de Janeiro. Abstracts. Rio de Janeiro, 2000. 1 CD-ROM.

Laurent O., Rapopo M., Stevens G., Moyen J.F., Martin H., Doucelance R., Bosq C. 2014. Contrasting petrogenesis of Mg-K and Fe-K granitoids and implications for post-collisional magmatism: Case study from the Late-Archean Matok pluton (Pietersburg block, South Africa). *Lithos,* **196**, 131–149. doi:10.1016/j.lithos.2014.03.006.

Le Maitre R.W. 2002. Igneous rocks; a classification and glossary of terms; recommendations of the International Union of geological Sciences Sub commission on the systematics of igneous rocks., 2nd ed. Cambridge University Press, University of Tasmania.

Leake B.E., Woolley A.R., Arps C.E.S., Birch, W.D., Gilbert C. m., Grice J.D., Hawthorne F.C., Kato A., Kisch H.J., Krivovichev V.G., Linthout K., Laird J., Mandarino J.A., Maresch W. V., Nickel E.H., Rock N.M.S.N.M.S., Schumacher J.C., Smith D.C., Stephenson N.C.N., Whittaker E.J.W., Youzhi G., Gurion B., Krivovichev V.G., Laird J., Mandarino J.A., Maresch W. V., Nickel E.H., Rock N.M.S.N.M.S., Schumacher J.C., Smith D.C., Stephenson N.C.N., Ungaretti L., Whittaker E.J.W., Youzhi G., Gilbert M.C., Grice J.D., Linthout K., Nicholaus M.S., Karort A., Krscnru H.J., H, D.G.F.C., Knns G.K., Jo, L., Mlnnarrnor A.,

Mannschrr W. V, Rocrrft H.N.N.M.S., Svrrrnr D.C., Srnphensonrr N.C.N., Scnurmcherrrr J.C., Uuc, L., Wnrrrakerrl J.W., Youznrl G. 1997. Nomenclature of amphiboles: Report of the Subcommittee on Amphiboles of the International Mineralogical Association, Commission on New Minerals and Mineral Names BnnN. *Can. Mineral*, **35**, 219–246.

Leite-Santos P.J. & Oliveira D.C. de. 2016. Geologia, petrografia e geoquímica das associações leucograníticas arqueanas da área de Nova Canadá: Província Carajás. Geol. USP - *Ser. Cient.* **16**, 37–66. doi:10.11606/issn.2316-9095.v16i2p37-66.

Leite A.A. da S., Dall'Agnol R., Macambira M.J.B., Althoff,F.J. 2004. Geologia e geocronologia dos granitoides arqueanos da região de Xinguara-PA e suas implicações na evolução do terreno granito-greenstone de Rio Maria, Cráton Amazônico. *Rev. Bras. Geociências*, **34**, 447–458.

Liégeois J.P. 1998. Preface – some words on the postcollisional magmatism. *Lithos*, **45**, xv–xvii.

Lindsley D.H. & Andersen D.J. 1983. A two-pyroxene thermometer. *J. Geophys. Res.* **88**, A887. doi:10.1029/JB088iS02p0A887.

Machado N., Lindenmayer Z., Krogh T.E., Lindenmayer D. 1991. U-Pb geochronology of Archean magmatism and basement reactivation in the Carajás area, Amazon shield, Brazil. *Precambrian Res.* **49**, 329–354. doi:10.1016/0301-9268(91)90040-H.

Marangoanha B., Oliveira, D.C.de., Oliveira V.E.S.de., Galarza M.A., Lamarão C.N. 2019. Neoarchean A-type granitoids from Carajás province (Brazil): New insights from geochemistry, geochronology and microstructural analysis. *Precambrian Res.* **324**, 86–108. doi:10.1016/j.precamres.2019.01.010.

Marangoanha B. Petrologia e evolução crustal na porção central do Domínio Canaã dos Carajás, Província Carajás. 2018. xxx, 193 f. (Ph.D. Thesis) - Universidade Federal do Pará, Instituto de Geociências, Programa de Pós-Graduação em Geologia e Geoquímica, 2018.

McDonough W.F., Sun S. 1995. The composition of the Earth. Chem. *Geology*, **120**, 223–253. doi:10.1016/0009-2541(94)00140-4.

Mendes J.C. & Campos C.M.P.de. 2012. Norite and charnockites from the Venda Nova Pluton, SE Brazil: Intensive parameters and some petrogenetic constraints. *Geosci. Front.* **3**, 789–800. doi:10.1016/j.gsf.2012.05.009.

Mikhalsky E. V., Sheraton J.W., Hahne K. 2006. Charnockite composition in relation to the tectonic evolution of East Antarctica. *Gondwana Res.* **9**, 379–397. doi:10.1016/j.gr.2005.11.007.

Miyashiro A. 1974. Volcanic rock series in island arcs and active continental margins. *Am. J. Sci.* **274**, 321–355. doi:10.2475/ajs.274.4.321.

Molin G. & Zanazzi P.F. 1991. Intracrystalline Fe2+-Mg ordering in augite: experimental study and geothermometric applications. Eur. J. Mineral. 3, 863–875.

doi:10.1127/ejm/3/5/0863.

Morimoto N. 1988. Nomenclature of Pyroxenes. *Mineral. Petrol.* **39**, 55–76. doi:10.1007/BF01226262

Mutch E.J.F., Blundy J.D., Tattitch B.C., Cooper F.J., Brooker R.A. 2016. An experimental study of amphibole stability in low-pressure granitic magmas and a revised Al-in-hornblende geobarometer. *Contrib. to Mineral. Petrol.* **171**, 85. doi:10.1007/s00410-016-1298-9.

Nachit H., Ibhi A., Abia E.H., Ben Ohoud M. 2005. Discrimination between primary magmatic biotites, reequilibrated biotites and neoformed biotites. *Comptes Rendus Geosci.* **337**, 1415–1420. doi:10.1016/j.crte.2005.09.002.

Nachit H., Razafimahefa N., Stussi J.M., Carron J.P. 1985. Composition chimique des biotites et typologie magmatique des granites. C.R. *Acad. Sci. Paris.* doi:10.1088/0031-9120/35/3/311.

Naney M.T. 1983. Phase equilibria of rock-forming ferromagnesian silicates in granitic systems. *Am. J. Sci.* **283**, 993–1033. doi:10.2475/ajs.283.10.993

Neves S.P. 2012. Granitos orogênicos: da geração dos magmas à intrusão e deformação. Synergia, Rio de Janeiro, 147 p.

Oliveira D.C., Dall'Agnol R., Corrêa da Silva J.B., Costa de Almeida J.A., 2008. Gravimetric, radiometric, and magnetic susceptibility study of the Paleoproterozoic Redenção and Bannach plutons, eastern Amazonian Craton, Brazil: Implications for architecture and zoning of A-type granites. *J. South Am. Earth Sci.* **25**, 100–115. doi:10.1016/j.jsames.2007.10.003.

Oliveira D.C. de, Neves S.P., Trindade R.I.F., Dall'Agnol R., Mariano G., Correia P.B., 2010. Magnetic anisotropy of the Redenção granite, eastern Amazonian craton (Brazil): Implications for the emplacement of A-type plutons. *Tectonophysics,* **493**, 27–41. doi:10.1016/j.tecto.2010.07.018.

Oliveira M.A. De., Dall'Agnol R., Althoff F.J., Silva Leite A.A.da. 2009. Mesoarchean sanukitoid rocks of the Rio Maria Granite-Greenstone Terrane, Amazonian craton, Brazil. *J. South Am. Earth Sci.* **27**, 146–160. doi:10.1016/j.jsames.2008.07.003.

Oliveira V.E.S. de, Oliveira D.C.de., Marangoanha B., Lamarão C.N. 2018. Geology, mineralogy and petrological affinities of the Neoarchean granitoids from the central portion of the Canaã dos Carajás domain, Amazonian craton, Brazil. *J. South Am. Earth Sci.* **85**, 135–159. doi:10.1016/j.jsames.2018.04.022.

Passchier C. & Trouw, R. 2005. Microtectonics, *Tectonophysics.* doi:10.1007/978-3-662-08734-3.

Paterson S.R., Vernon R.H., Tobisch O.T. 1989. A review of criteria for the identification of magmatic and tectonic foliations in granitoids. *J. Struct. Geol.* **11**, 349–363. doi:10.1016/0191-8141(89)90074-6.

Patiño Douce A.E. 1996. Effects of pressure and H2O content on the compositions of primary crustal melts, in: Special Paper 315: The Third Hutton Symposium on the Origin of Granites and Related Rocks. *Geological Society of America*, pp. 11–21. doi:10.1130/0-8137-2315-9.11.

Peccerillo A., Taylor, S.R. 1976. Geochemistry of eocene calc-alkaline volcanic rocks from the Kastamonu area, Northern Turkey. *Contrib. to Mineral. Petrol.* **58**, 63–81. doi:10.1007/BF00384745.

Petersen J.S. 1980. The zoned Kleivan granite - an end member of the anorthosite suite in southwest Norway. *Lithos*, **13**, 79–95. doi:10.1016/0024-4937(80)90065-1.

Pidgeon R.T., MacAmbira M.J.B., Lafon J.M. 2000. Th-U-Pb isotopic systems and internal structures of complex zircons from an enderbite from the Pium Complex, Carajas Province, Brazil: Evidence for the ages of granulite facies metamorphism and the protolith of the enderbite. *Chem. Geol.* **166**, 159–171. doi:10.1016/S0009-2541(99)00190-4.

Poldervaart A. & Hess H.H. 1951. Pyroxenes in the Crystallization of Basaltic Magma. *J. Geol.* **59**, 472–489. doi:10.1086/625891.

Rajesh H.M. 2012. A geochemical perspective on charnockite magmatism in Peninsular India. *Geosci. Front.* **3**, 773–788. doi:10.1016/j.gsf.2012.04.003.

Rajesh H.M. & Santosh, M. 2012. Charnockites and charnockites. *Geosci. Front.* **3**, 737–744. doi:10.1016/j.gsf.2012.07.001.

Rajesh H.M. & Santosh M. 2004. Charnockitic magmatism in southern India. Proc. Indian Acad. Sci. *Earth Planet. Sci.* **113**, 565–585. doi:10.1007/BF02704023.

Rajesh H.M., Santosh M., Proyer A., Wan Y., Liu D., Liu S.J., Belyanin G.A. 2014a. Think outside the box: There is no Limpopo orogeny-Reply to comment by Laurent et al. on paper by Rajesh et al. (2014). *Precambrian Res.* **255**, 459–466. doi:10.1016/j.precamres.2014.09.001.

Rajesh H.M., Santosh M., Wan Y., Liu D., Liu S.J., Belyanin G.A. 2014b. Ultrahigh temperature granulites and magnesian charnockites: Evidence for Neoarchean accretion along the northern margin of the Kaapvaal Craton. *Precambrian Res.* **246**, 150–159. doi:10.1016/j.precamres.2014.03.001.

Rapopo M., 2010. Petrogenesis of the Matok pluton, South Africa: implications on the heat source that induced regional metamorphism in the Southern Marginal Zone of the Limpopo Belt. Master Thesis - University of Stellenbosch, South Africa (197p).

Ridolfi F., Renzulli A., Puerini M. 2010. Stability and chemical equilibrium of amphibole in calc-alkaline magmas: an overview, new thermobarometric formulations and application to subduction-related volcanoes 45–66. doi:10.1007/s00410-009-0465-7.

Santos M. N. S. D. (2015). Granodiorito Rio Maria e rochas associadas de Ourilândia do Norte – Província Carajás: geologia e afinidades petrológicas. Orientador: Davis Carvalho de

Oliveira. 2015. 68 f. Dissertação (Mestrado em Geologia e Geoquímica) – Instituto de Geociências, Universidade Federal do Pará, Belém, 2015. Disponível em: http://repositorio.ufpa.br/jspui/handle/2011/10681.

Santos M. De, Jesus Pereira Dos C.N.L., Lima, P.H.A., Lima, A., I, M.A.G., Carlos, J., Mesquita, L. 2013. Granitoides arqueanos da região de Água Azul do Norte, Província Carajás, sudeste do estado do Pará: petrografia, geoquímica e geocronologia. *Bol. do Mus. Para. Emílio Goeldi*. **8**, 325–354 p.

Santos J. 2003. Geotectônica dos escudos das Guianas e Brasil Central. *In*: Geol. tectônica e Recur. minerais do Bras.

Santos M. De, Jesus Pereira Dos C.N.L., Lima, P.H.A., Lima, A., I, M.A.G., Carlos, J., Mesquita, L. 2013. Granitoides arqueanos da região de Água Azul do Norte, Província Carajás, sudeste do estado do Pará: petrografia, geoquímica e geocronologia. *Bol. do Mus. Para. Emílio Goeldi*. **8**, 325–354 p.

Sardinha A.S., Barros C.E. de M., Krymsky R. 2006. Geology, geochemistry, and U-Pb geochronology of the Archean (2.74 Ga) Serra do Rabo granite stocks, Carajás Metallogenetic Province, northern Brazil. *J. South Am. Earth Sci.* **20**, 327–339 p. doi:10.1016/j.jsames.2005.11.001.

Schmidt M.W. 1992. Amphibole composition in tonalite as a function of pressure: an experimental calibration of the Al-in-hornblende barometer. *Contrib. to Mineral. Petrol.* **110**, 304–310 p. doi:10.1007/BF00310745

Schumacher J.C., 1997. The estimation of ferric iron in electron micropobe analysis of amphiboles. In: Leake B.E. (Ed.), 1997 Nomenclature of Amphiboles. Reportof the Subcommittee on Amphiboles of the International Mineralogical Association Commission on New Minerals and Mineral Names. *European Journal of Mineralogy,* vol**. 9**, 623 - 651.

Shand S.J. 1950. Eruptive rocks their genesis, composition, classification and their relation to ore deposit, fourth ed. Murby, London, 488 pp.

Silva L.R. da, de Oliveira D.C., dos Santos M.N.S. 2018. Diversity, origin and tectonic significance of the Mesoarchean granitoids of Ourilândia do Norte, Carajás province (Brazil*). J. South Am. Earth Sci.* **82**, 33–61. doi:10.1016/j.jsames.2017.12.004.

Smith J. V., 1974. Chemical Properties, in: Feldspar Minerals. Springer Berlin Heidelberg, Berlin, Heidelberg, pp. 15–143. doi:10.1007/978-3-642-65743-6_2.

Souza Z.S., Dall'Agnol R., Althoff F.J., Leite A.A.S., Barros C.E.M. 1996. Carajás Mineral Province: geological, geochronological and tectonic contrasts on the Archean evolution of the Rio Maria granite – greenstone terranes and the Carajás Block. *In*: SBG, Symposium Archaean terranes of the South American Platform, Brasília. *Extended Abstracts*. p. 31–32.

Souza Z.S., Potrel de, A., Lafon J.-M., Althoff F.J., Martins Pimentel M., Dall'Agnol R., de Oliveira C.G. 2001. Nd, Pb and Sr isotopes in the Identidade Belt, an Archaean greenstone belt of the Rio Maria region (Carajás Province, Brazil): implications for the Archaean

geodynamic evolution of the Amazonian Craton. *Precambrian Res.* **109**, 293–315. doi:10.1016/S0301-9268(01)00164-4.

Tassinari C. & Macambira M. 2004. A evolução tectônica do Cráton Amazônico. **Geol. do Cont.** *In:* sul-americano evolução da obra Fernando Flávio Marques Almeida 28, 471–485.

Tavares F.M., Trouw R.A.J., da Silva C.M.G., Justo A.P., Oliveira J.K.M. 2018. The multistage tectonic evolution of the northeastern Carajás Province, Amazonian Craton, Brazil: Revealing complex structural patterns. *J. South Am. Earth Sci.* **88**, 238–252. doi:10.1016/j.jsames.2018.08.024.

Teixeira A.S., Ferreira Filho, C.F., Giustina M.E.S. Della Araújo S.M., da Silva H.H.A.B. 2015. Geology, petrology and geochronology of the Lago Grande layered complex: Evidence for a PGE-mineralized magmatic suite in the Carajás Mineral Province, Brazil. *J. South Am. Earth Sci.* **64**, 116–138. doi:10.1016/j.jsames.2015.09.006.

Vasquez L.V., Rosa-Costa L.R., Silva C.G., Ricci P.F., Barbosa J.O., Klein E.L., Lopes E.S., Macambira E.B., Chaves C.L., Carvalho J.M., Oliveira J.G., Anjos G.C., Silva H.R. 2008. *Geologia e Recursos Minerais do Estado do Pará: Sistema de Informações Geográficas — SIG: texto explicativo dos mapas Geológico e Tectônico e de Recursos Minerais do Estado do Pará*. Organizadores, Vasquez M.L., Rosa-Costa L.T. Escala 1:1.000.000. Belém: CPRM.

Vernon R.H. 2004. *A practical guide to rock microstructures*. Cambridge University Press, p. 594.

Watson E.B. & Harrison T.M. 1983. Zircon saturation revisited: temperature and composition effects in a variety of crustal magma types. *Earth Planet. Sci. Lett.* 64, 295–304. doi:10.1016/0012-821X(83)90211-X.

Wones D.R. 1981. Mafic Silicates as Indicators of Intensive Variables in Granitic Magmas. *Min. Geol.* **74,** 744-749. doi:10.11456/shigenchishitsu1951.31.191

Wood B.J. & Banno S. 1973. Garnet-Orthopyroxene and Orthopyroxene-Clinopyroxene Relationships in Simple and Complex Systems 24.

Yavuz F. 2013. WinPyrox: A Windows program for pyroxene calculation classification and thermobarometry. *Am. Mineral*, **98**: 1338–1359. doi:10.2138/am.2013.4292.

Yavuz F. & Döner Z. 2017. WinAmptb: A windows program for calcic amphibole thermobarometry. *Period. di Mineral,* **86**, 135–167. doi:10.2451/2017PM710.

CAPÍTULO 3 CONCLUSÕES

3.1   CONCLUSÕES E CONSIDERAÇÕES FINAIS

Estudos desenvolvidos nos granitoides e rochas máficas associadas da região de Ourilândia do Norte permitiram a caracterização de 4 grupos petrograficamente distintos: (i) ortopiroxênio granodiorito, (ii) clinopiroxênio monzogranito e (iii) anfibólio monzogranito, e (iv) gabronorito. Este último ocorre espacialmente associados à variedade ortopiroxênio granodiorito. Tais rochas configuram cinco corpos alongados na direção NE-SW e E-W, onde o plúton principal possui ~12 km de extensão e entre 2 e 3 km de largura. É formado pelas variedades clinopiroxênio monzogranito e ortopiroxênio granodiorito, enquanto a variedade anfibólio monzogranito forma três pequenos corpos lenticulares com cerca de 3 km cada. Estes são alongados na direção E-W, mostram foliações na direção NE-SW e E-W e mergulhos subverticais (70-80º). As rochas estudadas exibem textura magmática bem preservada, são leucocráticas (M'=21,1 – 32,9), e de granulação média a grossa. Os minerais acessórios primários são allanita, epídoto, zircão, apatita, magnetita e ilmenita, sendo que a titanita ocorre somente nos monzogranitos e a olivina é restrita à variedade gabronorítica. Geoquimicamente, estas rochas mostram afinidade magnesiana, seguem o *trend* cálcio alcalino e cálcio alcalino de alto K, e são exclusivamente metaluminosas. Os dados de química mineral permitiram estimar as razões Fe/(Fe+Mg) tanto nas biotitas quanto nos anfibólios, as quais indicam condições intermediarias de fO_2, que é corroborada pela razão $Fe^{3+}/(Fe^{3+}+Fe^{2+})$ nos anfibólios que indica moderadas condições de fO_2 durante a cristalização (acima do tampão QFM). As temperaturas de cristalização para os piroxênios variam entre 855 a 1061 °C, 713 a 800 nos anfibólios, e a pressão de cristalização é de 190 a 310 MPa. A atividade de água no magma varia de 4,1 a 6,5.

Textura em coroa formada por anfibólios bordejando piroxênios ocorre em todas as variedades, que pode ser explicado pela reação do *melt* anidro com água em estágio magmático, que resultaria na ausência de piroxênio na fácies anfibólio monzogranito. As microestruturas de recristalização em quartzo e feldspatos permitem inferir uma temperatura final de deformação cristal-plástica em torno de 400-450 ºC. Microfraturas submagmáticas preenchidas por quartzo e álcali feldspato também são encontradas, indicando que os charnoquitos de Ourilândia do Norte sofreram deformação na presença de *melt*. Isto está de acordo com a natureza sin-tectônica para colocação de seus magmas. Estes dados mostram que a associação granítica-charnoquítica de Ourilândia possui afinidades com os demais

granitoides neoarqueanos. No entanto, o empobrecimento de HFSE em relação às rochas neoarqueanas de Carajás indica que a associação estudada possui uma fonte distinta e/ou sofreu diferentes processos de evolução. Dados de modelamento geoquímico indicam que tais granitoides evoluíram por cristalização fracionada a partir de um magma parental máfico (grabronorítico), em contraponto à fusão parcial, admitida como principal processo responsável pela origem dos demais granitoides neoarqueanos de Carajás.

REFERÊNCIAS

Ague J.J. 1997. Thermodynamic calculation of emplacement pressures for batholithic rocks, California: implications for the aluminum-in-hornblende barometer. *Geology,* **25** (6):563-566. doi:10.1130/0091-7613(1997)025<0563:TCOEPF>2.3.CO;2

Almeida J.A.C. de., Dall'Agnol R., Oliveira M.A.de., Macambira M.J.B., Pimentel M.M., Rämö O.T., Guimarães F.V., Leite A.A. da S., Almeida J. de A.C., Dall'Agnol R., Oliveira M.A.de., Macambira M.J.B., Pimentel M.M., Rämö O.T., Guimarães F.V., Leite A.A.S.da., 2011. Zircon geochronology, geochemistry and origin of the TTG suites of the Rio Maria granite-greenstone terrane: Implications for the growth of the Archean crust of the Carajás province, Brazil. *Precambrian Research,* **187** (1-2): 201–221. doi:10.1016/j.precamres.2011.03.004.

Almeida J. de A.C. de., Dall'Agnol R., Leite A.A.S.da., 2013. Geochemistry and zircon geochronology of the Archean granite suites of the Rio Maria granite-greenstone terrane, Carajás Province, Brazil. *Journal of South American Earth Sciences,* **42**, 103–126.

Almeida F.F.M., Hasui Y., Brito Neves B.B.de., Fuck R.A., 1981. Brazilian structural provinces: an introduction. *Earth-Science Reviews,* **17**, 1–29. doi:10.1016/0012-8252(81)90003-9.

Almeida J. A.C.de., Dall'Agnol R., Dias S.B., Althoff F.J., 2010. Origin of the Archean leucogranodiorite-granite suites: evidence from the Rio Maria terrane and implications for granite magmatism in the Archean. *Lithos,* **120**, 235–257. doi:10.1016/j.lithos.2010.07.026.

Almeida J. Oliveira M., Dall'Agnol R., Althoff F. 2008. *Relatório de mapeamento geológico na escala 1: 100.000 da Folha Marajoara (SB-22-zc v).* Belém, CPRM–Serviço Geológico do Bras. 147p. (Programa GeoBrasil).

Althoff F., Barbey P., Boullier A.M., 2000. 2.8–3.0 Ga plutonism and deformation in the SE Amazonian craton: the Archaean granitoids of Marajoara (Carajás Mineral Province, Brazil). *Precambrian Research,* **104**, 187–206. doi:10.1016/S0301-9268(00)00103-0.

Andersen D.J., Lindsley D.H., Davidson P.M., 1993. QUILF: A pascal program to assess equilibria among FeMgMnTi oxides, pyroxenes, olivine, and quartz. *Computers and Geosciences,* **19**, 1333–1350. doi:10.1016/0098-3004(93)90033-2.

Anderson J.L., Barth A.P., Wooden J.L., Mazdab F., 2008. Thermometers and Thermobarometers in Granitic Systems. *Reviews in Mineralogy and Geochemistry,* **69**, 121–142. doi:10.2138/rmg.2008.69.4.

Anderson J.L., Smith D.R., 1995. The effects of temperature and fO2 on the Al-in-hornblende barometer. *American Mineralogist,* **80**, 549–559. doi:10.1016/0031-9201(95)03018-R.

Araújo O. & Maia R. 1991. *Serra dos Carajás, folha SB. 22-ZA.* Estado do Pará. CPRM. Relatório Final. 136 p.

Araújo O.J., Maia R.G., Jorge João X.., Costa J.B, S. 1988. A megaestrutura arqueana da Folha Serra dos Carajás. *In*: SBG, 7º Congresso Latino-Americano de Gelololiga. *Anais*, Belém, p. 324–338.

Avelar V.G., Lafon J.M., Correia Jr., F.C., Macambira E.M.B. 1999. O magmatismo arqueano da região de Tucumã - Província Mineral De Carajás: Novos resultados geocronológicos. *Revista Brasileira de Geociências,* **29**, 453–460.

Baker L.L., Rutherford M.J. 1996. The effect of dissolved water on the oxidation state of silicic melts. *Geochimica et Cosmochimica Acta*. Pergamon **60**, 2179–2187. doi:10.1016/0016-7037(96)00090-7.

Bard J.P. 1986. *Microtextures of igneous and metamorphic rocks*. Dordreche, Boston, Marechal, Marianne. D. Reidel Pub. Co. (Petrology and Structural Geology A4).

Barker F., Arth J.G. 1976. Generation of trondhjemitic-tonalitic liquids and Archaean bimodal trondhjemitie-basalt suites. *Geology,* **4**, 596–600. doi:10.1130/0091-7613(1976)4<596.

Barros C.E.M., Barbey P., Boullier A.M. 2001. Role of magma pressure, tectonic stress and crystallization progress in the emplacement of syntectonic granites. The A-type Estrela granite complex (Carajás Mineral Province, Brazil). *Tectonophysics,* **343**, 93–109. doi:10.1016/S0040-1951(01)00260-8.

Barros C.E.M., Sardinha A.S., Barbosa J.D.P.O. de, Macambira M.J.B., Barbey P., Boullier A.M. 2009. Structure, petrology, geochemistry and zircon u/pb and pb/pb geochronology of the synkinematic archean (2.7 ga) a-type granites fromthe carajás metallogenic province, northern Brazil. *Canadian Mineralogist,* **47**, 1423–1440. doi:10.3749/canmin.47.6.1423.

Beard J.S., Ragland P.C., Rushmer T. 2004. Hydration Crystallization Reactions between Anhydrous Minerals and Hydrous Melt to Yield Amphibole and Biotite in Igneous Rocks: description and implications. *J. Geol*, **112**, 617–621. doi:10.1086/422670.

Blenkinsop T. 2000. *Deformation microstructures and mechanisms in minerals and rocks*. Dordrecht, Kluwer Academic Publishers, p.150. doi:10.1007/0-306-47543-X

Blundy J.D. & Holland T.J.B. 1990. Calcic amphibole equilibria and a new amphibole-plagioclase geothermometer. *Contributions to Mineralogy and Petrology,* **2**, 208-224 doi:10.1007/BF00306444.

Bohlender F., Van Reenen D.D., Barton J.M. 1992. Evidence for metamorphic and igneous charnockites in the Southern Marginal Zone of the Limpopo Belt. *Precambrian Research,* **55**, 429–449. doi:10.1016/0301-9268(92)90038-P.

Bohlender F. 1992. Igneous and metamorphiccharnockitic ocks in the Southern Marginal Zone of the Limpopo Belt with spe-cial emphasis on the Matok enderbitic-granitic suite. Rand Afrikaans University, 261p. (Unpublished Ph.D. thesis).

Bouchez J.L., Delas C., Gleizes G., Nedelec A., Cuney M. 1992. Submagmatic microfractures in granites. *Geology,* **20**, 35–38. doi:10.1130/0091-7613(1992)020<0035:SMIG>2.3.CO.

Brown G.C., Hawkesworth C.J., Wilson R.C.L. 1992. *Understanding the Earth.* Milton Keynes, UK, Departament of Earth Sciences the open university, p. 229.

Bucher K., Frost B.R., 2006. Fluid Transfer in High-grade Metamorphic Terrains Intruded by Anorogenic Granites: the Thor Range, Antarctica. *Journal of Petrology,* **47**, 567–593. doi:10.1093/petrology/egi086.

Campos B.C.S., Vilalva F.C.J., Nascimento M.A.L. do., Galindo A.C., 2016. Crystallization conditions of porphyritic high-K calc-alkaline granitoids in the extreme northeastern Borborema Province, NE Brazil, And geodynamic implications. *Journal of South American Earth Sciences,* **70**, 224–236. doi:10.1016/j.jsames.2016.05.010.

Carlson W.D., Lindsley D.H., 1988. Thermochemistry of pyroxenes on the join Mg2Si2O6-CaMgSi2O6. *American Mineralogist,* **73** (3-4), 242-252.

Carmichael I.S.E., 1991. The redox states of basic and silicic magmas: a reflection of their source regions? *Contributions to Mineralogy and Petrology*. Springer-Verlag, **106**, 129–141. doi:10.1007/BF00306429.

Carroll M.R. & Wyllie P.J. 1990. The system tonalite-H2O at 15 kbar and the genesis of calc-alkaline magmas. *American Mineralogist,* **75**, 345–357. doi:10.1177/1525740109354775.

Chayes F., 1956. Petrographic Modal Analysis: An Elementary Statistical Appraisal, p.113.

Clowe C.A., Popp R.K., Fritz S.J., 1988. Experimental investigation of the effect of oxygen fugacity on ferric-ferrous ratios and unit-cell parameters of four natural clinoamphiboles. *American Mineralogis,t* **73**, 487.

Condie K.C., Allen P., Narayana B.L., 1982. Geochemistry of the Archean low- to high-grade transition zone, Southern India. *Contributions to Mineralogy and Petrology*, Springer-Verlag **81**, 157–167. doi:10.1007/BF00371293.

Costa J.B.S, Araújo O.J.B., Jorge João X.S. Maia R., Macambira E.M.B., Vale A.G., Santos A., Pena Filho J.I.C., Neves A.P. 1994. Panorama tectono-estrutural da região sudeste do estado do Pará. *In:* SBG, 4° Simpósio geologia da Amazônia, Belém. *Resumos*. p. 314–317.

Cunha I.R.V.da., Dall'Agnol R., Feio G.R.L., 2016. Mineral chemistry and magnetic petrology of the Archean Planalto Suite, Carajás Province – Amazonian Craton: Implications for the evolution of ferroan Archean granites. *Journal of South American Earth Sciences,* **67**, 100–121. doi:10.1016/j.jsames.2016.01.007.

Dall'Agnol R., Cunha I.R.V.da., Guimarães F.V., Oliveira D.C.de., Teixeira M.F.B., Feio G.R.L., Lamarão C.N., 2017. Mineralogy, geochemistry, and petrology of Neoarchean ferroan to magnesian granites of Carajás Province, Amazonian Craton: The origin of hydrated granites associated with charnockites. *Lithos,* **277**, 3–32. doi:10.1016/j.lithos.2016.09.032.

Dall'Agnol R., Oliveira, D.C.de., 2007. Oxidized, magnetite-series, rapakivi-type granites of Carajás, Brazil: implications for classification and petrogenesis of A-type granites. *Lithos,* **93**, 215–233. doi:10.1016/j.lithos.2006.03.065.

Dall'Agnol R., Oliveira D.C.de, Guimarães F. V., O., Gabriel E.O., Feio G.R.L., Lamarão C.N., Althoff F.J., Patrick A. S., Teixeira M.F.B., Alice C. Silva, Daniel S. Rodrigues, Max J. P. Santos, Chrystophe R. P. Silva, Roseli D. Santos, P.J.L.S., 2013. Geologia do subdomínio de transição do domínio carajás – implicações para a evolução arqueana da província carajás – pará. *In:* 13 Simpósio Geol. da Amazônia. *Anais.* 1 CDrom.

Dall'Agnol R., Oliveira M.A., Almeida J.A.C., Althoff F.J., Leite A.A.S., Oliveira D.C., Barros C.E.M., 2006. Archean and Paleoproterozoic granitoids of the Carajás metallogenetic province, eastern Amazonian craton. *In:* Symp. Magmat. Crustal Evol. Metallog. Amaz. Craton. *Abstr.* Vol. F. Trips Guid.

Dall'Agnol R., Teixeira N.P., Rämö O.T., Moura C.A.V., Macambira M.J.B., de Oliveira, D.C., 2005. Petrogenesis of the Paleoproterozoic rapakivi A-type granites of the Archean Carajás metallogenic province, Brazil. *Lithos,* **80**, 101–129. doi:10.1016/j.lithos.2004.03.058.

Debon F. & Le Fort P. 1983. A Chemical-Mineralogical Classification of Common Plutonic Rocks and Associations. *Transactions of the Royal Society of Edinburgh: Earth Sciences*, **73** (3): 135-149. doi:10.1017/S0263593300010117

Debon F. & Lefort P. 1988. A cationic classification of common plutonic rocks and their magmatic associations: principles, method, applications. *Bulletin de Minéralogie*. **5,** 493-510 p.

Deer W.A., Howie R.A., Zussman J. 2013. *An introduction to rock-forming minerals.* 2nd ed. London, Longmans, 696 p.

DOCEGEO 1988. Revisão litoestratigráfica da Província Mineral de Carajás, Pará. In: *Congr. Bras. Geol.* **35**, 11–59.

Elliott B.A. 2003. Petrogenesis of the Post-kinematic Magmatism of the Central Finland Granitoid Complex II; Sources and Magmatic Evolution. *J. Petrol,* **44**, 1681–1701. doi:10.1093/petrology/egg053

Ellis D.J., Thompson A.B. 1986. Subsolidus and partial melting reactions in the quartz-excess $CaO + MgO + Al_2O_3 + SiO_2 + H_2O$ system under water excess and water-deficient

conditions to 10 kbar: some implications for the origin of peraluminous melts from mafic rocks. *J. Petrol,* **27**, 91–121.

Evensen N.M.M., Hamilton P.J.J., O'Nions R.K.K. 1978. Rare-earth abundances in chondritic meteorites. *Geochim. Cosmochim. Acta,* **42**, 1199–1212. doi:10.1016/0016-7037(78)90114-X.

Fegley B. 2013. Practical Chemical Thermodynamics for Geoscientists, Practical Chemical Thermodynamics for Geoscientists. doi:10.1016/C2009-0-22615-8.

Feio G.R.L. & Dall'Agnol R. 2012. Geochemistry and petrogenesis of the Mesoarchean granites from the Canaã dos Carajás area, Carajás Province, Brazil: Implications for the origin of Archean granites. *Lithos,* **154**, 33–52. doi:10.1016/j.lithos.2012.06.022.

Feio G.R.L., Dall'Agnol R., Dantas E.L., Macambira M.J.B., Gomes A.C.B., Sardinha A.S., Oliveira D.C., Santos R.D., Santos P.A. 2012. Geochemistry, geochronology, and origin of the Neoarchean Planalto Granite suite, Carajás, Amazonian craton: A-type or hydrated charnockitic granites? *Lithos,* **151**, 57–73. doi:10.1016/j.lithos.2012.02.020.

Feio G.R.L., Dall'Agnol R., Dantas E.L., Macambira M.J.B., Santos J.O.S., Althoff F.J., Soares J.E.B. 2013. Archean granitoid magmatism in the Canaã dos Carajás area: Implications for crustal evolution of the Carajás province, Amazonian craton, Brazil. *Precambrian Res,* **227**, 157–185. doi:10.1016/j.precamres.2012.04.007.

Frost B.R., Barnes C.G., Collins W.J., Arculus R.J., Ellis D.J., Frost C.D. 2001. A geochemical classification for granitic rocks. *J. Petrol,* **42,** doi:10.1093/petrology/42.11.2033.

Frost B.R. & Frost C.D. 2009. On charnockites: Reply to the discussion by C. Bhattacharyya and B. Goswami. *Gondwana Res,* **15**, 218–219. doi:10.1016/J.GR.2008.09.003.

Frost B.R. & Frost C.D. 2008. On charnockites. *Gondwana Res,* **13**, 30–44. doi:10.1016/j.gr.2007.07.006.

Frost B.R., Frost C.D., Hulsebosch T.P., Swapp S.M. 2000. Origin of the Charnockites of the Louis Lake Batholith, Wind River Range, Wyoming. *J. Petrol,* **41**, 1759–1776.

Frost B.R. & Lindsley D.H. 1991. Occurrence of Iron-Titanium Oxides in Igneous Rocks. *Rev. Mineral.* doi:10.2138/rmg.1991.25.12.

Frost R. 1991. Oxide minerals: Petrologic and magnetic significance. *Rev. Mineral.* **25**, 481–509. doi:10.1016/0037-0738(93)90062-A.

Gabriel E.O., Oliveira D.C., Macambira M.J.B. 2010. Caracterização geológica, petrográfica e geocronológica de ortopiroxênio-trondhjemitos (leucoenderbitos) da região de Vila Cedere III, Canaã dos Carajás-PA, Província Mineral de Carajás. *In:* SBG, Congresso Brasileiro de Geologia, 45. CDrom (in Portuguese).

Gabriel E.O. & Oliveira D.C. 2014. Geologia, petrografia e geoquímica dos granitoides arqueanos de alto magnésio da região de Água Azul do Norte, porção sul do Domínio Carajás, Pará. *Bol. do Mus. Para. Emílio Goeldi* - Série Ciências Nat. **9**, 533–564.

Gomes A.C.B. & Dall'Agnol R. 2007. Nova associação tonalítica-trondhjemítica neoarqueana na região de Canaã dos Carajás: TTGS com altos conteúdos de Ti, Zr e Y. *Rev. Bras. Geociências,* **37**, 182–193. doi:10.25249/0375-7536.2007371182193.

Hammarstrom J.M. & Zen E. 1986. Aluminum in hornblende: an empirical igneous geobarometer. *Am. Mineral.* doi:10.1016/S0022-2836(03)00574-6.

Harker A. 1965. *The natural history of igneous rocks*. New York, Macmillan.

Hawthorne F.C., Oberti R., Harlow G.E., Maresch W. V., Martin R.F., Schumacher, J.C., Welch, M.D. 2012. Nomenclature of the amphibole supergroup. *Am. Mineral.* **97**, 2031–2048. doi:10.2138/am.2012.4276.

Hibbard M. 1995. *Petrography to petrogenesis*. London, Macmillan Pub.

Holland T., Blundy J., 1994. Non-ideal interactions in calcic amphiboles and their bearing on amphibole-plagioclase thermometry. *Contrib. to Mineral. Petrol.* **116**, 433–447. doi:10.1007/BF00310910.

Holland T.H. 1900. The charnockite series, a group of Archaean hypersthenic rocks in peninsular India. *Geol. Surv. India Mem.*

Hollister L.S., Grissom G.C., Peters E.K., Stowell H.H., Sisson V.B. 1987. Confirmation of the empirical correlation of Al in hornblende with pressure of solidification of calc-alkaline plutons. *Am. Mineral.*

Howie R.A. 1955. The Geochemistry of the Charnockite Series of Madras, India. *Trans. R. Soc. Edinburgh,* **62**, 725–768. doi:10.1017/S0080456800009431

Hubbard F.H. 1988. Basic intrusion, charnockite-rapakivi granite plutonism and crustal depletion, S.W. Sweden. *Soc. Ital. di Mineral. e Petrol.* **43**, 543–554.

Hutchison C., 1974. Laboratory handbook of petrographic techniques.

Irvine T.N. & Baragar W.R.A. 1971. A Guide to the Chemical Classification of the Common Volcanic Rocks. Can. *J. Earth Sci.* **8**, 523–548. doi:10.1139/e71-055.

Johnson M.C. & Rutherford M.J. 1989. Experimental calibration of the aluminum-in-hornblende geobarometer with application of Long Valley caldera (California) volcanic rocks. *Geology*, **17**, 837–841. doi:10.1130/0091-7613(1989)017<0837:ECOTAI>2.3.CO;2.

Kerr P. 1959. *Optical mineralogy*. McGraw-Hill New York, 549 p.

Köhler T. & Brey G. 1990. Calcium exchange between olivine and clinopyroxene calibrated as a geothermobarometer for natural peridotites from 2 to 60 kb with applications. *Geochim. Cosmochim. Acta,* **54**, 2375–2388. doi:10.1016/0016-7037(90)90226-B.

Lafon J., Rodrigues E., Duarte K.D. 1994. Le granite Mata Surrão: un magmatisme monzogranitique contemporain des associations tonalitiques-trondhjemitiques-granodioritiques archéennes de la région de. *Comptes rendus l'Académie des.*

Lafon J.M.; Macambira M.J.B.; Pidgeon R.T. Zircon U-Pb SHRIMP dating of Neoarchean magmatism in the southwestern part of the Carajás Province (eastern Amazonian Craton, Brazil). *In:* International Geological Congress, 31., 2000, Rio de Janeiro. Abstracts. Rio de Janeiro, 2000. 1 CD-ROM.

Laurent O., Rapopo M., Stevens G., Moyen J.F., Martin H., Doucelance R., Bosq C. 2014. Contrasting petrogenesis of Mg-K and Fe-K granitoids and implications for post-collisional magmatism: Case study from the Late-Archean Matok pluton (Pietersburg block, South Africa). *Lithos*, **196**, 131–149. doi:10.1016/j.lithos.2014.03.006.

Le Maitre R.W. 2002. Igneous rocks; a classification and glossary of terms; recommendations of the International Union of geological Sciences Sub commission on the systematics of igneous rocks., 2nd ed. Cambridge University Press, University of Tasmania.

Leake B.E., Woolley A.R., Arps C.E.S., Birch, W.D., Gilbert C. m., Grice J.D., Hawthorne F.C., Kato A., Kisch H.J., Krivovichev V.G., Linthout K., Laird J., Mandarino J.A., Maresch W. V., Nickel E.H., Rock N.M.S.N.M.S., Schumacher J.C., Smith D.C., Stephenson N.C.N., Whittaker E.J.W., Youzhi G., Gurion B., Krivovichev V.G., Laird J., Mandarino J.A., Maresch W. V., Nickel E.H., Rock N.M.S.N.M.S., Schumacher J.C., Smith D.C., Stephenson N.C.N., Ungaretti L., Whittaker E.J.W., Youzhi G., Gilbert M.C., Grice J.D., Linthout K., Nicholaus M.S., Karort A., Krscnru H.J., H, D.G.F.C., Knns G.K., Jo, L., Mlnnarrnor A., Mannschrr W. V, Rocrrft H.N.N.M.S., Svrrrnr D.C., Srnphensonrr N.C.N., Scnurmcherrrr J.C., Uuc, L., Wnrrrakerrl J.W., Youznrl G. 1997. Nomenclature of amphiboles: Report of the Subcommittee on Amphiboles of the International Mineralogical Association, Commission on New Minerals and Mineral Names BnnN. *Can. Mineral*, **35**, 219–246.

Leite-Santos P.J. & Oliveira D.C. 2014. Trondhjemitos da área de Nova Canadá: novas ocorrências de associações magmáticas tipo TTG no Domínio Carajás. Bol. do Mus. Para. *Emílio Goeldi.* Ciências Nat, **9**, 635–659.

Leite-Santos P.J. & Oliveira D.C. 2016. Geologia, petrografia e geoquímica das associações leucograníticas arqueanas da área de Nova Canadá: Província Carajás. Geol. USP - *Ser. Cient.* **16**, 37–66. doi:10.11606/issn.2316-9095.v16i2p37-66.

Leite A.A. da S., Dall'Agnol R., Macambira M.J.B., Althoff,F.J. 2004. Geologia e geocronologia dos granitoides arqueanos da região de Xinguara-PA e suas implicações na evolução do terreno granito-greenstone de Rio Maria, Cráton Amazônico. *Rev. Bras. Geociências,* **34**, 447–458.

Leite A.A.D.S., Dall'agnol R., Althoff F.J. 1999. Geoquímica e Aspectos Petrogenéticos Do Granito Xinguara, Terreno Granito-Greenstone Arqueano De Rio Maria - Cráton Amazônico. *Rev. Bras. Geociências* **29**, 429–436. doi:10.25249/0375-7536.199929429436.

Liégeois J.P., 1998. Preface – some words on the postcollisional magmatism. *Lithos*, **45**, xv–xvii.

Lindsley D.H. & Andersen D.J. 1983. A two-pyroxene thermometer. *J. Geophys. Res.* **88**, A887. doi:10.1029/JB088iS02p0A887.

Macambira E.M.B. & Vale A.G. São Félix do Xingu: folha SB.22-Y-B, Estado do Pará, escala 1:250.000. Texto Explicativo. Brasília: CPRM, 1997. 344 p., il. Programa Levantamentos Geológicos Básicos do Brasil (PLGB).

Machado N., Lindenmayer Z., Krogh T.E., Lindenmayer D. 1991. U-Pb geochronology of Archean magmatism and basement reactivation in the Carajás area, Amazon shield, Brazil. *Precambrian Res.* **49**, 329–354. doi:10.1016/0301-9268(91)90040-H.

MacKenzie W., Donaldson C., Guilford C. 1982. Atlas of igneous rocks and their textures.

Marangoanha B., Oliveira, D.C.de., Oliveira V.E.S.de., Galarza M.A., Lamarão C.N. 2019. Neoarchean A-type granitoids from Carajás province (Brazil): New insights from geochemistry, geochronology and microstructural analysis. *Precambrian Res.* **324**, 86–108. doi:10.1016/j.precamres.2019.01.010.

Marangoanha B. Petrologia e evolução crustal na porção central do Domínio Canaã dos Carajás, Província Carajás. 2018. xxx, 193 f. (Ph.D. Thesis) - Universidade Federal do Pará, Instituto de Geociências, Programa de Pós-Graduação em Geologia e Geoquímica, 2018.

McDonough W.F., Sun S. -s., 1995. The composition of the Earth. Chem. *Geology*, **120**, 223–253. doi:10.1016/0009-2541(94)00140-4.

Medeiros H. & Dall'Agnol R. 1988. Petrologia da porção leste do Batólito Granodiorítico Rio Maria, sudeste do Pará. *In:* SBG, Congr. Bras. Geol. Belém, *Anais*, 3:1488-1499.

Mendes J.C. & Campos C.M.P. 2012. Norite and charnockites from the Venda Nova Pluton, SE Brazil: Intensive parameters and some petrogenetic constraints. *Geosci. Front.* **3**, 789–800. doi:10.1016/j.gsf.2012.05.009.

Mikhalsky E. V., Sheraton J.W., Hahne K. 2006. Charnockite composition in relation to the tectonic evolution of East Antarctica. *Gondwana Res.* **9**, 379–397. doi:10.1016/j.gr.2005.11.007.

Miyashiro A., 1974. Volcanic rock series in island arcs and active continental margins. *Am. J.*

Sci. **274**, 321–355. doi:10.2475/ajs.274.4.321.

Molin G., Zanazzi P.F., 1991. Intracrystalline Fe2+-Mg ordering in augite: experimental study and geothermometric applications. Eur. J. Mineral. 3, 863–875. doi:10.1127/ejm/3/5/0863.

Moreto C.P.N., Monteiro L.V.S., Xavier R.P., Amaral W.S., dos Santos T.J.S., Juliani C., de Souza Filho C.R. 2011. Mesoarchean (3.0 and 2.86 Ga) host rocks of the iron oxide–Cu–Au Bacaba deposit, Carajás Mineral Province: U–Pb geochronology and metallogenetic implications. *Miner. Depos.* **46**, 789–811. doi:10.1007/s00126-011-0352-9.

Morimoto N. 1988. Nomenclature of Pyroxenes. *Mineral. Petrol.* **39**, 55–76. doi:10.1007/BF01226262.

Mutch E.J.F., Blundy J.D., Tattitch B.C., Cooper F.J., Brooker R.A. 2016. An experimental study of amphibole stability in low-pressure granitic magmas and a revised Al-in-hornblende geobarometer. *Contrib. to Mineral. Petrol.* **171**, 85. doi:10.1007/s00410-016-1298-9.

Nachit H., Ibhi A., Abia E.H., Ben Ohoud M. 2005. Discrimination between primary magmatic biotites, reequilibrated biotites and neoformed biotites. *Comptes Rendus Geosci.* **337**, 1415–1420. doi:10.1016/j.crte.2005.09.002.

Nachit H., Razafimahefa N., Stussi J.M., Carron J.P. 1985. Composition chimique des biotites et typologie magmatique des granites. C.R. *Acad. Sci. Paris*. doi:10.1088/0031-9120/35/3/311.

Naney M.T. 1983. Phase equilibria of rock-forming ferromagnesian silicates in granitic systems. *Am. J. Sci.* **283**, 993–1033. doi:10.2475/ajs.283.10.993

Neves S.P. 2012. Granitos orogênicos: da geração dos magmas à intrusão e deformação. Synergia, Rio de Janeiro, 147 p.

O'Connor J. 1965. A classification for quartz-rich igneous rocks based on feldspar ratios. US Geol. *Surv. Prof. Pap. B.*

Oliveira D.C., Dall'Agnol R., Corrêa da Silva J.B., Costa de Almeida J.A. 2008. Gravimetric, radiometric, and magnetic susceptibility study of the Paleoproterozoic Redenção and Bannach plutons, eastern Amazonian Craton, Brazil: Implications for architecture and zoning of A-type granites. *J. South Am. Earth Sci.* **25**, 100–115. doi:10.1016/j.jsames.2007.10.003.

Oliveira, D.C. de, Neves, S.P., Trindade, R.I.F., Dall'Agnol, R., Mariano, G., Correia, P.B. 2010. Magnetic anisotropy of the Redenção granite, eastern Amazonian craton (Brazil): Implications for the emplacement of A-type plutons. *Tectonophysics,* **493**, 27–41. doi:10.1016/j.tecto.2010.07.018.

Oliveira M.A. De., Dall'Agnol R., Althoff F.J., Silva Leite A.A.da. 2009. Mesoarchean sanukitoid rocks of the Rio Maria Granite-Greenstone Terrane, Amazonian craton, Brazil. *J. South Am. Earth Sci.* **27**, 146–160. doi:10.1016/j.jsames.2008.07.003.

Oliveira V.E.S. de, Oliveira D.C.de., Marangoanha B., Lamarão C.N., 2018. Geology, mineralogy and petrological affinities of the Neoarchean granitoids from the central portion of the Canaã dos Carajás domain, Amazonian craton, Brazil. *J. South Am. Earth Sci.* **85**, 135–159. doi:10.1016/j.jsames.2018.04.022.

Passchier C. & Trouw R. 2005. Microtectonics, *Tectonophysics.* doi:10.1007/978-3-662-08734-3.

Passchier C.W. & Trouw R.A.J. 1996. *Microtectonics.* Berlin, Springer-Verlag. 289p.

Paterson S.R., Vernon R.H., Tobisch O.T. 1989. A review of criteria for the identification of magmatic and tectonic foliations in granitoids. *J. Struct. Geol.* **11**, 349–363. doi:10.1016/0191-8141(89)90074-6.

Patiño Douce A.E. 1996. Effects of pressure and H2O content on the compositions of primary crustal melts, in: Special Paper 315: The Third Hutton Symposium on the Origin of Granites and Related Rocks. *Geological Society of America*, pp. 11–21. doi:10.1130/0-8137-2315-9.11.

Peccerillo A. & Taylor, S.R. 1976. Geochemistry of eocene calc-alkaline volcanic rocks from the Kastamonu area, Northern Turkey. *Contrib. to Mineral. Petrol.* **58**, 63–81. doi:10.1007/BF00384745.

Petersen J.S. 1980. The zoned Kleivan granite - an end member of the anorthosite suite in southwest Norway. *Lithos*, **13**, 79–95. doi:10.1016/0024-4937(80)90065-1.

Pidgeon R.T., MacAmbira M.J.B., Lafon J.M. 2000. Th-U-Pb isotopic systems and internal structures of complex zircons from an enderbite from the Pium Complex, Carajas Province, Brazil: Evidence for the ages of granulite facies metamorphism and the protolith of the enderbite. *Chem. Geol.* **166**, 159–171. doi:10.1016/S0009-2541(99)00190-4.

Poldervaart A. & Hess, H.H. 1951. Pyroxenes in the Crystallization of Basaltic Magma. *J. Geol.* **59**, 472–489. doi:10.1086/625891.

Ragland P.C. 1989. *Basic analytical Petrology*. New York, Oxford University Press.

Rajesh H.M. 2012. A geochemical perspective on charnockite magmatism in Peninsular India. *Geosci. Front.* **3**, 773–788. doi:10.1016/j.gsf.2012.04.003.

Rajesh H.M. & Santosh, M. 2012. Charnockites and charnockites. *Geosci. Front.* **3**, 737–744.

doi:10.1016/j.gsf.2012.07.001.

Rajesh H.M. & Santosh M. 2004. Charnockitic magmatism in southern India. Proc. Indian Acad. Sci. *Earth Planet. Sci.* **113**, 565–585. doi:10.1007/BF02704023.

Rajesh H.M., Santosh M., Proyer A., Wan Y., Liu D., Liu S.J., Belyanin G.A. 2014a. Think outside the box: There is no Limpopo orogeny-Reply to comment by Laurent et al. on paper by Rajesh et al. (2014). *Precambrian Res.* **255**, 459–466. doi:10.1016/j.precamres.2014.09.001.

Rajesh H.M., Santosh M., Wan Y., Liu D., Liu S.J., Belyanin G.A. 2014b. Ultrahigh temperature granulites and magnesian charnockites: Evidence for Neoarchean accretion along the northern margin of the Kaapvaal Craton. *Precambrian Res.* **246**, 150–159. doi:10.1016/j.precamres.2014.03.001.

Rapopo M. 2010. Petrogenesis of the Matok pluton, South Africa: implications on the heat source that induced regional metamorphism in the Southern Marginal Zone of the Limpopo Belt. Master Thesis - University of Stellenbosch, South Africa (197p).

Ridolfi F., Renzulli A., Puerini M. 2010. Stability and chemical equilibrium of amphibole in calc-alkaline magmas: an overview, new thermobarometric formulations and application to subduction-related volcanoes 45–66. doi:10.1007/s00410-009-0465-7

Rodrigues D., Oliveira D., Macambira M. 2010. Geologia, geoquímica e geocronologia do magmatismo granítico da porção SW de Vila Sedere III, município de Água Azul do Norte-Província Mineral de Carajás. XLV *Congr. Bras. Geol.* **45**.

Rollinson H.R. & Hugh R. 1993. Using geochemical data: evaluation, presentation, interpretation. *Longman Scientific & Technical.*

Santos M. De, Jesus Pereira Dos C.N.L., Lima, P.H.A., Lima, A., I, M.A.G., Carlos, J., Mesquita, L. 2013. Granitoides arqueanos da região de Água Azul do Norte, Província Carajás, sudeste do estado do Pará: petrografia, geoquímica e geocronologia. *Bol. do Mus. Para. Emílio Goeldi.* **8**, 325–354 p.

Santos M.N.S.dos. & Oliveira D.C. 2016. Rio Maria granodiorite and associated rocks of Ourilândia do Norte – Carajás province: Petrography, geochemistry and implications for sanukitoid petrogenesis. *J. South Am. Earth Sci.* **72**, 279–301 p. doi:10.1016/j.jsames.2016.09.002

Santos J. 2003. Geotectônica dos escudos das Guianas e Brasil Central. Geol. tectônica e Recur. minerais do Bras.

Santos M. N. S. D. 2015. *Granodiorito Rio Maria e rochas associadas de Ourilândia do Norte – Província Carajás*: geologia e afinidades petrológicas. Orientador: Davis Carvalho de Oliveira. MD Dissetation em Geologia e Geoquímica, Instituto de Geociências, Universidade Federal do Pará, Belém, 2015. 68 p. Disponível em: http://repositorio.ufpa.br/jspui/handle/2011/10681.

Santos P. 2014. Geologia, petrografia e geoquímica das associações leucograníticas e TTG arqueanos da área de Nova Canadá (PA) Domínio Carajás. *Geologia USP. Série Científica*, **16**(2): 37-66. doi:10.11606/issn.2316-9095.v16i2p37-66

Santos R. D., Galarza M. A., Oliveira D. C. 2013. Geologia, geoquímica e geocronologia do Diopsídio-Norito Pium, Província Carajás Geology , geochemistry and geochronology of the Pium Diopside-Norite , Carajás Province. *Bol. Mus. Para. Emílio Goeldi.* Cienc. Nat. **8**, 355–382 p.

Sardinha A.S., Barros C.E. de M., Krymsky R. 2006. Geology, geochemistry, and U-Pb geochronology of the Archean (2.74 Ga) Serra do Rabo granite stocks, Carajás Metallogenetic Province, northern Brazil. *J. South Am. Earth Sci.* **20**, 327–339 p. doi:10.1016/j.jsames.2005.11.001.

Schmidt M.W. 1992. Amphibole composition in tonalite as a function of pressure: an experimental calibration of the Al-in-hornblende barometer. *Contrib. to Mineral. Petrol.* **110**, 304–310 p. doi:10.1007/BF00310745

Schumacher J.C. 1997. The estimation of ferric iron in electron micropobe analysis of amphiboles. In: Leake B.E. (Ed.), 1997 Nomenclature of Amphiboles. Reportof the Subcommittee on Amphiboles of the International Mineralogical Association Commission on New Minerals and Mineral Names. *European Journal of Mineralogy,* vol**. 9**, 623 - 651.

Silva A.C., Dall'Agnol R., Guimarães F.V., Oliveira D.C. 2014. Geologia, petrografia e geoquímica de Associações Tonalíticas e Trondhjemíticas Arqueanas de Vila Jussara, Província Carajás, Pará. *Bol. do Mus. Para. Emílio Goeldi - Série Ciências Nat.* 9, 13–45.

Silv, F.F.da., Oliveira D.C.de., Antonio P.Y.J., D'Agrella Filho M.S., Lamarão C.N. 2016. Bimodal magmatism of the Tucumã area, Carajás province: U-Pb geochronology, classification and processes. *J. South Am. Earth Sci.* **72**, 95–114. doi:10.1016/j.jsames.2016.07.016.

Silva L.R., Oliveira, D.C., Santos M.N.S.dos. 2018. Diversity, origin and tectonic significance of the Mesoarchean granitoids of Ourilândia do Norte, Carajás province (Brazil*). J. South Am. Earth Sci.* **82**, 33–61. doi:10.1016/j.jsames.2017.12.004.

Silva M., Oliveira D., Macambira M. 2010. Geologia, petrografia e geocronologia do magmatismo de alto K da região de Vila Jussara, Água Azul do Norte—Província Mineral de Carajás. *In*: SBG, 45º Congresso Brasileiro de Geologia, *Anais,* Belém, 1 CDrom.

Shand S.J. 1950. *Eruptive rocks their genesis, composition, classification and their relation to ore deposit.* Fourth ed. London, Murby, 488 p.

Smith J. V. 1974. Chemical properties. *In*: Autor(es). *Feldspar minerals*. Berlin, Heidelberg, Springer. p. 15–143. doi:10.1007/978-3-642-65743-6_2.

Souza Z.S., Dall'Agnol R., Althoff F.J., Leite A.A.S., Barros C.E.M. 1996. Carajás Mineral Province: geological, geochronological and tectonic contrasts on the Archean evolution of the Rio Maria granite – greenstone terranes and the Carajás Block. *In*: SBG, Symposium Archaean terranes of the South American Platform, Brasília. *Extended Abstracts*. p. 31–32.

Souza Z.S., Potrel A.de., Lafon J.-M., Althoff F.J., Martins Pimentel M., Dall'Agnol R., Oliveira, C.G. 2001. Nd, Pb and Sr isotopes in the Identidade Belt, an Archaean greenstone belt of the Rio Maria region (Carajás Province, Brazil): implications for the Archaean geodynamic evolution of the Amazonian Craton. *Precambrian Res*. **109**, 293–315. doi:10.1016/S0301-9268(01)00164-4.

Sousa S.D., Monteiro L.V.S., Oliveira D.C., Delinardo M.A.S., Moreto C.P.N., Juliani C. 2013. O greenstone belt Sapucaia na região de Água Azul do Norte, Província Mineral de Carajás: Contexto geológico e caracterização petrográfica. *In:* SBG, Congresso Brasileiro de Geologia, 47, *Anais*, Salvador, CDrom.

Streckeisen A., 1976. To each plutonic rock its proper name. *Earth Sci. Rev*. doi:10.1016/0012-8252(76)90052-0.

Tassinari C. & Macambira, M. 2004. A evolução tectônica do Cráton Amazônico. **Geol. do Cont.** *In:* sul-americano evolução da obra Fernando Flávio Marques Almeida 28, 471–485.

Tassinar, C.C.G.G. & Macambira M.J.B.B. 1999. Geochronological provinces of the Amazonian Craton. *Episodes* **22**, 174–182. doi:10.1080/00206819709465329.

Tavares F.M., Trouw R.A.J., da Silva C.M.G., Justo A.P., Oliveira J.K.M. 2018. The multistage tectonic evolution of the northeastern Carajás Province, Amazonian Craton, Brazil: Revealing complex structural patterns. *J. South Am. Earth Sci*. **88**, 238–252. doi:10.1016/j.jsames.2018.08.024.

Teixeira A.S., Ferreira Filho C.F., Giustina M.E.S., Araújo, S.M., da Silva H.H.A.B., 2015. Geology, petrology and geochronology of the Lago Grande layered complex: Evidence for a PGE-mineralized magmatic suite in the Carajás Mineral Province, Brazil. *J. South Am. Earth Sci*. **64**, 116–138. doi:10.1016/j.jsames.2015.09.006.

Teixeira M.F.B., Dall'Agnol R., Santos J.O.S., de Sousa L.A.M., Lafon J.M. 2017. Geochemistry, geochronology and Nd isotopes of the Gogó da Onça Granite: A new Paleoproterozoic A-type granite of Carajás Province, Brazil. *J. South Am. Earth Sci*. **80**, 47–65. doi:10.1016/j.jsames.2017.09.017.

Teixeira M.F.B., Dall'Agnol R., Silva A.C., Santos P.A. 2013. Geologia, petrografia e geoquímica do Leucogranodiorito Pantanal e dos leucogranitos arqueanos da área a norte de Sapucaia, Província Carajás, Pará: implicações petrogenéticas. *Bol. do Mus. Para. Emílio Goeldi.* Série Ciências Nat., **8** (3): 291–323.

Vasquez L.V., Rosa-Costa L.R., Silva C.G., Ricci P.F., Barbosa J.O., Klein E.L., Lopes E.S., Macambira E.B., Chaves C.L., Carvalho J.M., Oliveira J.G., Anjos G.C., Silva H.R. 2008. Unidades litoestratigráficas. *In*: Vasquez M.L. & Rosa-Costa L.T. (org.). *Geologia e recursos*

minerais do Estado do Pará: Sistema de Informações Geográficas — SIG: texto explicativo dos mapas Geológico e Tectônico e de Recursos Minerais do Estado do Pará. Escala 1:1.000.000. Belém, CPRM. p. 113-215.

Vernon R.H. 2004. *A practical guide to rock microstructures*. Cambridge, Cambridge University Press, 594p.

Watson E.B. & Harrison T.M. 1983. Zircon saturation revisited: temperature and composition effects in a variety of crustal magma types. *Earth Planet. Sci. Lett.* **64**(2): 295–304. doi:10.1016/0012-821X(83)90211-X.

Wells P.R.A. 1977. Pyroxene thermometry in simple and complex systems. *Contrib. to Mineral. Petrol.* **62**: 129–139. doi:10.1007/BF00372872.

Wones D.R. 1981. Mafic silicates as indicators of intensive variables in granitic magmas. *Min. Geol.* **74**:744-749. doi:10.11456/shigenchishitsu1951.31.191

Wood B.J. & Banno S. 1973. Garnet-orthopyroxene and orthopyroxene-clinopyroxene relationships in simple and complex systems 24. *Contributions to Mineralogy and Petrology*, **42**(2): 109-124.

Yavuz F. 2013. WinPyrox: a windows program for pyroxene calculation classification and thermobarometry. *Am. Mineral*, **98**: 1338–1359. doi:10.2138/am.2013.4292.

Yavuz F. & Döner Z. 2017. WinAmptb: a windows program for calcic amphibole thermobarometry. *Period. di Mineral,* **86**: 135–167. doi:10.2451/2017PM710.